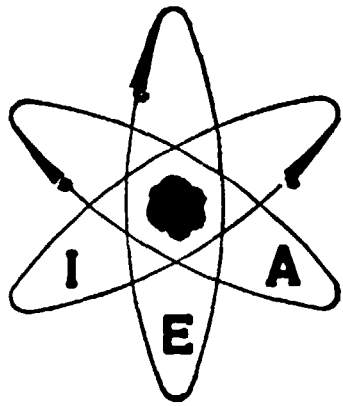

"HEALTH PHYSICS"
(PROTEÇÃO RADIOLÓGICA)

J. W. POSTON

INFORMAÇÃO IEA N.º 38

Dezembro — 1974

INSTITUTO DE ENERGIA ATÔMICA
Caixa Postal 11049 (Pinheiros)
CIDADE UNIVERSITÁRIA "ARMANDO DE SALLES OLIVEIRA"
SÃO PAULO — BRASIL

"HEALTH PHYSICS"
(PROTEÇÃO RADIOLOGICA)

J W Poston

Coordenadoria de Proteção Radiológica
Instituto de Energia Atômica
São Paulo Brasil

Informação IEA Nº 38
Dezembro 1974

* Research sponsored by the U S Atomic Energy Commission under contract with the Union Carbide Corporation

Instituto de Energia Atômica

Conselho Superior

Engº Roberto N. Jafet - Presidente
Prof. Dr. Emilio Mattar - Vice-Presidente
Prof. Dr. José Augusto Martins
Prof. Dr. Milton Campos
Engº Helcio Modesto da Costa

Superintendente

Prof. Dr. Rômulo Ribeiro Pieroni

"HEALTH PHYSICS"
(PROTEÇÃO RADIOLÓGICA)

J W Poston

LECTURE Nº 1

INTERACTION OF RADIATION WITH MATTER

Introduction

In 1896, Henri Becquerel found that uranium salts emitted penetrating radiations similar to those which Roentgen had produced only a year earlier with a gas discharge tube The tremendous importance of this discovery was not apparent until a few years later when Pierre and Marie Curie announced the isolation from a uranium mineral pitchblende of two substances many times more radioactive than uranium itself These two substances were subsequently shown to be two new elements polonium and radium

Skillful physicists worked for several years before they were able to identify the mysterious radiations emitted by the radioactive elements By use of magnetic fields Rutherford showed that there were three distinct types of radiations I am sure that all of you have seen a drawing similar to that shown in Figure 1 1 In this drawing a radium source is shown inside a lead block into which a small diameter hole has been bored The block is thick enough to absorb the penetrating rays. therefore they can only emerge through the opening This arrangement provides a parallel beam of rays escaping from the sorce If it were possible to see these invisible rays in the presence of a magnetic field, they would appear as sketched in the figure Those most easily deflected by the magnetic field are called beta (β) particles Those only slightly deflected by the field are called alpha (α) particles, and those which are unaffected are known as gamma (γ) rays

Alpha particles were rapidly identified as positively charged particles based on the direction of deflection in the magnetic field The same evidence showed beta particles were negatively charged, and gamma rays to be electrically neutral The relative radii of the deflected beams showed either that the alpha particle was much more massive than the beta particle or that it was emitted with a much greater energy The latter alternative seemed unlikely since alpha particles had little ability to penetrate absorbers

Alpha particles emitted from radioactive nuclei are completely stopped by a few sheets of paper or by a few centimeters of air Beta particles have a range of a few meters in air or several millimeters in an absorber such as aluminum Gamma rays were found to be very penetrating, being attenuated but not completely absorbed by several centimeters of aluminum or lead

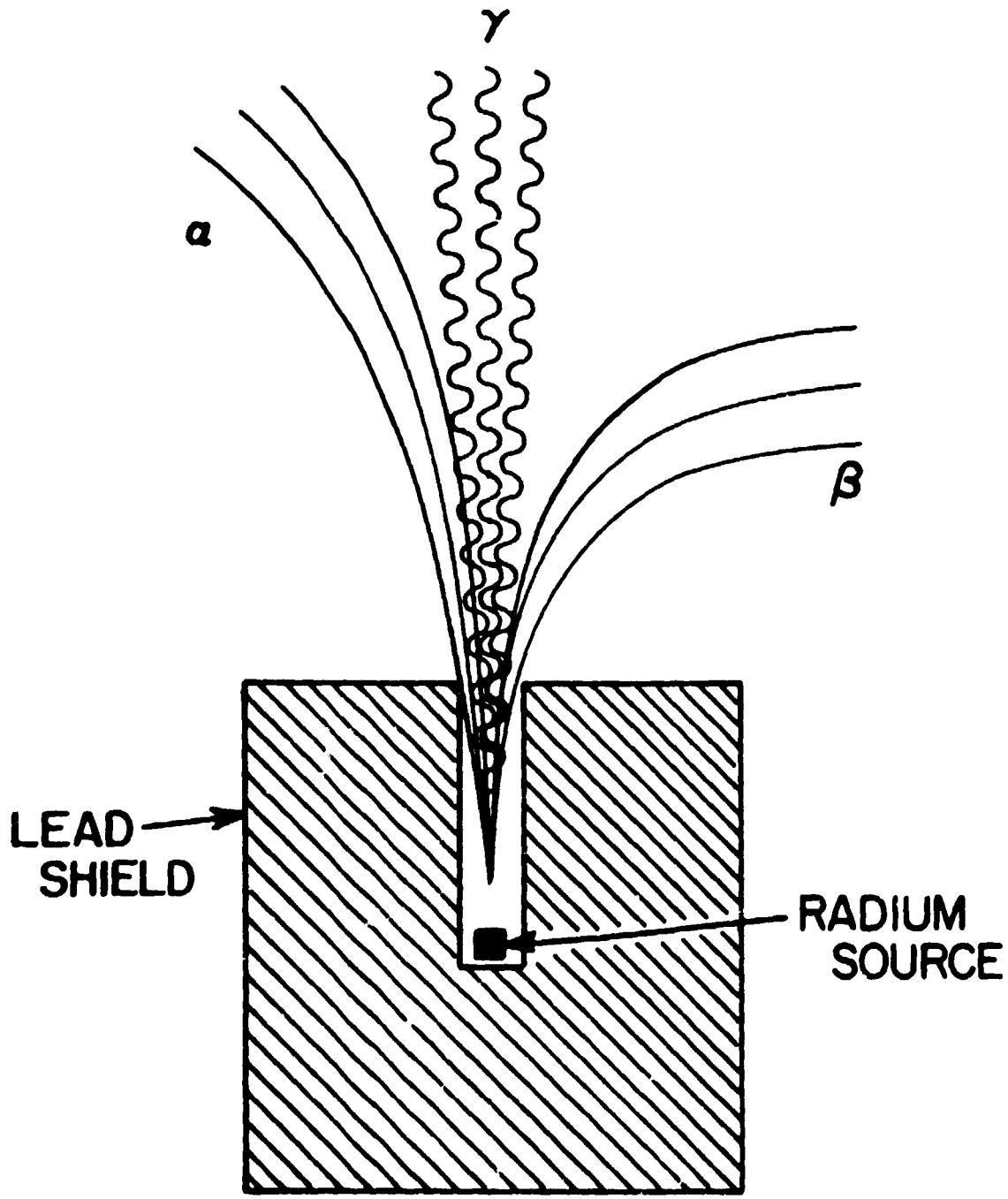

Figure 1-1

Deflections of the Radiations Emitted from Radium by a Magnetic Field Directed into the Paper

General Properties of Alpha Particles

Each alpha particle has a positive electric charge equal in magnitude to twice the electron charge. The alpha particle mass is that of a nucleus of ^4He, and an early experiment by Rutherford established the identity.

Because of the double charge, the alpha particle has a strong coulomb field and interacts strongly with any matter through which it passes. Thus would predict a rapid loss of energy and a short range.

A given nucleus emits alpha particles with, at most, a few unique values of energy. This constitutes a strong argument for the existence of discrete nuclear energy levels.

General Properties of Beta Particles

Magnetic analysis shows that beta particles have a single negative charge and a mass equal to that of the electron. They are, then, high speed electrons ejected from the nucleus as the result of a nuclear disintegration. Although beta particles originate in the nucleus, they do not exist there as such prior to emission. Considerations of magnetic dipole moments alone exclude the electron as a nuclear particle.

Positively-charged beta particles, or *positrons*, are ejected from some artificially produced radioactive nuclei. Many of the properties of the positron are identical with those of the negative beta particle, or *negatron*.

Beta particles are ejected from nuclei with velocities ranging from zero to nearly the velocity of light. In contrast to alpha particles, beta particles have a continuous distribution of energies from zero up to a maximum value that is a characteristic of each species of radioactive nuclide. Beta particles showing this continuous energy distribution are known as *primary beta particles*. Tables of disintegration constants always list the maximum energy of emission. In some calculations, as for energy deposition or absorbed dose, mean beta energy rather than the maximum is required. There is no simple general relation between mean and maximum beta energies, but for rough calculations, the mean may be taken as one third of the maximum.

The maximum beta energy really represents the energy of a transition. The missing two thirds of the total available energy is carried off by the neutrino, ν, which accompanies the emission of each primary beta particle. Since the neutrino interacts very weakly with matter, it deposits essentially no energy locally and need not be taken account of in dose calculations.

General Properties of Gamma Rays

Gamma rays are electromagnetic radiations or photons whose emission permits a nucleus in an excited state to go toward or to the ground state. A radioactive nucleus may, for example, emit either an alpha or a beta particle to produce a *daughter* nucleus of different atomic number. If the daughter nucleus is formed in its lowest energy state, the transition is completed with the particle emission. Should the daughter be left in an excited state, particle emission will be followed promptly by gamma ray emission until the ground state is reached. This process is the nuclear analog to the emission of visible or ultraviolet light when excited atoms return to

the ground state.

Gamma rays are also emitted in the process of *isomeric transition*. These are transitions of relatively low energy where there is a large difference between the angular momenta of the excited and the ground states. As a consequence, the excited state can exist for a measurable time before gamma emission occurs. The term *measurable* becomes progressively shorter as experimental techniques improve, but in all cases, isomeric transitions take place from a state which has had a long existence compared to that of the state preceding simple gamma-ray emission. In either case, the gammas are emitted with discrete energies since they represent the energy differences between definite nuclear energy levels.

The most important properties of these radiations are summarized in Table 1.1.

Interaction with Matter

Charged and neutral particles and electromagnetic waves penetrate matter and alter it in various ways. In this section, we shall discuss the ways in which these radiations interact with matter and the physical effects these interactions have. These effects are important both because they provide insight into chemical and biological actions of radiations, and because they provide a basis for the detection and measurement of radiation.

According to atomic theory, each electron in the atom is in a discrete, or quantized, energy state. If the electrons fill levels at which their total energy is at its minimum value, the atom is said to be in its *ground state*. All atoms have unfilled levels to which electrons can be "promoted" by energy absorption. When electron promotion occurs, the atom is said to be electronically exited. If enough energy is absorbed to remove an electron from the influence of the nucleus, the atom may be *ionized*. The minimum energies which electrons in various levels must acquire to be freed from the atom are called their *ionization potential*. When an electron absorbs energy in excess of its ionization potential, this excess appears as the kinetic energy of the electron.

When an alpha, beta, or other energetic charged particle approaches an atom or molecule, several processes of energy loss occur. The interaction leading to energy loss results from electric forces between the charged particle and the electrons in the atoms. Energy losses are due essentially to *excitation* and *ionization* of atoms. Although there are other processes (such as dissociation) which may occur, the most important energy loss processes are the electronic losses due to exitation and ionization.

The ionization process produces a free electron and a positively-charged ion; this combination is called an *ion pair*. The energy required to produce an ion pair varies only slightly with type of particle and gas. An average value of 34 eV may be used in most cases.

Alpha Particles

The number of ion pairs produced per centimeter of path varies as a function of the alpha particle energy. To see this move clearly, let's picture the passage of an alpha particle through a gas. The relatively massive particle with its double charge makes frequent electrostatic interactions with the outer, loosely bound electrons. The electrons are accelerated and often pulled away

TABLE 1 · 1

Characteristics of Different Radiations

Radiation	Type	Charge	Range of Typical Energy	Length of Typical Trajectory		Primary Mechanism of Energy Loss	General Comments
				Air	Solid		
Alpha	Particle	+ 2	4 · 10 MeV	3 · 5 cm	25 · 40 μ	Ionization, Excitation	Essentially a He Nucleus (He^{++})
Beta	Particle	1	0 · 4 MeV	0 10 cm	0 · 1 mm	Ionization, Excitation	Identical to Electron
Neutron	Particle	0	0 10 MeV	0 · 100 m	0 1 cm	Elastic Collision with Nucleus	Primarily from Nuclear Bombardment
X Rays	Electromagnetic Radiation	0	1 eV 100 keV	1 μ 10 m	1 μ 1 cm	Photoelectric Effect	Photons from Transition of Orbital Electrons
γ Rays	Electromagnetic Radiation	0	10 keV 3 MeV	1 cm 100 m	1 mm 10 cm	Photoelectric Compton Pair Production	Photons from Nuclear Transitions

from their parent atoms (ionization). As the alpha particle gives up energy and slows, it spends more time in the vicinity of each atom in its path and, consequently, has a higher probability of ionizing. One would expect specific ionization to increase slowly as the particle first leaves the source; near the end of its path, ionization should increase rapidly and then drop to zero as the particle acquires two electrons, becoming a neutral atom.

Figure 1-2 shows the variation of specific ionization for the alpha particles emitted by ^{214}Po. The values first rise slowly, then more rapidly as the *residual range* (path length left to travel) decreases. After reaching a maximum just before the end of the range, specific ionization rapidly drops to zero.

Range determinations may be performed as illustrated in Figure 1-3. Variation in the intensity of the source is plotted as a function of distance from the source d. If each alpha particle had the same initial energy and made an equal number of identical collisions, there should be a sharp break in the curve when d equals the range R. Actually, the curve bends downward at A, drops almost linearly along BC, and tails off at D. An extrapolation of the linear portion to the axis gives what is called the *extrapolated range*. The *mean range,* which is the distance of one-half maximum intensity, is usually a few millimeters shorter than the extrapolated range.

The tailing off at D is known as *straggling*. This is due to the statistical nature of the collision process, both in numbers and in the amount of energy transferred. Because of these fluctuations, there is a gradual rather than an abrupt approach to zero intensity.

An accurate range-energy relationship for alpha particles is of importance, since these ranges are used in a variety of calculations. Figure 1-4 shows an experimentally determined range curve. In the 4-7 MeV region, the curve is fairly well fit by

$$R = 3.09\, E^{3/2}$$

$$E = 2.12\, R^{2/3}$$

where R = range in air in centimeters, E = initial energy in MeV.

These expressions hold only for a limited range, at low energies, $R \propto E^{3/4}$; at high energies, the dependence is more nearly $R \propto E^{2}$.

Comparison of the range of alphas in air and in a solid is often made by using the *stopping power* concept. Stopping power is defined as the rate at which the alpha particle loses energy per increment of path, i.e., $-dE/dx$, in the absorber. A concept which is more easily visualized is that of *relative stopping power,* which is simply the ratio of the stopping power in air to the stopping power in the solid absorber. This assumes that the alpha particles are compared over the same energy range. Typical values for common absorbers are tabulated in Table 1-2.

An approximate expression for alpha-particle range in solids in given by the Bragg Kleeman relation:

$$R_s = \frac{3.2 \times 10^{-4}\, RA^{1/2}}{\rho}$$

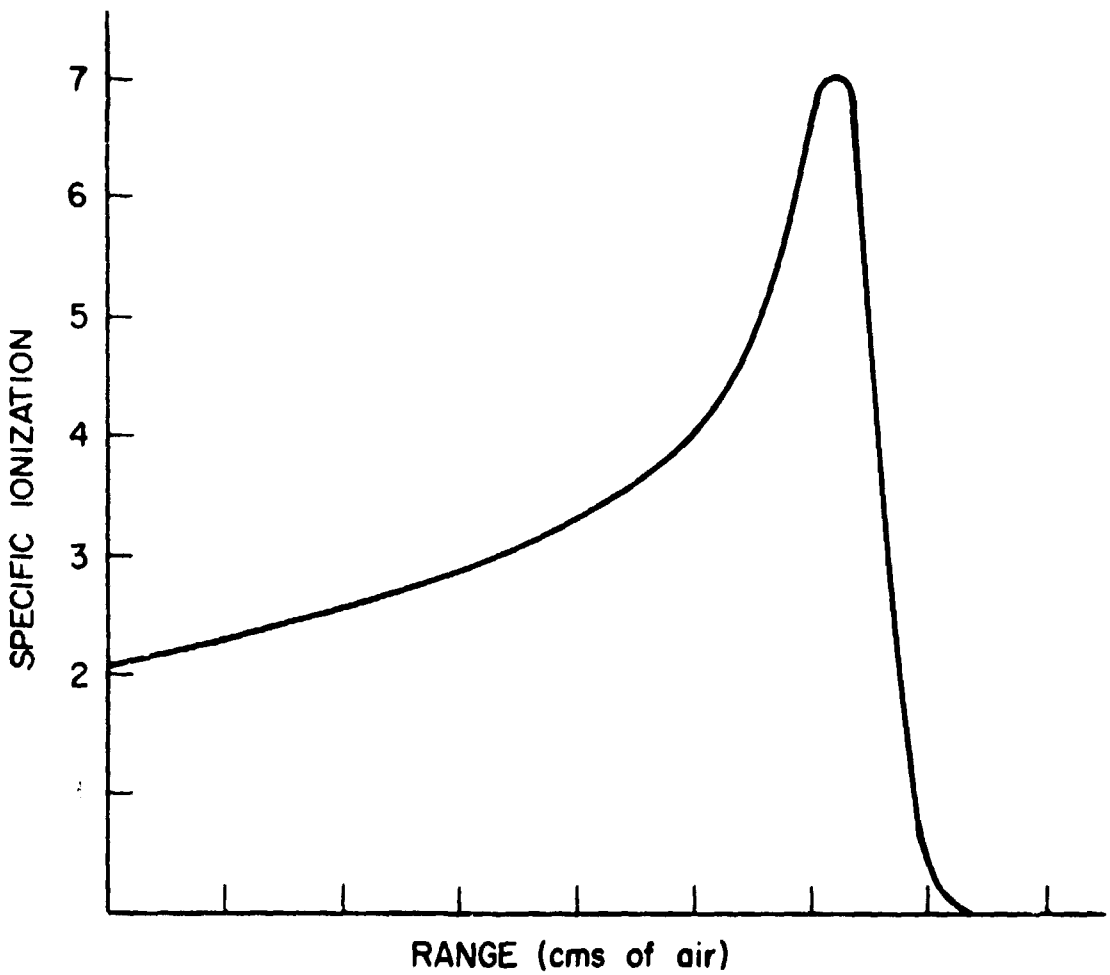

Figure 1-2

Specific Ionization of Alpha Particles as a Function of Distance from the Source

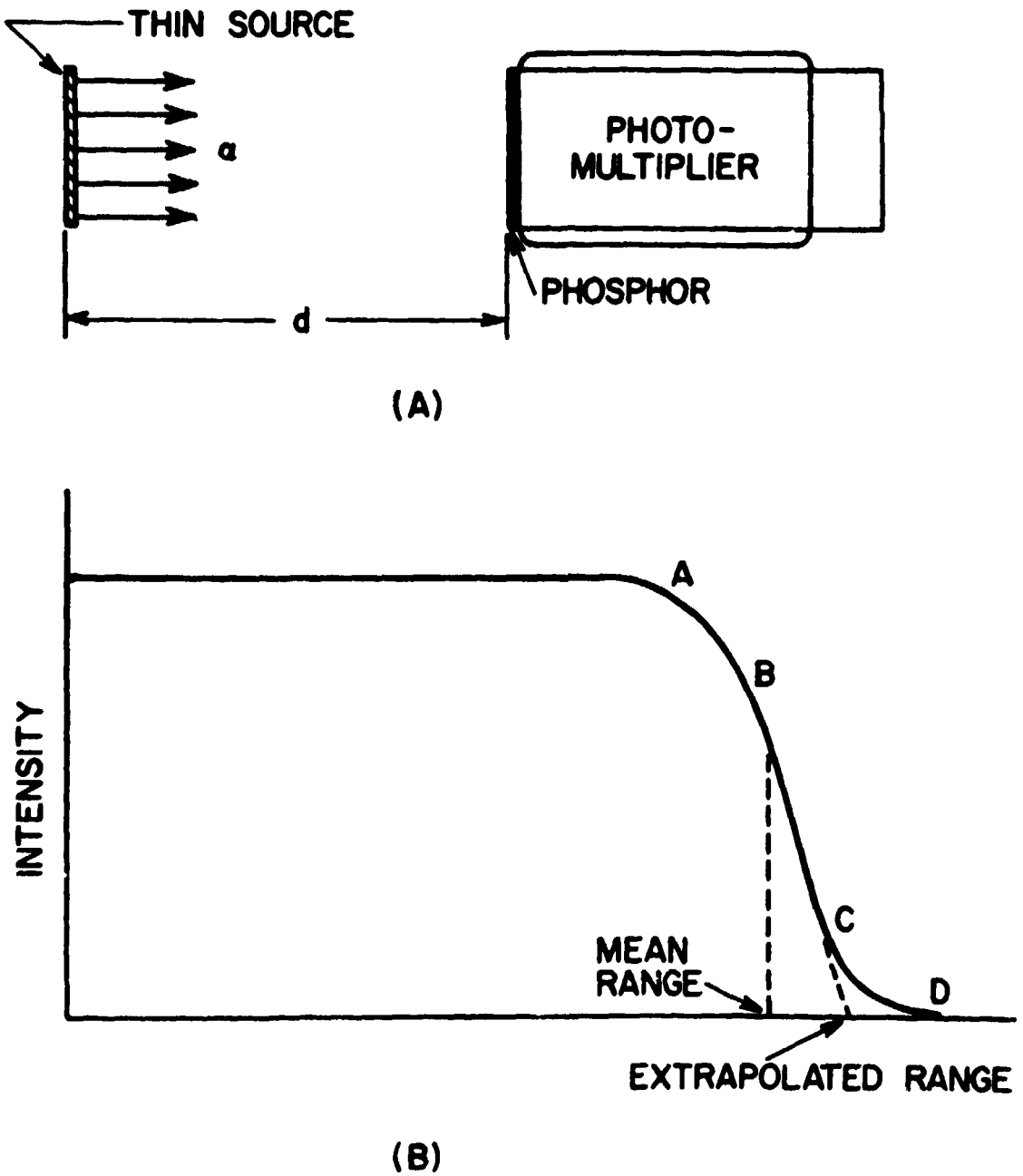

Figure 1-3

(a) Measurement of Alpha Particle Range.
(b) Intensity-Range Relationship.

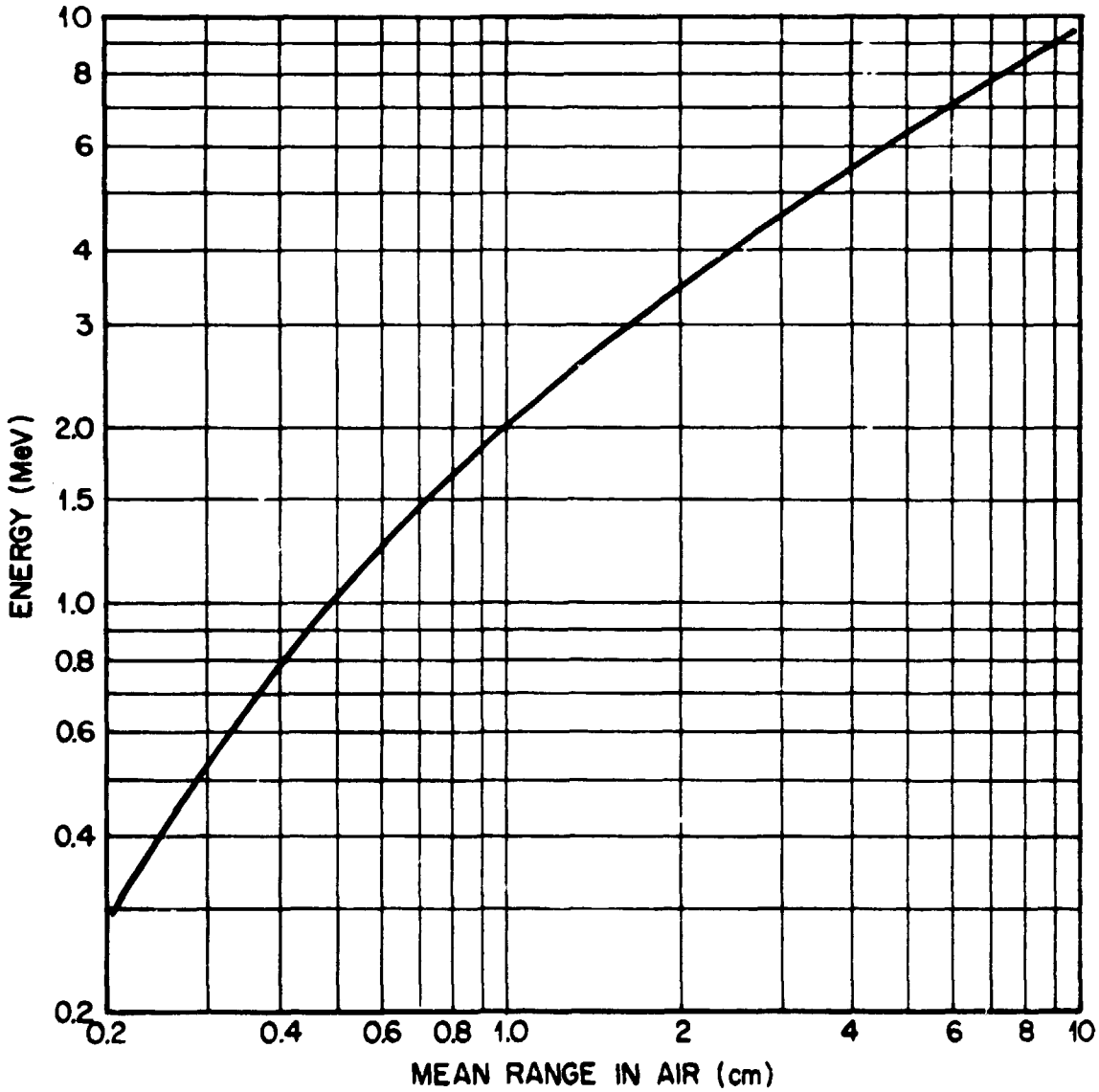

Figure 1 4

Range Energy Relationship for Alpha Particles in Standard Air

TABLE 1 2

Absorber:	Mica	Aluminium	Copper	Silver	Gold
Relative Stopping Power:	2000	1660	4000	3700	4800
mg/cm^2 = 1 cm air:	1 4	1 62	2 26	2 86	3 96
microns = 1 cm air:	5 0	6.0	2 5	2 7	2 1

where R_3 is the range in the solid of density ρ, and of mass number A, R is the range in air. A convenient relation between range in air and in tissue is of interest to biologists and medical scientists. The approximate rule

$$R_{air}\rho_{air} = R_{tissue}\rho_{tissue}$$

is easily remembered. Wherever it is necessary to deal with the mass number of a compound or mixture of elements, the value to substitute in equations such as those above is the effective atomic weight obtained by taking the square of the sum of the square roots of the individual atomic weights, the sum being taken in proportion to the percentage of to elements present For example, the effective value of A for air would be the square of the expression $(0.8\sqrt{14} + 0.2\sqrt{16})$, since nitrogen of mass number 14 makes up close to 80% of air molecules while oxygen (A = 16) may be assumed to be 20% for these calculations. Thus A for air would be 14.4.

Beta Particles

Early magnetic deflection measurements showed that beta particles had a single negative charge and an *e/m* ratio identical with that of electrons produced in a variety of ways. This identification was strong but incomplete evidence that the emitted negative particles were indeed electrons. As new properties of electrons became known and measured with precision, the identity between them and beta particles was strengthened. Except for origin, there is no known difference today between the negative beta particle and the electron, no matter how produced.

Beta particles originate in the nucleus, and it was assumed for some time that they existed there prior to emission. Before the discovery of the neutron, nuclear electrons were postulated to account for the difference between the number of nuclear charges and the number of nuclear masses. It is now evident that electrons as such cannot exist inside the nucleus Perhaps the strongest evidence comes from the magnetic moment of the electron, which is far too large to be associated with a nucleus. Spin considerations and the "size" of the electron as measured by its wave structure add to the evidence against nuclear electrons.

Lacking preexistence, the electron must be created at the moment of emission As we know now, the negatron arises from a neutron to proton conversion; the positron from the reverse, or proton to neutron conversion.

Early work showed that the beta particle, unlike other known radiations, had a continuous energy spectrum. This discovery jeopardized the entire concept of discrete nuclear energy levels, until Pauli brought forth what has now been shown to be the correct explanation

In 1931, Pauli suggested that the principles of conservation of energy and discrete nuclear energy levels could be retained by assuming a second particle emitted along with each beta particle. Conservation of electric charge in beta decays was already satisfied without the new particle which must then be electrically neutral. This requirement led to the name *neutrino*. Nuclear-mass relations were also satisfied to a high degree of precision without the neutrino, whose mass must, therefore, be very small compared to that of an electron. To fit the requirements of beta emission, the neutrino must be able to carry away energy momentum and angular momentum, and must have an inherent spin of 1/2.

According to Pauli, the energy E_m available at each beta emission is divided between beta particle and neutrino in all possible ratios. On the average, the neutrino receives about twice the energy imparted to the beta. In 1934, Fermi developed a theory of beta decay, which included the probability of energy division between the two particles. The success of the Fermi theory has furnished additional evidence for the validity of the neutrino concept.

A neutral particle of extremely small (or zero) mass will interact very weakly with any matter through which it passes. Measurements and theory agree on a neutrino interaction cross section of the order of 10^{-43} cm^2. This almost inconceivably small cross section leads to, at most, a few encounters in lead one light-year thick. It is understandable that the energy left by neutrinos within beta particle calorimeters is undetectable!

Unlike alpha particles, electrons are not characterized by linear paths and discrete ranges. Particularly at low energies, an electron path is tortuous as the result of multiple scattering encounters with the atoms along its path. In considering electron absorption, care must be taken to distinguish between *range*, which is linear thickness of material needed to just absorb the particle, and *path length*, which is the actual distance traveled before all kinetic energy is lost.

With a monoenergetic source of electrons, an approximately linear relation is found between ionization and absorber thickness. This linear trend is partly because the electrons are strongly scattered and so may be lost completely from the beam. The linear absorption for monoenergetic electrons differs sharply from that observed with the continuous energy distribution of a pure beta emitter.

Electrons lose energy through inelastic collisions, or more exactly, through interactions with the coulomb fields of atoms. These interactions lead to ionization and excitation of the absorber atoms. These coulomb interactions are highly variable depending on the exact details of each collision. Energy losses by the electron may range from a few to several hundred eV.

Electrons also lose energy by radiative collisions or bremsstrahlung production, usually important only at high energy in absorbers of high atomic number.

An expression for collision energy loss has been developed by Bethe and Ashkin,

$$-\left(\frac{dE}{dx}\right)_c = \frac{2\pi e^4 NZ}{m_o v^2}\left[\ln\frac{m_o v^2 E}{2I^2(1-\beta^2)} - \ln 2\left(2\sqrt{1-\beta^2}-1+\beta^2\right) + (1-\beta^2) + \frac{1}{8}\left(1-\sqrt{1-\beta^2}\right)^2\right]$$

where N = number of absorbing atoms per cubic centimeter
Z = atomic number of absorbing medium
v = *velocity of electron*
E = kinetic energy of electron, ergs
I = average ionization energy of absorber, ergs
e = electron charge, esu

Collision energy loss results from an interaction with orbital electrons and hence should be proportionl to electron density, NZ, as is the case. Phisical state or chemical combination does not play a role, except as may affect N.

Average ionization energy, I, has been the subject of extensive theoretical investigation, but values are probably beast obtained from experiment. Bakker and Segre measured the first four values in Table 1-3; the rest were obtained by interpolation or extrapolation.

TABLE 1 - 3

Average Ionization Energy

Material	Z	I (eV)
H	1	15 6
C	6	76 5
Al	13	150
Air		80 5
N	7	88
O	8	98
Water		68
Fe	26	400
Pb	82	1100

Bethe and Ashkin have also developed an expression for radiative energy loss in electron interactions.

$$-\left(\frac{dE}{dx}\right)_r = \frac{NEZ(Z+1)e^4}{137\, m_0^2 c^4}\left(4 \ln \frac{2E}{m_0 c^2} - \frac{4}{3}\right)$$

from this equation, we see that the rate of energy loss is roughly proportional to E and Z^2. Since path-length is inversely proportional to Z, the total bremsstrahlung production will be nearly proportional to E^2Z. This is in accord with the empirical results.

It has become customary to measure electron ranges in aluminum with either grams per square centimeter or milligrams per square centimeter as the range parameter. Except for the most exacting calculations, these ranges may be used for other absorbers. For energies above 1 MeV, the relation between range and energy is essentially linear. At low energies, the ionization losses and elastic scattering are very large, and the curve deviates from the linearity exhibited at higher energies. The linear part of the curve obeys a relation given by L. E. Glendenin and C. D. Coryell:

$$E = 1.85R + 0.245 \text{ for } R > 0.3 \text{ gram/cm}^2$$

or

$$R = 0.542E - 0.133 \text{ for } E > 0.8 \text{ MeV}$$

and is a more exact equation than that which was first given by Feather in 1938. The range equation is one that was empirically determined from precision measurements made on a series of beta emitters ranging in maximum energy values from 0.8 to 3.07 MeV. For energies lower than 0.8 MeV, the relation that fits the nonlinear curve is give by Glendenin and Coryell.

$$E = 1.92R^{0.725} \text{ for } R < 0.3 \text{ gram/cm}^2$$

and

$$R = 0.407E^{1.38} \text{ for } E < 0.8 \text{ MeV}$$

This energy equation should not be applied where the range, R, is less than 30 mg/cm^2. The range energy relation given above was established on the basis of precision absorption studies with beta emitters having an energy from 53 KeV to 0.8 MeV. Actually, for ranges less than 0.5 gram/cm^2, it is better to use the empirical curve of Bethe and Ashkin, which was given previously.

X Rays and Gamma Rays

In December, 1895, Wilhelm Conrad Roentgen announced the discovery of a new type of penetrating radiation, a discovery that was to affect the lives of all mankind. In his own words:

"A discharge from a large induction coil is passed through a Hittorf's vacuum tube, or through a well-exhausted Crooke's or Lenard's tube. The tube is surrounded by a fairly close fitting shield of black paper; it is then possible to see, in a completely darkened room that paper covered on one side with barium platinocyanide lights up with brilliant fluorescence when brought into the neighborhood of the tube, whether the painted side or the other be turned towards the tube."

In a remarkably thorough series of experiments, Roentgen determined many of the basic properties of these radiations, which he called *x rays* because of their unknown nature. The outstanding characteristic of the x ray was its ability to penetrate even solid matter. Medical fluoroscopy and radiography were the outgrowths of Roentgen's observation: "If the hand be held before the fluorescent screen, the shadow shows the bones darkly, with only faint outlines of the surrounding tissues."

Within five years, the French physicist, Villard, found that a radioactive material emitted penetrating rays similar to x rays. These rays became known as gamma (γ) rays, but their identity with x radiation was not established at the time. About this time, alpha and beta particles were discovered and certain scientists contended that gamma rays were themselves particles. Experiments conducted by Rutherford and Andrade showed clearly that gamma rays were not particulate but were, in fact, electromagnetic radiation. Despite the fact that x rays and gamma rays have a different origin, they have precisely the same characteristics. The old distinction that x rays were less penetrating than gamma rays is now a thing of the past, for modern technology has produced accelerators yielding x rays of far higher energy then any gamma radiation emitted from any radio element.

When x-or γ-ray photons traverse matter, some are absorbed, some pass through without interaction, and some are scattered, which really means that new photons are created, to move off in quite different directions from that of the original photon Figure 1-5 shows two arrangements for studying the attenuation of a photon beam by absorbers.

A photon source at S is collimated by heavy lead to provide a *narrow beam* of radiation at absorber C and detector D The arrangement in Figure 1-5A is said to have *good geometry*, since a negligible number of scattered photons reach the detector. Readings taken before and after the insertion of the absorber will provide a measure of the number of photons removed from the beam, or the *total absorption*. In *poor geometry*, Figure 1-5B, the detector will receive a considerable number of scattered photons. Readings taken before and after the introduction of an absorber will give a measure of the energy passed by it This is a measure of energy locally deposited in the absorber, or the *true absorption*

Attenuation measurements are also made under *broad beam* conditions Now, even in good geometry, the detector will receive some radiation due to photons scattered from regions where there were no primary photons with a narrow beam The photon intensity measured under broad-beam conditions will be greater than that measured with a narrow bear. The difference, called *build up*, represents the contribution due to photons scattered from one part of the broad beam to another. In a narrow beam, all scatter is out of the beam; none is in. Obviously, build-up is a complicated function of beam size, photon energy, and the geometrical arrangement of the measuring equipment.

With *monoenergetic* or monochromatic photons, measurements show an absorption which is an exponential function of absorber-thickness x. Beam intensities I_o, before, and I, after the introduction of the absorber, are related by

$$I = I_o e^{-\mu x}$$

where μ is the linear absorption coefficient.

The linear absorption coefficient is a function of photon energy as well as of absorber material, so the simple exponential form of the equation given above will not hold in general for a heteroenergetic photon beam. Absorption will always introduce some scattered low-energy photons, so even an initialy monoenergetic beam will not remain so, and measurements with thick absorbers may show an appreciable deviation from a constant value of μ.

Absorption coefficients depend upon the atomic compositon and the amount of absorber in the beam but not upon the chemical or physical state, Thus a given mass of water, ice, or steam will produce equal beam attenuations, although the three values of μ will differ widely because of density differences To avoid this it is convenient to introduce a *mass* absorption coefficient, $\mu_m = \mu/\rho$, which will be independent of absorber density The beam fraction, μ_m, is removed by unit areal density (1 gram/cm^2) regardless of the thickness required to obtain this density. Thus, the above equation becomes

$$I = I_o e^{-\mu_m (x\rho)}$$

where ρ is the absorber density in grams per cubic centimeter.

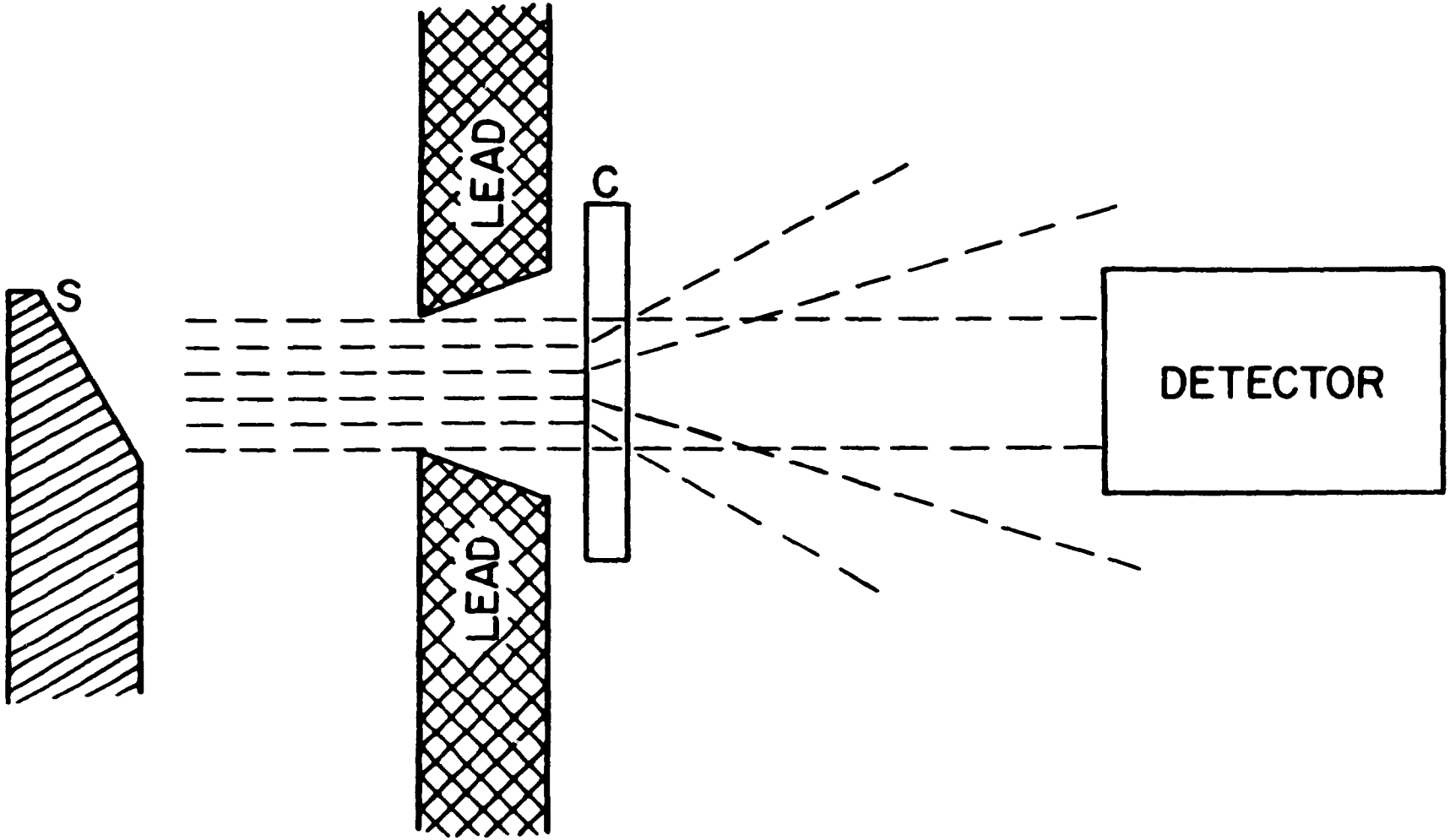

Figure 1-5A

Good Geometry Experiment.

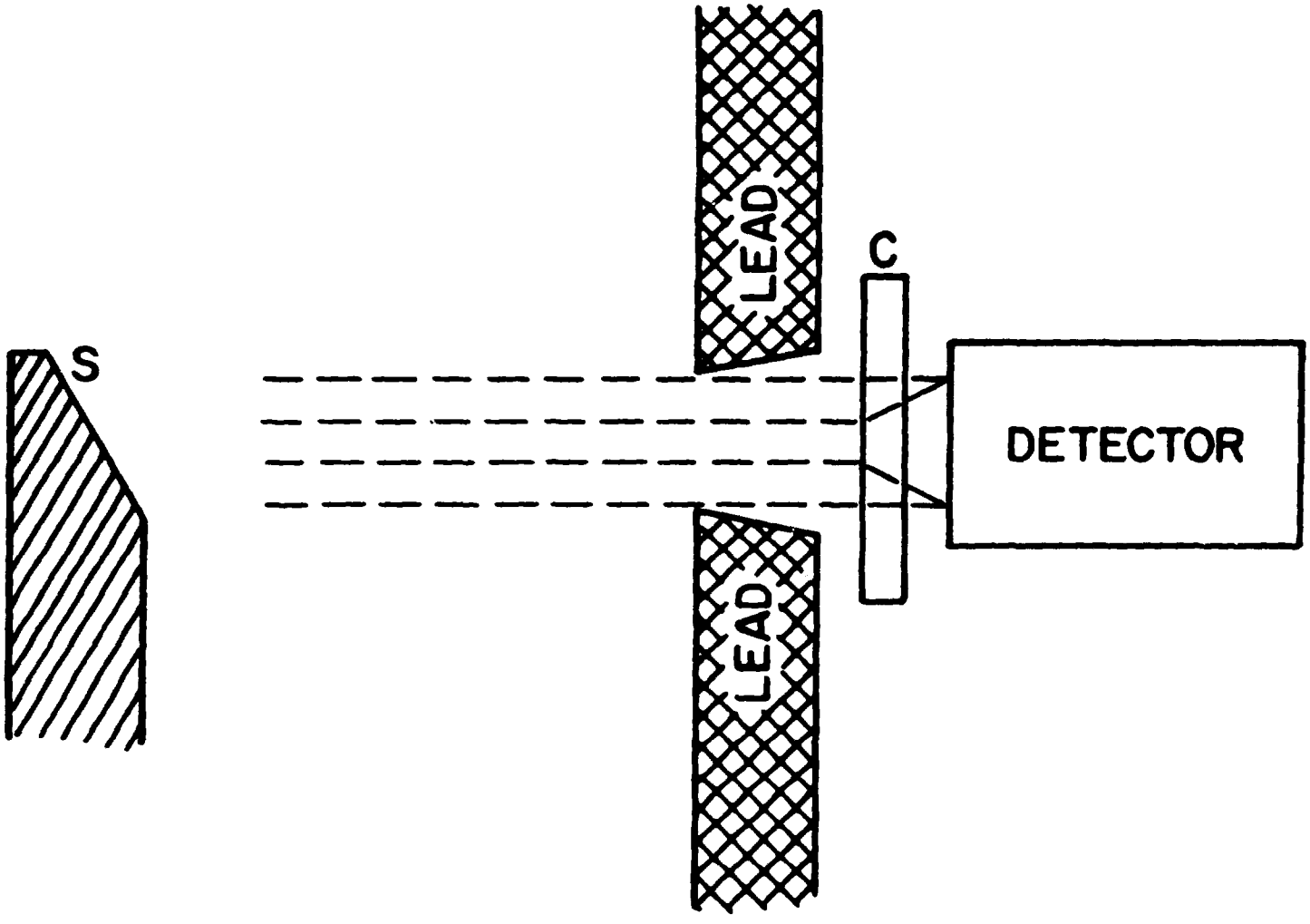

Figure 1-5B

Poor Geometry Experiment.

Thus far, we have considered the phenomena of photon absorption without regard to the details of their interaction with matter. Actually each absorption coefficient is the sum of three components. For example,

$$\mu_m = \tau_m + \mu_{mc} + \mu_{mp}$$

where τ_m = mass absorption coefficient for photoelectric effect
μ_{mc} = mass absorption coefficient for Compton effect
μ_{mp} = mass absorption coefficient for pair production

These are the three principal processes by which photons give up energy to matter, and each will be discussed.

When an x-ray quantum or photon collides with an atom, it may impinge upon an orbital electron and transfer all of its energy to this particle by ejecting it from the atom. If the incident photon carried more energy than that necessary to remove the orbital electron from the atom, it imparts to the electron its additional energy in the form of kinetic energy. This process is known as the *photoelectric effect* and obeys the Einstein photoelectric equation:

$$h\nu = \phi + E_k$$

Here $h\nu$ represents the total energy of the incident photon, ϕ the energy required to remove the electron from its atom, and E_k the kinetic energy of the ejected electron. (See Figure 1-6.)

Electrons thus ejected from atoms are called *photoelectrons*. Since these photoelectrons are produced by a process which completely absorbs the energy of the incident photon, they may carry considerable kinetic energy. This means that the photoelectrons, themselves, become a source of ionization, for as they pass close to neighboring atoms, they strip off electrons from them.

Photoelectric absorption increases as Z^5 and decreases as $E^{7/2}$. For low Z materials, such as living tissue, photoelectric absorption becomes negligible at photon energies above about 200 keV. In high Z materials, photoelectric absorption is appreciable at 1-2 MeV.

In some interactions, the incident photon is absorbed, as in the photoelectric process, but only a portion of the available energy goes into kinetic energy of the ejected electron. Instead, a new photon of lower energy than the original is created, with a division of energy between it and the electron. In this process, the electrons are called *recoil* or *Compton* electrons after the discoverer, A. H. Compton. In general, the new or scattered photon will not have the direction of the original as shown in Figure 1-7. Compton absorption falls of with increasing energy, but at a slower rate than photoelectric absorption. Compton interactions may contribute an appreciable fraction of the total absorption out to a few MeV. Under broad beam conditions, which include most practical shielding situations, Compton scattering acts to soften the beam by replacing high energy photons by those of a lower energy. However, beam hardening results from the fact that the photoelectric and Compton coefficients increase with decreasing photon energy. Detailed calculations for high energy photons are complex, since these involve the relative probabilities of the Compton and photoelectric process.

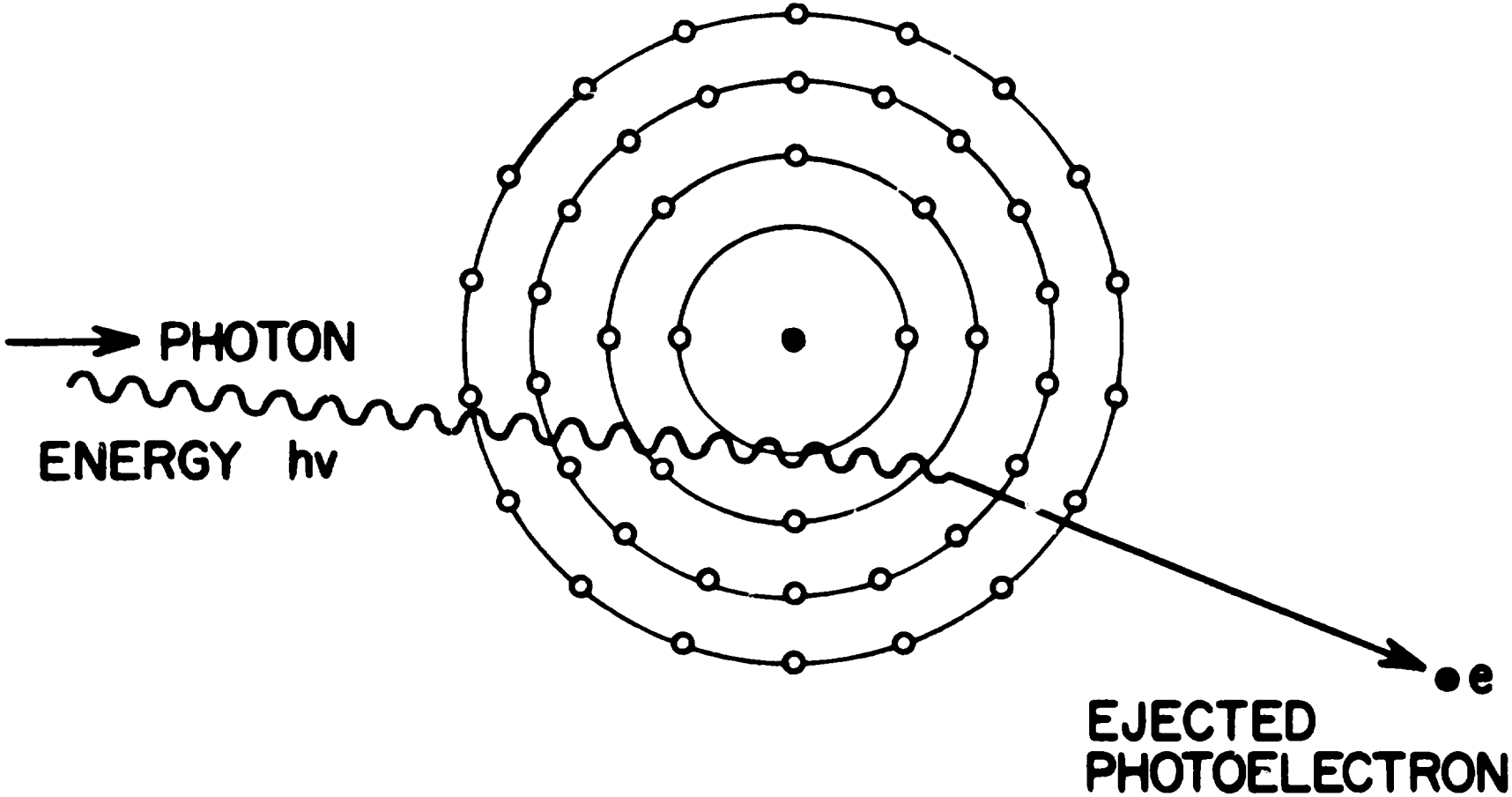

Figure 1-6

The Photoelectric Effect.

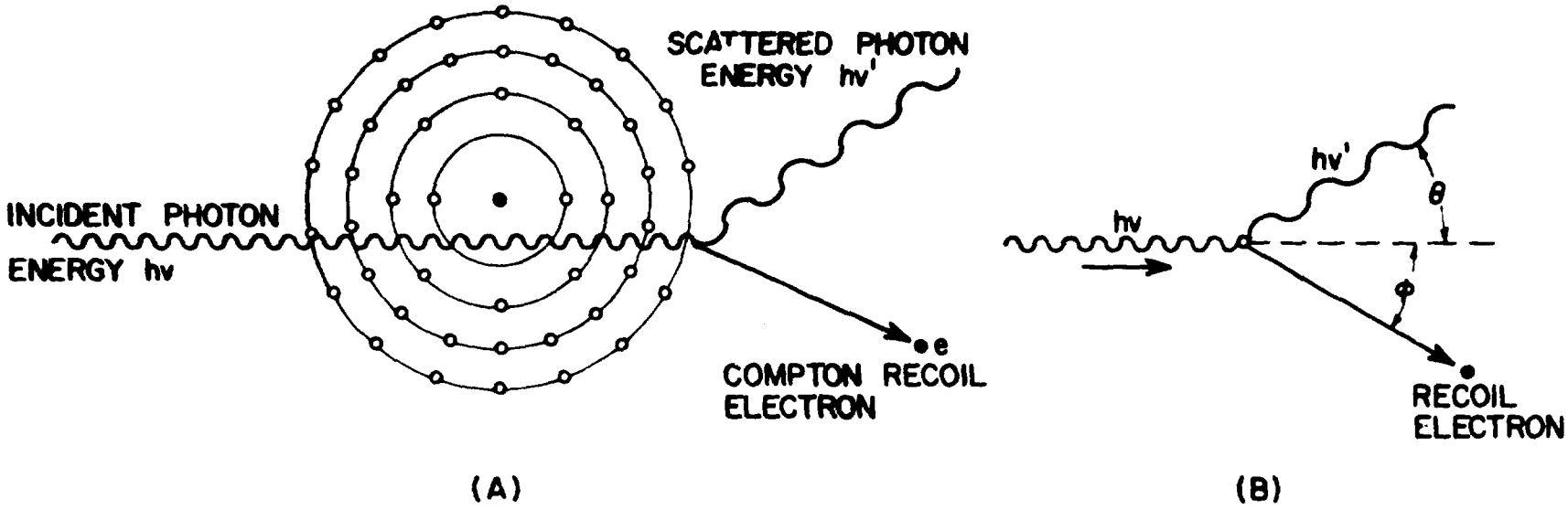

Figure 1-7

(a) The Compton Effect.
(b) Relationships Between the Quantities Involved.

An entirely different type of photon absorption *pair production* has a threshold at 1.02 MeV and becomes increasingly important at higher photon energies. In pair production (Figure 1-8), a photon in the field of a charged particle may disappear, giving up its energy to the *creation* of a positron-negatron electron pair. Interaction with a nuclear field is preferred, but orbital electrons are also effective. Pair production is not ionization of the involved molecule by the ejection of orbital electrons. Two previously nonexistent electron masses appear as a result of the disappearance of the photon energy. All of the photon energy is given up to the two electrons, with the exception of a very small amount going into the recoiling nucleus. The reaction is

$$h\nu \rightarrow e^{+} + e^{-} + 2E_k$$

The energy equivalent of each electron mass is 0.51 MeV, which establishes the reaction threshold at 1.02 MeV. Any excess energy is divided almost equally between the two particles, with the positron receiving slightly more than the negatron.

Each electron of the pair loses energy by ionization as it moves off from the point of origin. When the positron energy becomes low it combines with a negatron in a process that is the reverse of that by which it was created.

$$e^{+} + e^{-} \rightarrow 2\,h\nu$$

The two gamma rays in the above equation are called *annihilation radiation*, since they result from the disappearance of the mass of the two electrons. This equation is highly favored at low kinetic energies; hence in most reactions, energy comes only from the electron masses. This leads to photons producing photons with energies somewhat above 0.51 MeV. The two annihilation photons move off in almost exactly opposite directions, which permits some localization measurements by simultaneous counting.

Part of the energy initially derived from a photon absorbed by pair production goes into secondary photons, and is removed to a considerable distance from the primary interaction. This requires the use of two absorption coefficients, true and total, as for Compton scattering. Total absorption coefficients can be calculated directly; true absorption by pair production requires that the total coefficient be reduced by the factor

$$\frac{h\nu - 1.02}{h\nu}$$

where $h\nu$ must be in MeV. Near the threshold, there will be a substantial difference between the two coefficients.

The annihilation process is pictured as the formation, initially, of a hydrogen-like structure, *positronium*, in which the nucleus is the positron. This positron-negatron structure can be quantized exactly like the hydrogen atom. Like hydrogen, the ground state of positronium is an S state with zero angular momentum. The calculated lifetime of the singlet state (spins of positron and negatron anti-parallel) is only 10^{-10} sec. *Orthopositronium*, the triplet state in which the spins are parallel, has a mean life of about 10^{-7} sec, which is long enough to permit identification and to measure some of its optical properties.

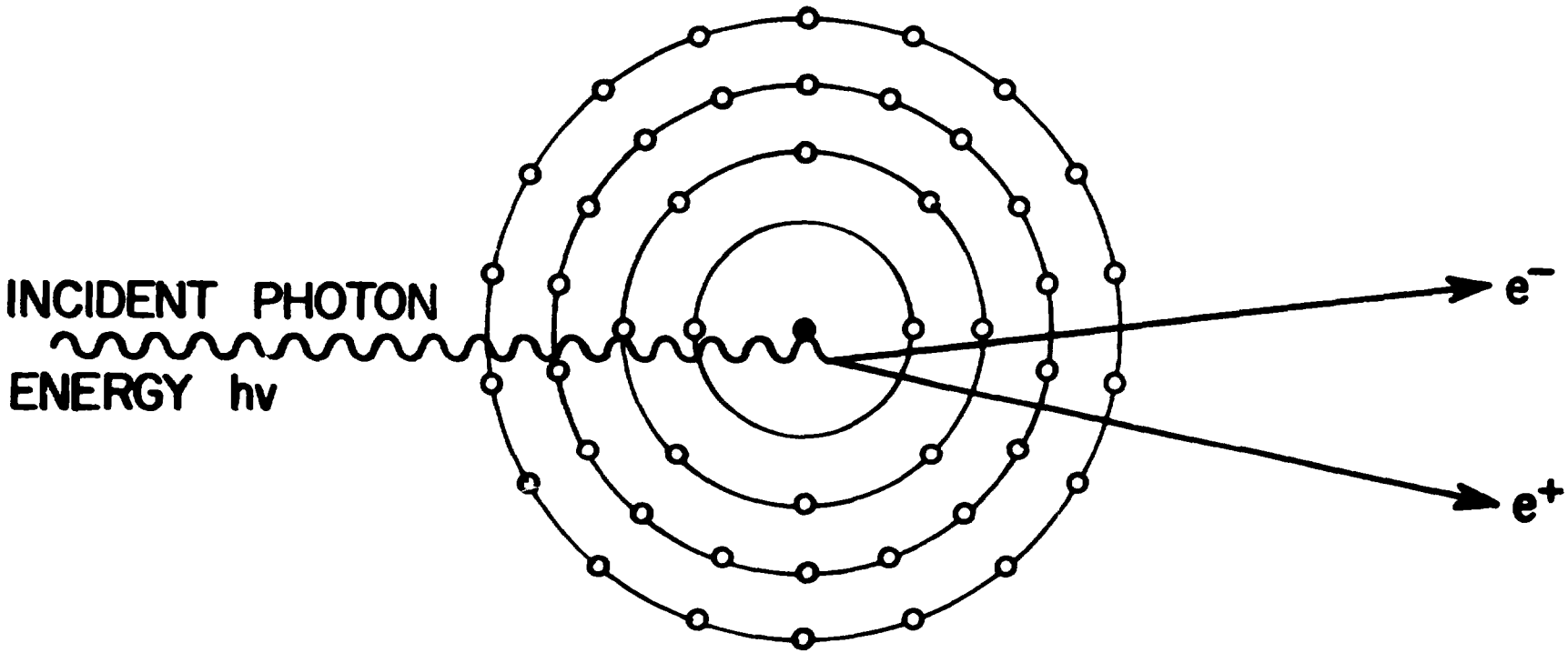

Figure 1-8

Pair Production.

BIBLIOGRAPHY

1. H. A. Bethe and J. A. Ashkin, *Experimental Nuclear Physics*, E. Segre, Ed., John Wiley and Sons, Inc., New York, 1953, Vol. 1.

2. C. J. Bakker and E. Segre, Phys. Rev. 811, 489 (1951).

3. R. E. Lapp and H. L. Andrews, *Nuclear Radiation Physics*, 3rd ed., Prentice-Hall, Inc., Englewood Cliffs, New Jersey, 1963.

4. G. S. Hurst and J. E. Turner, *Elementary Radiation Physics*, John Wiley and Sons, Inc., New York, 1970.

LECTURE Nº 2

RADIATION QUANTITIES AND UNITS

The purpose of this section is to introduce and define the main concepts, quantities and units used in radiation dosimetry. Since these concepts occur continually throughout the remainder of this course, it is prudent to examine them in great detail. It is the intent of this lecture to introduce these concepts through a historical review and through a logical development that emphasizes the important relationships existing between various quantities.

It would seem apparent that dosimetry is simply the measurement of dose by means of dosimeters. And essentially this is correct. In radiation dosimetry, at the present time, the sole proper use of the term *dose* is as an abbreviation for absorbed dose. The latter is defined as the energy imparted to matter by ionizing radiation per unit mass of material. However, in the literature, dose has been used in several senses; this reflects the fact that there are several different types of measurements that have been found possible and useful in the study and control of the effects of ionizing radiation on matter. The major types of measurements are:

1. Measurement of the absorbed dose in the matter at the point of interest.
2. Measurement of the energy released by indirectly ionizing particles per unit mass of some reference material at the point of interest. This serves as a convenient abbreviated description of the radiation there. The reference material may be either the actual material present at the point of interest, or some other material.
3. Measurement of the number of particles and quanta, or their energy, incident at a given point.
4. Measurement of some function of the number and energy of the particles and quanta incident at a given point.

Radiation dosimetry is commonly applied to all of these types of measurements, not just the measurement of absorbed dose.

Before we proceed with this discussion, let's go back many years and take a closer look at some of the concepts, etc. which are necessary in radiation dosimetry. The following discussion was taken in large part from Report 10a, 'Radiation Quantities and Units', of the International Commission on Radiological Units and Measurements.

Dosimetry has always been closely related to the practice of radiology, because radiologists were, until recent years, the largest group of users of radiation sources. The primary goal of radiologists was simply to control the amount of radiation delivered by their x-ray machines from one time to the next. This was not easy with the early gas-filled x-ray tubes. These could not be manufactured reproducibly and were not stable in operation. The problem was considerably simplified with the introduction in 1913 of the relatively stable Coolidge hot-filament, high vacuum x-ray tube, but even these required some mode of output calibration.

Many different physical effects were used in early measurements of x radiation, including calorimetric, chemical, photographic, and solid state coloration and fluorescence effects. In the early days of radiotherapy, a widely used indicator of radiation dose was the threshold

erythema dose. This is the amount of radiation required to produce a mild reddening of the skin; it provided a gross measure of the total absorbed dose By 1925, ionization chambers had become the method of choice because of their convenience, stability, and reproducibility I will discuss these chambers in detail in a later lecture It soon became apparent that two air filled chambers, identical except for the materials of the chamber walls, could give quite different values of ionization current in the same radiation field. To eliminate this wall effect and to make the response dependent upon ionization in air only, the free air chamber was developed during the 1920's and 1930's. During this period, concern over the measurement of x rays in radiological practice led to the organization of an international body to deal with the problem.

The First International Congress of Radiology (1925) created an organization known as the International Commission on Radiological Units (ICRU) to deal with the problems of radiation measurement and standardization in radiology Later the words "and Measurements" were added to the name of the organization, but "ICRU" was retained as the abbreviation

In 1928, the ICRU established a unit for that quantity which was measured by the free-air chamber. It was called the Roentgen, after the discoverer of x rays, and abbreviated, "r". The roentgen was originally defined to provide the best quantitative measure of exposure to medium energy x-radiation which the measuring techniques of that day permitted The choice of air as a standard substance was not only convenient but also appropriate for a physical quantity which was to be correlated with the biological effect of x rays, since the effective atomic number of air is not very different from that of tissue Thus a given biological response could be reproduced approximately by an equal exposure in roentgens for x ray energies available at that time. Since 1928, the definition has been changed several times, and this has reflected some feeling of dissatisfaction with the clarity of the concept

The most serious source of confusion was the failure to define adequately the radiation quantity of which the roentgen was said to be the unit [1] As a consequence of this omission, the roentgen had gradually acquired a double role. The use of this name for the unit had become recognized as a way of specifying not only the magnitude but also the nature of the quantity measured. This practice conflicts with the general usage in physics, which permits, within the same field, the use of a particular unit for all quantities having the same dimensions.

Even before this, the need for accurate dosimetry of neutrons and of charged particles from accelerators or from radionuclides had compelled the International Commission on Radiological Units and Measurements (ICRU) to extend the number of concepts. It was also desirable to introduce a new quantity which could be more directly correlated with the local biological and chemical effects of radiation. This quantity, *absorbed dose*, has a generality and simplicity which greatly facilitated its acceptance, and in a very few years, it has become widely used in every branch of radiation dosimetry.

The introduction of absorbed dose into the medical and biological field was further assisted by defining a special unit - the *rad*. **One rad is approximately equal to the absorbed dose delivered when soft tissue is exposed to one roentgen of medium voltage X radiation.** This is in many situations of interest to medical radiology, but not in all, the numbers of roentgens and rads associated with a particular medical or biological effect are approximately equal, and experience with the earlier unit could be readily transferred to the new one. Although the *rad* is merely a convenient multiple of the fundamental unit, *erg/g*, it has already

acquired, at least in some circles, the additional connotation that the only quantity which can be measured in rads is absorbed dose. On the other hand, the rad has been used by some authors as a unit for a quantity called by them *first collision dose*; this practice is deprecated by the Commission.

Definitions

1. The *absorbed dose (D)* is the quotient of ΔE_D by Δm, where ΔE_D is the energy imparted by ionizing radiation to the matter in a volume element, Δm is the mass of the matter in that volume element.

$$D = \Delta E_D / \Delta m$$

The symbol Δ precedes symbols for quantities that may be concerned with averaging procedures.

The special unit of absorbed dose is the *rad*.

$$1 \text{ rad} = 100 \text{ erg/gm} = 1/100 \text{(J/kg)}$$

Note: J is the abbreviation for Joule.

2. The *particle fluence*or fluence (Φ)* of particles is the quotient of ΔN by Δa, where ΔN is the number of particles which enter a sphere** of cross sectional area Δa.

$$\Phi = \Delta N / \Delta a$$

3. The *particle flux density or flux density (ϕ)* of particles is the quotient of $\Delta\Phi$ by Δt where $\Delta\Phi$ is the particle fluence in time Δt.

$$\phi = \Delta\Phi / \Delta t$$

Note. This quantity may also be referred to as particle fluence rate.

4. The *energy fluence (F)* of particles is the quotient of ΔE_F by Δa, where ΔE_F is the sum of the energies, exclusive of rest energies, of all the particles which enter a sphere of cross sectional area Δa.

$$F = \Delta E_F / \Delta a$$

---

* This quantity is the same as the quantity, nvt, commonly used in neutron physics.

** This quantity is sometimes defined with reference to a plane of area Δa, instead of a sphere of cross-sectional area Δa. The plane quantity is less useful for the present purposes, and it will not be defined. The two quantities are equal for a unidirectional beam of particles perpendicularly incident upon the plane area.

5. The *energy flux density* or *intensity (I)* is the quotient of ΔF by Δt where ΔF is the energy fluence in the time Δt.

$$I = \Delta F/\Delta t$$

Note: This quantity may also be referred to as energy fluence rate.

6. The *kerma* (K)* is the quotient of ΔE_K by Δm, where ΔE_K is the sum of the initial kinetic energies of all the charged particles liberated by indirectly ionizing particles in a volume element of the specified material, Δm is the mass of the matter in that volume element.

$$K = \Delta E_K/\Delta m$$

Note: (a) Since ΔE_K is the sum of the initial kinetic energies of the charged particles liberated by the indirectly ionizing particles, it includes not only the kinetic energy these charged particles expend in collisions but also the energy they radiate in bremsstrahlung. The energy of any charged particles is also included when these are produced in secondary processes occurring within the volume element. Thus the energy of Auger electrons is part of ΔE_K.

(b) In actual measurements, Δm should be so small that its introduction does not appreciably disturb the radiation field. This is particularly necessary if the medium for which kerma is determined is different from the ambient medium; if the disturbance is appreciable, an appropriate correction must be applied.

(c) It may often be convenient to refer to a value of kerma or of kerma rate for a specified material in free space or at a point inside a different material. In such a case, the value will be that which would be obtained if a small quantity of the specified material were placed at the point of interest. It is, however, permissible to make a statement such as: "The kerma for air at the point P inside a water phantom is ...," recognizing that this is a shorthand version of the fuller description given above.

(d) A fundamental physical description of a radiation field is the intensity (energy flux density) at all relevant points. For the purpose of dosimetry, however, it may be convenient to describe the field of indirectly ionizing particles in terms of the kerma rate for a specified material. A suitable material woud be air for electromagnetic radiation of moderate energies, tissue for all radiations in medicine or biology, or any relevant material for studies of radiation effects.

Kerma can also be a useful quantity in dosimetry when charged particle equilibium exists at the positon and in the material of interest, and bremsstrahlung losses are negligible. It is then equal to the absorbed dose at that point. In beams of x or gamma rays or neutrons, whose energies are moderately high, transient charged particle equilibrium can occur; in this condition the kerma is just slightly less than the absorbed dose. At very high energies the difference becomes appreciable. In general, if the range of directly ionizing particles becomes comparable with the mean free path of the indirectly ionizing particles, no equilibrium will exist.

---

* Various other methods of specifying a radiation field have been used, e.g., for a neutron source the "first collision dose" in a standard material at a specified point.

7. The *exposure (X)* is the quotient of ΔQ by Δm, where ΔQ is the sum of the electrical charges on all the ions of one sign produced in air when all the electrons (negatrons and positrons), liberated by photons in a volume element of air whose mass is Δm, are completely stopped in air.

$$X = \Delta Q/\Delta m$$

The special unit of exposure is the roentgen (R)*.

$$1\,R = 2.58 \times 10^{-4}\ C/kg$$

Note: (a) The words "charges on all the ions of one sign" should be interpreted in the mathematically absolut sense.

(b) The ionization arising from the absorption of bremsstrahlung emitted by the secondary electrons is not to be included in ΔQ. **Except for this small difference, significant only at high energies, the exposure as defined above is the ionization equivalent of the kerma in air.**

(c) With present techniques, it is difficult to measure exposure when the photon energies involved lie above a few MeV or below a few keV.

(d) As in the case of kerma, it may often be convenient to refer to a value of exposure or of exposure rate in free space or at a point inside a material different from air. In such a case, the value will be that which would be determined for a small quantity of air placed at a point of interest. It is, however, permissible to make a statement such as: "The exposure at the point P inside a water phanton is..."

8. The *linear energy transfer (L)* of charged particles in a medium is the quotient of dE_L by dl where dE_L is the average energy locally imparted to the medium by a charged particle of specified energy in traversing a distance of dl.

$$L = dE_L/dl$$

Note: (a) The term "locally imparted" may refer either to a maximum distance from the track or to a maximum value of discrete energy loss by the particle beyond which losses are no longer considered as local. In either case, the limits chosen should be specified.

(b) The concept of linear energy transfer is different from that of stopping power. The former refers to energy imparted within a limited volume, the latter to loss of energy regardless of where this energy is absorbed.

9. The *average energy (W) expended in a gas per ion pair formed* is the quotient of E by N_w, where N_w is the average number of ion pairs formed when a charged particle of initial energy E is completely stopped by the gas.

$$W = E/N_w$$

---

* This unit is numerically identical with the old one defined as 1 e.s.u. of charge per 0.001293 gram of air. C is the abbreviation for coulomb.

Note: (a) The ions arising from the absorption of bremsstrahlung emitted by the charged particles are not to be counted in N_w.

(b) In certain cases, it may be necessary to consider the variation in W along the path of the particle, and a differential concept is then required, but is not specifically defined here.

10. The *activity (A)* of a quantity of a radioactive nuclide is the quotient of ΔN by Δt where ΔN is the number of nuclear transformations which occur in this quantity in time Δt.

$$A = \Delta N/\Delta t$$

The special unit of activity is the curie (Ci).

$$1 \text{ Ci} = 3.7 \times 10^{10} \text{ s}^{-1} \text{ (exactly)}$$

Note: In accordance with the former definition of the curie as a unit of quantity of a radioactive nuclide, it was customary and correct to say: "Y curies of P-32 were administered..." It is still permissible to make such statements rather than use the longer form which is now correct: "A quantity of P-32 was administered whose activity was Y curies."

11. The *dose equivalent* (DE) is defined as the product of the absorbed dose and other necessary modifying factors. The ICRU wishes to reserve the term RBE for use in radiobiology only. The term *quality factor* (QF) should be used for protection purposes. The product of an absorbed dose and a suitable quality factor expresses the irradiation in terms of a common scale for all ionizing radiations. The *distribution factor* (DF) is used to correct for nonuniform distribution in the case of internally deposited radionuclides. Thus, the dose equivalent is given by:

$$DE = D(QF)(DF)\ldots\ldots$$

DE is numerically equal to the dose in rads times the appropriate factors. The unit of dose equivalent is the *rem.*

Table 2.1 summarizes the quantities and units discussed in the lecture.

BIBLIOGRAPHY

1. *Radiation Quatities and Units,* International Commission on Radiological Units and Measurements (ICRU) Report 10a, U.S. National Bureau of Standard Handbook 84, 1962

2. F. H. Attix and W. C. Roesch, eds., *Radiation Dosimetry, Vol. I Fundamentals,* Academic Press, New York, 1968.

TABLE 2 - 1

Table of Quantities and Units

No	Name	Symbol	Dimensions *	Units		
				MKSA	cgs	Special
4	Energy Imparted (Integral Absorbed Dose)	-	E	J	erg	gm rad
5	Absorbed Dose	D	EM^{-1}	Jkg^{-1}	$erg\ gm^{-1}$	rad
6	Absorbed Dose Rate	-	$EM^{-1}T^{-1}$	$Jkg^{-1}s^{-1}$	$erg\ gm^{-1}s^{-1}$	$rad\ s^{-1}$ etc.
7	Particle Fluence or Fluence	ϕ	L^{-2}	m^{-2}	cm^{-2}	
8	Particle Flux Density	Φ	$L^{-2}T^{-1}$	$m^{-2}s^{-1}$	$cm^{-2}s^{-1}$	
9	Energy Fluence	F	EL^{-2}	Jm^{-2}	$erg\ cm^{-2}$	
10	Energy Flux Density or Intensity	I	$EL^{-2}T^{-1}$	$Jm^{-2}s^{-1}$	$erg\ cm^{-2}s^{-1}$	
11	Kerma	K	EM^{-1}	Jkg^{-1}	$erg\ gm^{-1}$	
12	Kerma Rate	-	$EM^{-1}T^{-1}$	$Jkg^{-1}s^{-1}$	$erg\ gm^{-1}s^{-1}$	
13	Exposure	X	QM^{-1}	Ckg^{-1}	$esu\ gm^{-1}$	R(roentgen)
14	Exposure Rate	-	$QM^{-1}T^{-1}$	$Ckg^{-1}s^{-1}$	$esu\ gm^{-1}s^{-1}$	Rs^{-1} etc.
15	Mass Attenuation Coefficient	μ/ρ	L^2M^{-1}	m^2kg^{-1}	cm^2gm^{-1}	
16	Mass Energy Transfer Coefficient	μ_k/ρ	L^2M^{-1}	m^2kg^{-1}	cm^2gm^{-1}	
17	Mass Energy Absorption Coefficient	μ_{en}/ρ	L^2M^{-1}	m^2kg^{-1}	cm^2gm^{-1}	
18	Mass Stopping Power	S/ρ	EL^2M^{-1}	Jm^2kg^{-1}	$erg\ cm^2gm^{-1}$	
19	Linear Energy Transfer	L	EL^{-1}	Jm^{-1}	$erg\ cm^{-1}$	$keV(\mu m)^{-1}$
20	Average Energy per Ion Pair	W	E	J	erg	eV
22	Activity	A	T^{-1}	s^{-1}	s^{-1}	Ci (curie)
23	Specific Gamma-Ray Constant	Γ	QL^2M^{-1}	cm^2kg^{-1}	$esu\ cm^2gm^{-1}$	$Rm\ h^{-1}Ci^{-1}$ etc.
	Dose Equivalent	DE	-	-		rem

* It was desired to present only one set of dimensions for each quantity, a set that woud be suitable in both the MKSA and electrostatic cgs systems. To do this, it was necessary to use a dimension Q, for the electrical charge, that is not a fundamental dimension in either system. In the MKSA system (fundamental dimensions M, L, T, I) Q represents the product IT; in the electrostatic cgs system (M, L, T) it represents $M^{1/2}L^{3/2}T^{-1}$.

LECTURE N° 3

THE PHYSICAL BASIS OF RADIATION DOSIMETRY

Introduction

Implied in the term radiation dosimetry is the central problem in the field. One is given an environment consisting of corpuscular radiations distributed in an unknown fashion with respect to quantity, nature, direction, and energy. The problem of dosimetry is that of relating physical measurements of this environment to doses which are important from the standpoint of radiation physics and radiobiology.

Two approaches to radiation dosimetry may be considered. The first approach gives primary attention to the radiation field itself; in concept, measurements of the energy-angle distribution of particles in the field coud be carried out to obtain a complete description of the radiation environment in a given locale. This information could be employed, e.g., to compute the detailed distribution of radiation dose within a human placed there. The second approach characterizes the field primarily in terms of its interaction with matter located in the region of interest. This approach is of great practical importance and has formed the basis for almost all of radiation dosimetry.

The distinction between the two approaches is somewhat arbitrary in that one knows the radiation field only through its interaction with matter. The point of the second approach is to avoid a complete characterization of the field by taking advantage of the fact that the doses of interest are usually integral ones, requiring sums over the various spectral components of the field, weighted by more or less well known importance factors at the different energies. Thus, rather than obtaining a complete description of the energy distribution of the field only to perform a sum over this distribution to find the dose, one tries to utilize methods by which the sums are in a sense automatically performed.

The term *dose* is biologically oriented and originated during the early medical use of x rays. It is now defined in terms of physically measurable quantities. The ideal unit of dose from the standpoint of radiation protection and biophysics would be one which would produce the same biological effect independent of the kind and energy of the radiation. Such an ideal is probably unattainable because of the extreme complexity of radiation induced damage in living systems. In practice, one employs a physical dose unit which gives nearly the same biological effect independent of the energy of a given kind of radiation.

A reasonable choice for dose is the energy absorbed by (or alternately imparted to) a unit mass of matter. Hence, a unit such as the rad accupies a useful position in modern dosimetry, even though more sophisticated measure of radiation fields, such as linear energy transfer (LET), have assumed important positions in recent years. Definitions of various units of radiation dose were discussed in Lecture 2.

In the present lecture, the physical concepts upon which the second approach to dosimetry is based will be discussed. A well-known prescription for relating a phisical measurement in a radiation field to a dose in that field is embodied in the Bragg-Gray principle. This principle is important historically and in the practical design of many gamma and neutron

dosimeters. It has been considered in great detail by various authors since its original formulation and will be discussed below in the framework of a more general principle of radiation dosimetry.

Variation of Dose with Energy

The first collision dose to a given material and its variation with the energy of the impinging corpuscular radiation are important concepts in radiation dosimetry. The physical situation implied by the term "first collision" is one in which a beam of ionizing radiation is incident on a mass so small that the attenuation of the beam in the material is small. The first collision dose is usually expressed in terms of the energy imparted to a unit mass of the material per unit time and per unit flux of the incident beam. The term *first collision dose* has, as you know, been replaced by the term *kerma*. However, first collision dose is very often used even today, since the words are very descriptive of the physical interaction processes.

The central importance of this quantity is due (in addition to its simplicity) to the fact that many radiation measuring instruments have an energy response approximating the first collision dose energy relationship. Such an instrument may be used to measure the first collision dose in a free radiation field, or, equally important, it may be employed in the form of a small probe to measure the dose inside a large mass of material placed in the field. In the latter situation, it gives a physical measure of the dose to a small element of mass inside the larger one in a region where the dose may have a large spatial gradient and a magnitude quite different from the free field value.

Because of the importance of the first collision dose to radiation dosimetry, numerical data are given below for certain important materials.

First Collision Dose from Gamma Radiation

There are three important ways in which gamma rays interact with matter in the range of photon energies from 10 keV to 10 MeV. These are (1) the photoelectric effect, (2) Compton scattering, and (3) pair production. These processes of importance to dosimetry were discussed in Lecture 1.

In the photoelectric process, the ejected electron acquires kinetic energy equal to the photon energy minus the binding energy of the electron in its initial state in the atom. In the case of Compton scattering, the struck electron may assume different kinetic energies depending upon the angle of scatter of the photon. At energies above twice the electron rest energy ($2 mc^2$) where pair production is possible, the photon energy in excess of this value is taken up as kinetic energy be the electron positron pair. The energy of annihilation photons is not included in the definition of first collision dose, since their attenuation in matter occurs in a distance comparable with the attenuation length of the primary photons.

For purposes of calculating first collision dose, we assume that the energy of secondary ionizing radiations, e.g., electrons and positrons, liberated in these processes is dissipated locally (i.e., in a distance small compared with the mean range of the primary radiation). This a good approximation in the energy range to be considered here, where one may choose a mass of material to be small compared with the attenuation length of the primary gamma rays and large

compared with range of the electrons.

Defining $D^{(\gamma)}(E)$ to be the first collision dose from gamma rays of energy E in units of rad/(photon . cm^{-2}), one may write for an arbitrary material composition,

$$D^{(\gamma)}(E) = 1.602 \times 10^{-8} \sum_i N_i \left[\tau_i(E)\epsilon_i^{pe}(E) + \sigma_i(E)\epsilon^{c}(E) + k_i(E)\epsilon^{pp}(E)\right]$$

where

N_i = number of atoms of the i^{th} element per gram of the material,

$\tau_i(E)$ = photoelectric cross section of the i^{th} element (in cm^2/atom),

$\sigma_i(E)$ = Compton scattering cross section of the i^{th} element (in cm^2/atom),

$k_i(E)$ = pair production cross section of the i^{th} element (in cm^2/atom),

$\epsilon_i^{pe}(E)$ = average kinetic energy acquired by electrons ejected from atoms of the i^{th} element (in MeV); ($\epsilon_i^{pe} = E - E_B^i$ where E_B^i is the average binding energy of electrons in the i^{th} atom),

$\epsilon^{c}(E)$ = average kinetic energy transferred to electrons in the Compton scattering process (in MeV),

$\epsilon^{pp}(E)$ = average kinetic energy absorbed by the electron positron pair (in MeV) ($\epsilon^{pp} = E - 1.022$).

The summation extends over all types of element i in the target. The factor 1.602×10^{-8} converts MeV per gram to rads. Both ϵ^c and ϵ^{pp} have been taken independent of the kind of atom, because in the range of energies where these processes are important, the photon energy is much larger than the electronic binding energy. This is not necessarily true for the photoelectric process, where for some elements, both K and L-shell photoelectric processes may be important. In this case, an average binding energy $\bar{E}_B^i$ must be employed.

Figure 3-1 shows the relation between first collision dose in rad/ (photon . cm^{-2}) and the photon energy for soft tissue, bone, air, and carbon. An approximate expression for the first collision tissue dose-energy relationship is

$$D^{(\gamma)}(E) = 3.7 \times 10^{-9} \; E \text{ rad/(photon . } cm^{-2})$$

Where E is the photon energy in MeV. This equation is valid to ± 30% in the energy range .05 MeV $< E <$ 7 MeV. The ratios of the rad doses in bone, air, and carbon to that in tissue at various energies are given in Figure 3-2.

The salient aspects of these curves is easily understood. At low energies, the dominant interaction between photons and atoms results in photoelectric ejection of electrons. The cross section for this process increases very rapidly as the photon energy decreases and varies with Z, the atomic number of the atom, approximately as Z^n at a given photon energy. Here n is roughly 4 or 5. Thus in the energy range below $\sim$0.03 MeV, the first collision dose to bone is an order of magnitude larger than that to soft tissue because of the presence of relatively high-Z atoms in the former. At photon energies in the region 0.02 - 1 MeV, the dominant interaction is Compton scattering. Since the cross section for this process is proportional to the total number of electrons in a given atom and since the electronic density in most materials is approximately constant, one finds only minor differences in dose in this energy range. Similar considerations

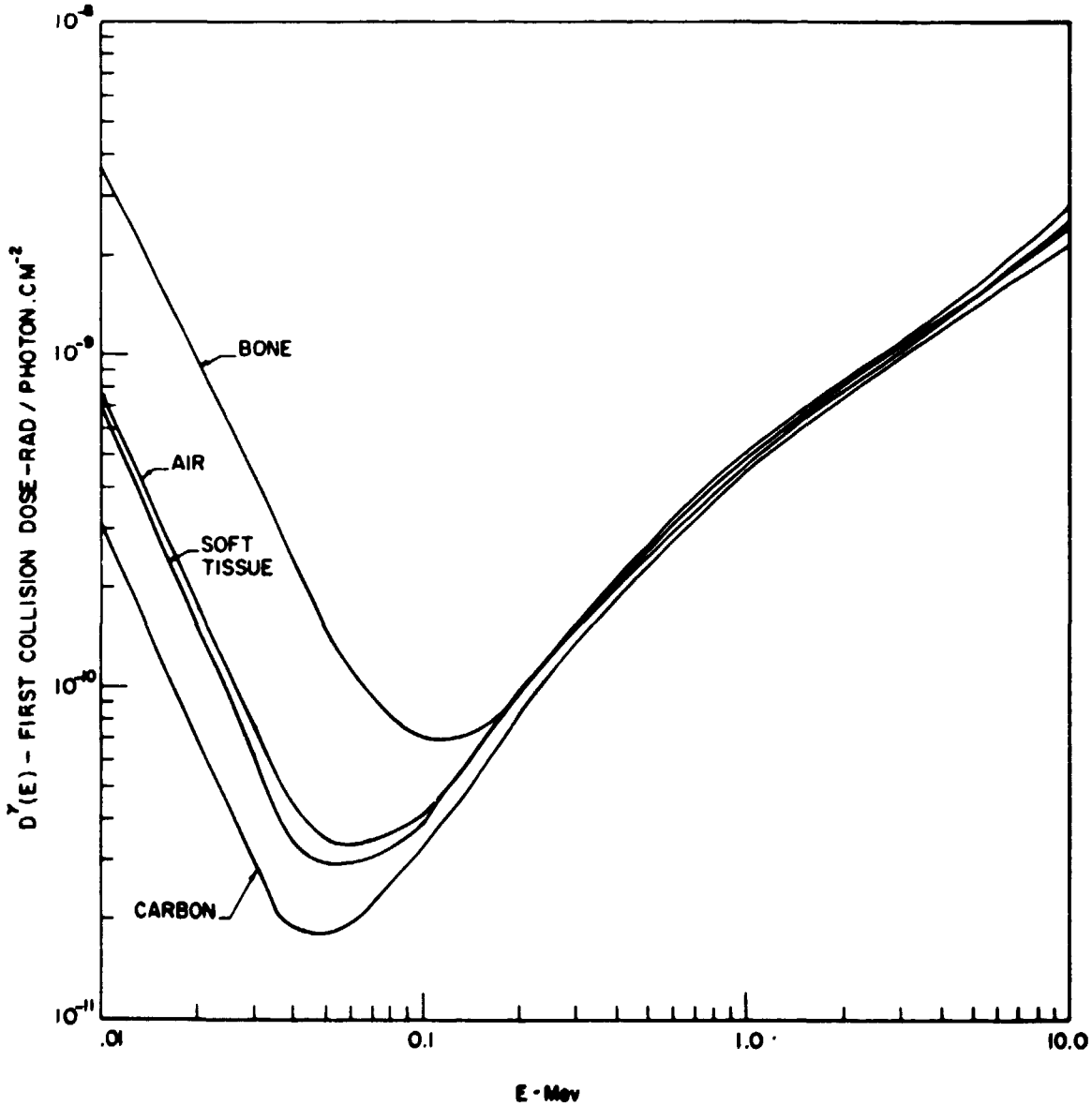

Figure 3-1

Variation with Gamma Ray Energy of the First-Collision Gamma Dose to Bone, Air, Soft Tissue and Carbon

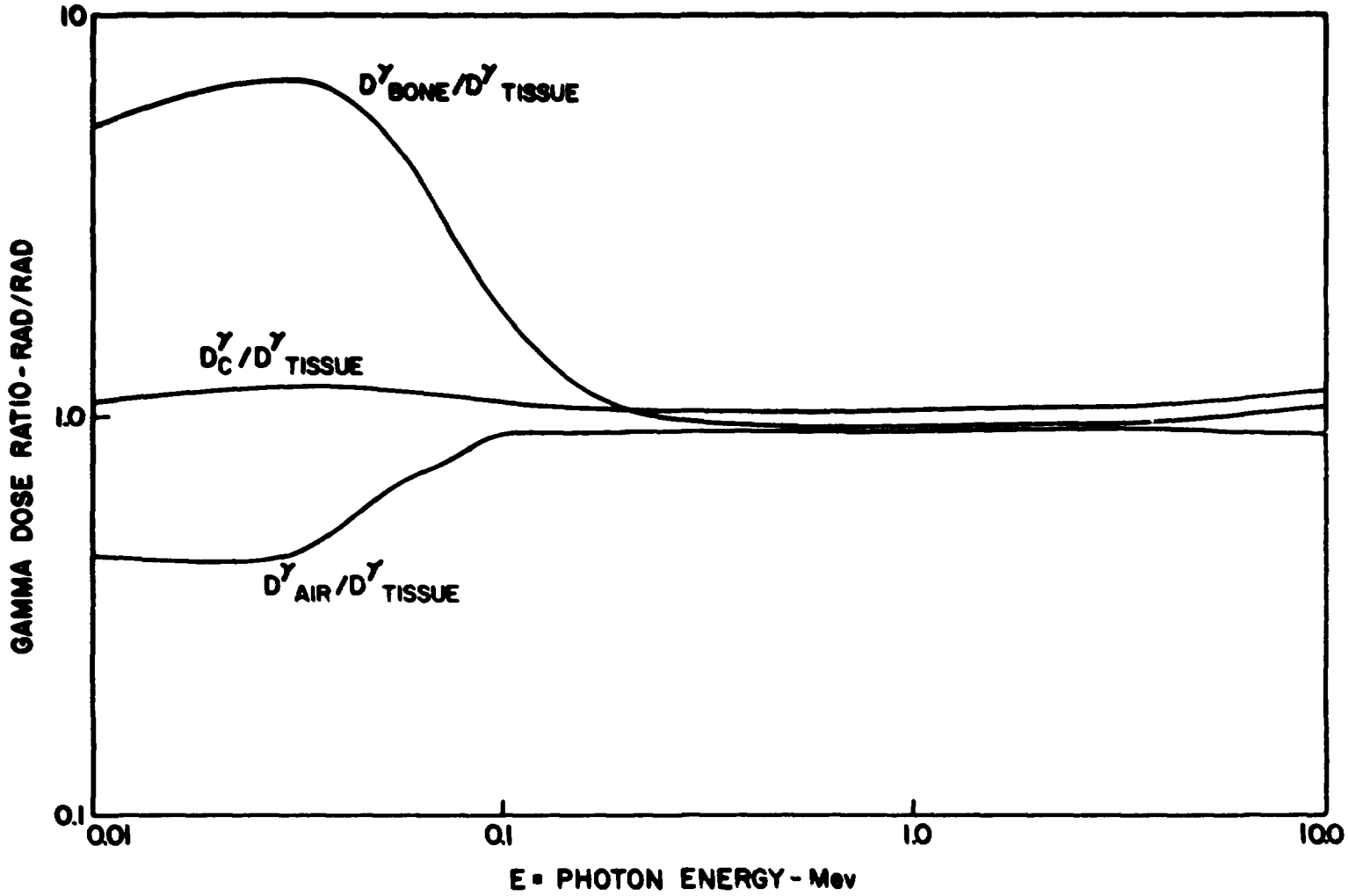

Figure 3-2

First-Collision Gamma Dose Ratios for Several Substances as a Function of Gamma-Ray Energy.

hold for higher energies where pair production becomes important

First Collision Dose for Neutrons

The first collision neutron dose $D^{(n)}$ imparted to a particular substance when irradiated by neutrons of energy E may be written

$$D^{(n)}(E) = 1.602 \times 10^{-8} \sum_i \sum_j N_i \sigma_{ij}(E) \bar{\epsilon}_{ij}(E)$$

where

N_i = number of nuclei of type i per gram of substance,

σ_{ij} = cross section of the i^{th} kind of nucleus for the reaction in which ionizing particles of type j are produced,

$\bar{\epsilon}_{ij}$ = average kinetic energy acquired by the j^{th} kind of ionizing secondary ejected in an interaction between a neutron and the i^{th} type of nucleus.

The averaging process used to obtain $\bar{\epsilon}_{ij}$ is understood to be carried out over all possible energies which the j^{th} kind of particle may acquire. In the simple case of elastic scattering which is isotropic in the center of mass system of the neutron and the struck nucleus, one has

$$\bar{\epsilon}_{ij}(E) = \frac{2mM_i}{(m + M_i)^2} E$$

where m and M_i are the masses of the neutron and the i^{th} kind of nucleus, respectively. This kind of elastic encounter obtains for the scatter of neutrons on hydrogen nuclei in the range $0 < E < 14$ MeV. When E becomes as small as a few eV, the chemical binding of hydrogen nuclei in molecules becomes important, and this relation is no longer valid. In the case of nuclei heavier than hydrogen anisotropic center of mass scattering sets in at considerably lower energies. In general, the larger M_i becomes, the more limited is the range of energies in which the above equation is valid. However, in substances rich in hydrogen, such as soft tissue, the first collision dose may be computed with the reasonable accuracy up to $\sim$ 10 MeV, using this equation to compute the energy imparted in elastic encounters with all nuclei. This is so because collisions of neutrons with H nuclei are responsible for most of the energy absorbed in this case. (See Figure 3.3.)

If elastic scattering is anisotropic in the center of mass system (sometimes called "forward" elastic scattering), one may write

$$\bar{\epsilon}_{ij}(E) = \frac{2mM_i}{(c + M_i)^2} [1 - f_1^{(i)}(E)] E$$

where the differential elastic scattering cross section of the i^{th} nucleus in center of mass coordinates is expanded as follows:

$$\sigma_i^e(E,\theta) = \frac{\sigma_{io}^e(E)}{4\pi} \sum_{\ell=0} (2\ell + 1) f_\ell^{(i)}(E) P_\ell(\cos\theta)$$

In this formula $\sigma_{io}^e(E)$ is the total elastic scattering cross section of the i^{th} nucleus ($f_o^{(i)} = 1$), $P_\ell(x)$ is the ℓ^{th} Legendre polynomial and θ is the scattering angle

If the neutrons induce a nuclear reaction of the i^{th} kind of nucleus in which a charged particle is emitted with reaction energy Q_{ij}, then

$$\epsilon_{ij}(E) = (E + Q_{ij})\, St(E + Q_{ij}),$$

where Q_{ij} may be either positive or negative, depending upon whether the reaction is exoergic or endoergic, and St(x) is the unit step function

For purposes of computing first collision dose, gamma rays emitted subsequent to inelastic neutron scattering on nuclei are not considered, since these are not absorbed locally.

Figure 3-3 shows the first collision dose (or kerma) to soft tissue as a function of neutron energy. Curve A includes contributions from 33 reactions which take place in tissue. The other curves show the relative contributions of certain types of interaction processes. Special note should be paid to curve B for hydrogen elastic collisions. One concludes, for neutrons above 100 eV, that the first collision dose to matter containing an appreciable atom number fraction of hydrogen may be computed with good accuracy considering only elastic scattering with hidrogen.

Figure 3-4 gives the first collision dose to CH_2, H_2O, bone and C. Isotropic center of mass scattering was assumed for the first three of these substance, while for carbon anisotropic scattering data were used. Figure 3-5 shows the ratio of CH_2 dose to soft tissue dose as a function of energy. Both doses are first-collision values computed assuming isotropic center of mass scattering for all elements. This ratio varies in an irregular way with energy, but the variations are rather narrow in width, and when averaged over a reasonably smooth spectrum of energies may be considered constant at ~ 1.45 to a good approximation for many purposes. CH_2 is important since it is used in the Hurst absolute fast neutron dosimeter which will be described in a subsequent lecture.

The Bragg-Gray Principle

Many effects of a biological and physical nature are related to the energy charged particles impart to matter, and measuring it is an ever present problem. A historically preferred method is to measure the ionization in a gas and infer from this measurement the energy absorbed in the surrounding medium. An estimate can also be made of the absorbed dose in other materials which might be placed in the same geometrical configuration. For instance, a measurement might be made of the ionization in an air cavity surrounded by an air equivalent wall, and this information used to infer the absorbed dose in a volume of tissue placed at the same position. A prescription for obtaining the dose to the walls of a small gas-filled cavity from ionization measured in the cavity is contained in the Bragg Gray Principle. This principle has assumed great practical importance in the design of gamma dosimeters.

The use of cavity ionization chambers for the measurement of x- and γ-ray dose was put on a firm basis by the careful work of Gray, who also considered the cavity chamber for the measurement of fast neutron dose. He showed that for a cavity chamber, the "Bragg-Gray" relation may be written

$$D^{(\gamma)} = WJS/100$$

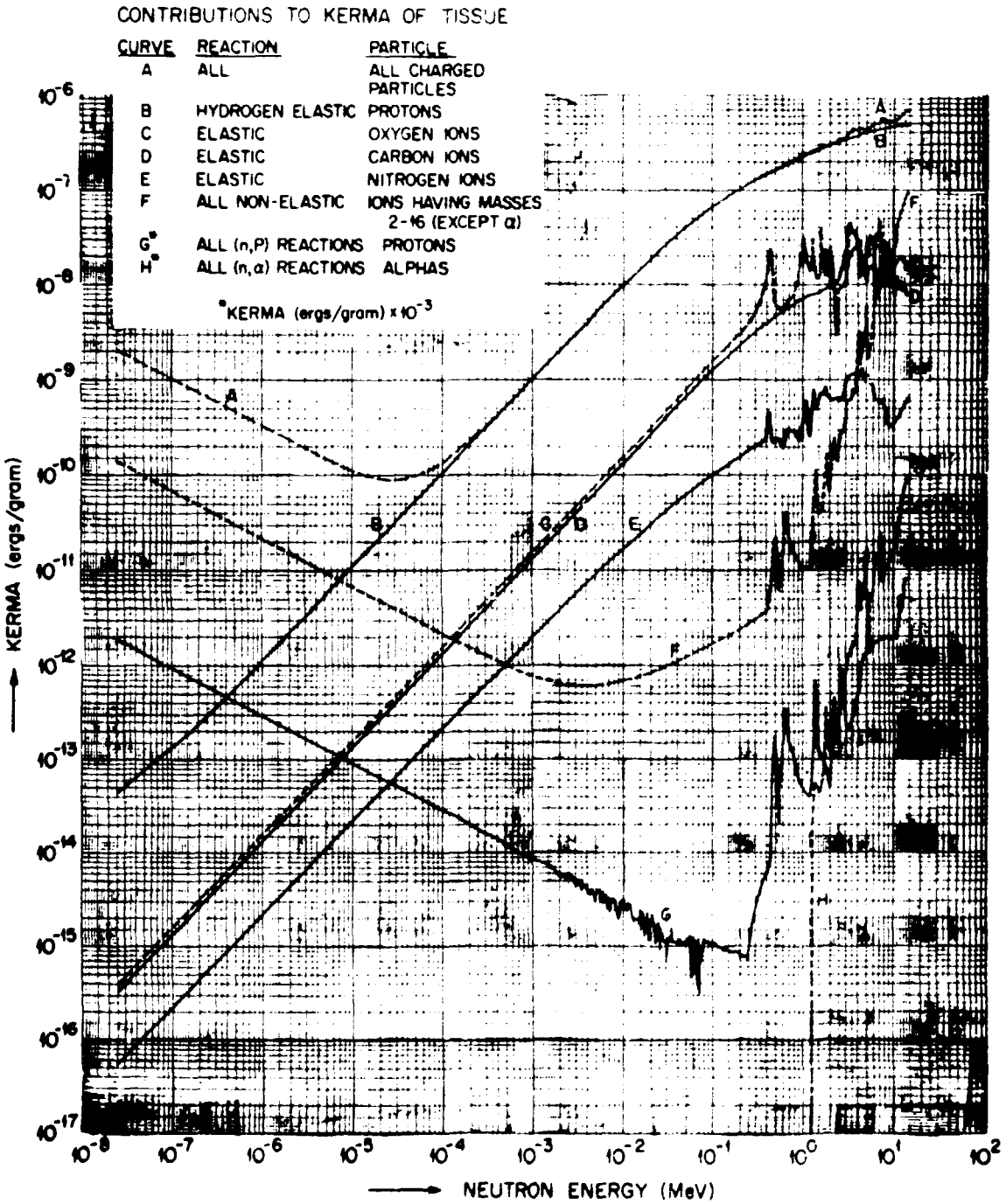

Figure 3 3

First Collision (Kerma) Neutron Dose to Soft Tissue as a Function of Neutron Energy

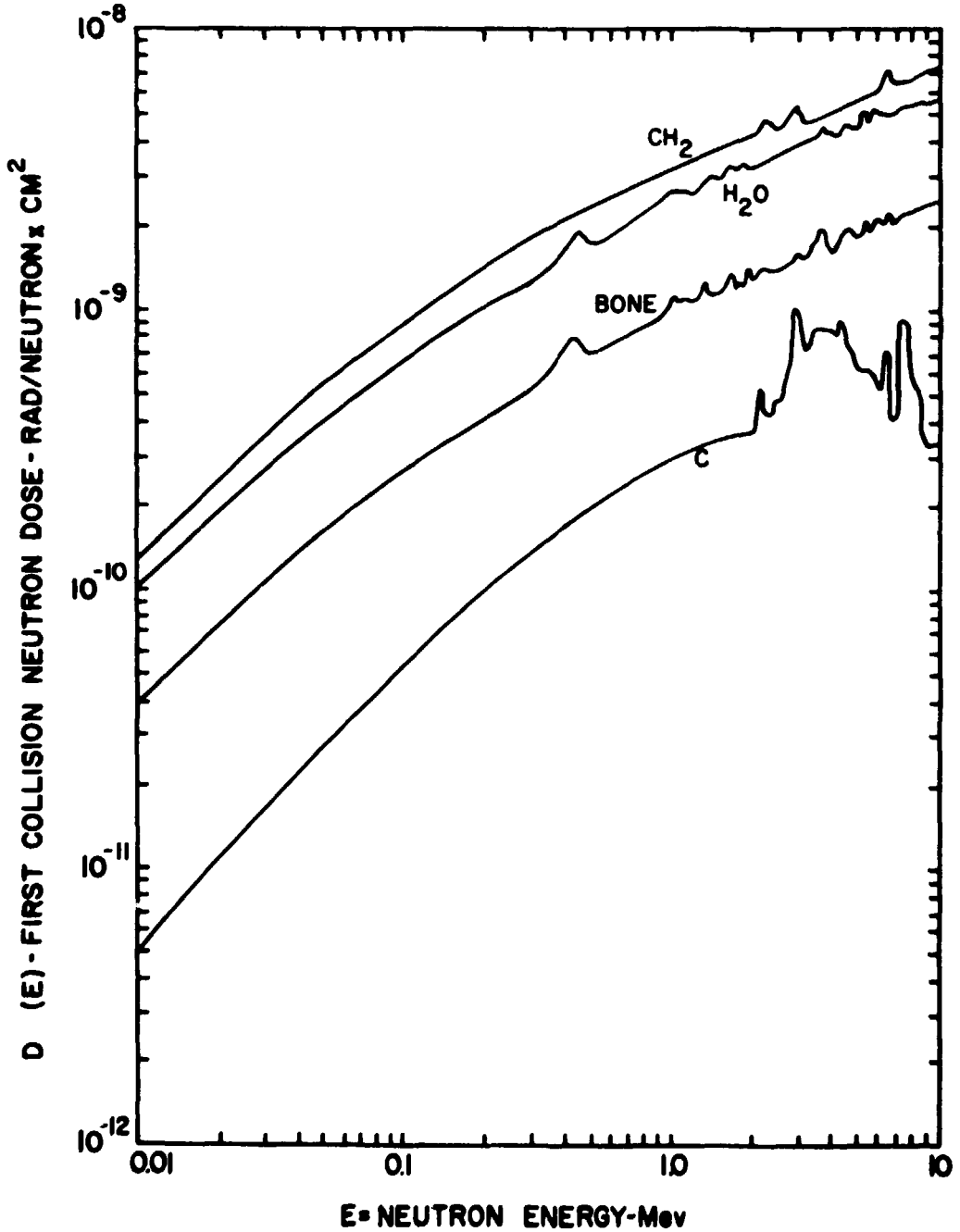

Figure 3-4

First Collision Neutron Dose to CH_2, H_2O, Bone and Carbon as a Function of Neutron Energy

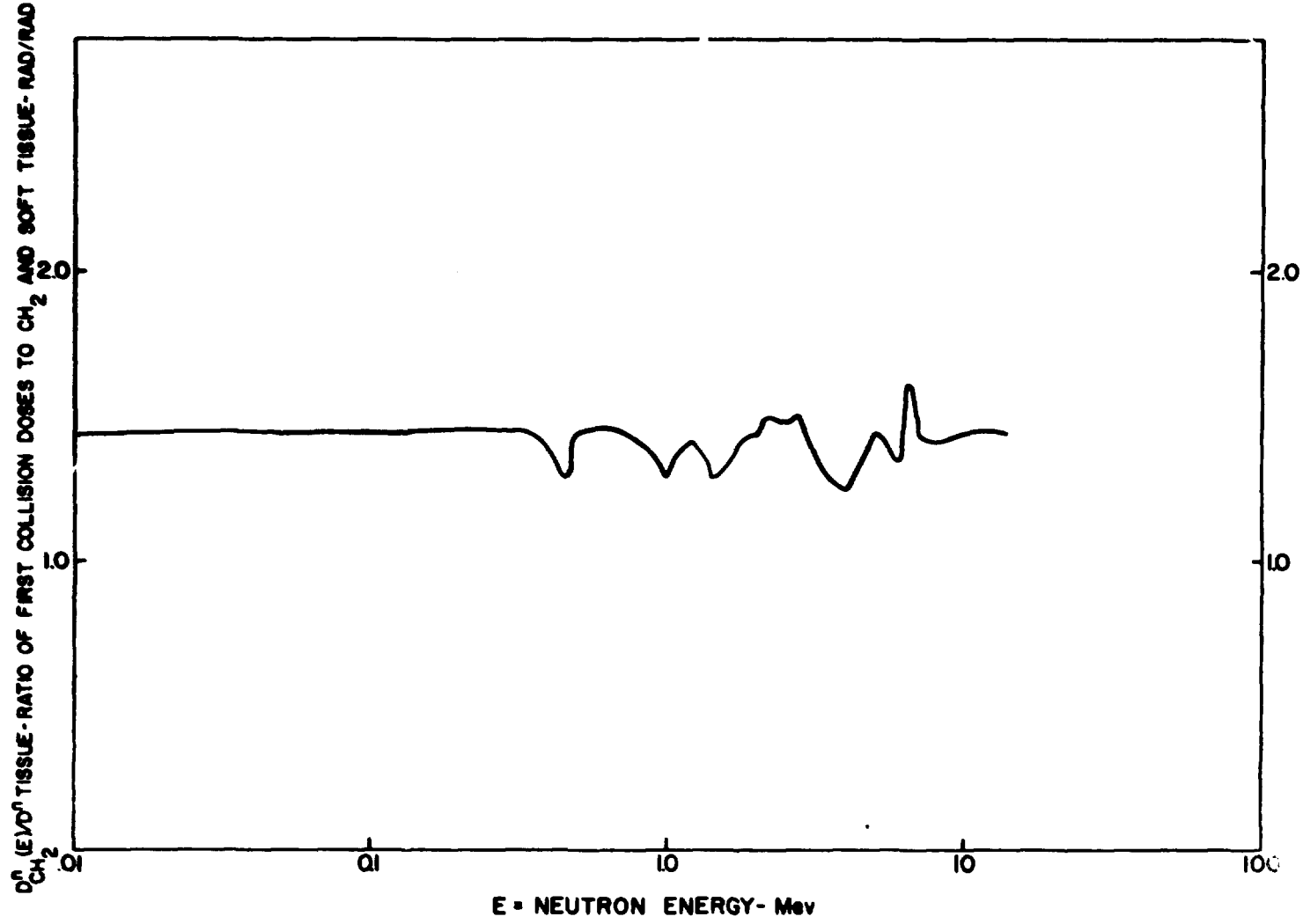

Figure 3-5

The Ratio of First Collision Neutron Dose in Ch_2 to that in Soft Tissue as a Function of Neutron Energy

where

$D^{(\gamma)}$ = dose to the wall in rad,

W = energy in ergs required to produce an ion pair in the gas contained in the cavity,

J = number of ion pairs formed per gram of the gas

S = mass stopping power of the wall material relative to that of the gas for the ionizing particles associated with the primary radiation.

Gray concluded from a detailed examination of data then available that W was a constant for electrons in air irrespective of their energy. The value he gave was 32.5 eV/ion pair while more recent data indicate that a value somewhat less than 34 eV is probably more nearly correct. The independence of electron energy seems valid for electrons of initial energies above $\sim$0.5 MeV. W for both electrons and α particles may vary rather markedly from one gas to another.

The original treatment of Gray assumed that S was the ratio of stopping power in the wall material relative to that in the gas and that S was not dependent upon energy. Laurence later made a natural extension of this treatment, taking S to be averaged over the spectrum of ionizing particles which cross the cavity. Other workers have considered the production of energetic delta rays in the cavity to obtain still another approximation to S. This consideration is commonly called the Spencer Attix extension of the Bragg Gray theory. It is found that where the gas and the cavity wall are reasonably close in atomic number, the use of an average S gives an excellent approximation for most purposes.

In order for the Bragg Gray relation to hold it is necessary(1) that the dimensions of the cavity be small compared with the range of the secondaries in the cavity and(2) that charged particle equilibrium shall obtain, i.e. that the wall thickness be greater than the range of the most energetic secondaries in the wall and small compared with the attenuation length of the primary radiation in the wall. If the cavity gas and wall material have the same atomic composition, the first requirement may be relaxed. In this case, neglecting the effect of chemical binding upon stopping power which is known to be small as long as the velocity of the secondaries is not too low, one may write $S = \rho$, where ρ is the ratio of the density of the wall material to that of the gas.

BIBLIOGRAPHY

1. K. Z. Morgan and J. E. Turner, *Principles of Radiation Protection*. John Wiley and Sons, Inc., New York, 1967.

2. F. H. Attix, W. C. Roesch, and E. Tochilin, *Radiation Dosimetry. Vol I*, Academic Press, New York, 1968.

3. *Physical Aspects of Irradiation*, National Bureau of Standards Handbook 85, March, 1964.

LECTURE Nº 4

DETECTION AND MEASUREMENT OF RADIATION

Introduction

It has long been known that radiation which has sufficient energy to ionize matter can damage living tissue. In fact, the earliest commonly used unit of radiation exposure dose, the roentgen, was defined in terms of the ionization produced in air. More recently, the trend has been to specify instead the absorbed dose measured in terms of the quantity of energy deposited by the radiation per unit of mass of irradiated material at the place of interest. Many of the practical devices employed in the determination of dose or dose rate depend upon an evaluation of the ionization produced in the detector by the radiation in question. In such instruments as ionization chambers and count-rate meters which employ gasfilled detectors, we are concerned with the quantity of ionization produced by the radiation and with the subsequent history of the electrons and gaseous ions produced for information leading to the dose or dose rate being measured. Ionization in gases and the behavior of the products of ionization in typical detectors will be the subjects of primary concern in this lecture.

Creation of Ions

Basic Ideas of Excitation and Ionization

When an ionizing particle traverses a gas, part of its energy is lost in ionizing the gas molecules, and part is lost in processes other than ionization. Hence, the number of ion pairs (electrons and positive ions) produced will always be less than the ratio of the energy lost by the ionizing particle and the ionization potential V_I of the gas. From the point of view of ion yield, a portion of the energy is wasted, since the ion yeld is the measurable quantity. The situation is simplified somewhat if attention is restricted, for the present, to ionizing particle velocities large compared to the Bohr orbit velocity ($v_o = e^2/H$). With this restriction, energy losses occur predominantly by direct impact between the particle and single orbital electrons of the gas and may be generally classified into three types:

(a) Excitation collisions in which the molecule is raised to a higher energy state, but in which ionization does not occur.

(b) Light ionizing collisions in which the energy lost is of the order of the ionization potential V_I of the gas.

(c) Violent collisions in which energetic secondary electrons, called delta rays, are produced.

Types (a) and (b) are most important from the standpoint of the total energy lost by the primary particle. Violent collisions are relatively rare and contribute little to the final total ionization; furthermore, the energetic secondary electrons dissipate their energy ultimately in collisions of the types (a) and (b). Since the relative numbers of excitation and light ionization collisions are practically independent of the nature and velocity of the primary particle, a constant amount of wasted energy, on the average, is associated with the formation of an ion

pair. Because of this constancy it has been found convenient to define the parameter W, the average energy lost per ion pair produced by

$$W = \frac{E}{N_w}$$

where E is the energy lost by the particle and N_w is the number of ion pairs formed. From the above arguments it follows that W will have a characteristic value for each gas but will be nearly independent of the nature and velocity of the primary particle for velocities appreciably greater than v_0.

W Values and Their Application to Dosimetry

Historically, the early indication of a direct proportionality between energy lost by an ionizing particle and the ionization produced in a gas together with the general application of gas-filled detectors to dosimetry measurements gave importance to accurate experimental determinations of W for various gases and different ionizing particles. Calculations of W are complex and have been made only for the simplest gases. A detailed calculation of W for atomic hydrogen using theoretical cross sections gave a value of 36 eV/ion pair compared with the measured value of 36.3 eV/ion pair for molecular hydrogen. Another calculation yielded a value of 43 eV/ion pair for helium in good agreement with experiment. Calculations for more complex gases have not yet been made.

The experimental determination of W for electrons has been the subject of investigations for more than 40 years. Various investigators have used beta rays, photons, and accelerated electron beams from heated filaments as sources ranging in energy from a few electron volts to more than 20 MeV. Measurements have been made in various types of ionization chambers, in proportional counters, in cloud chambers, and in calorimeters. While air has been the most frequently studied gas, all of the more common gases have been investigated by one technique or another. Much of the earlier work suffered from questionable gas purity, yet, considering the variety of techniques employed, the results are in rather good agreement.

Impurities

It was mentioned previously that early measurements of W were sometimes inaccurate due to impurities in the gas. This is particularly true of the noble gases and the measurements in helium best illustrate the large change in ionization efficiency which result from even trace amounts of other gases. Although early measurements gave values of W of about 30 eV/ion pair for He, theoretical calculations indicated that the value should be greater than 40 eV/ion pair. Using very carefully purified helium gas, Jesse and Sadauskis and Bortner and Hurst obtained experimental values of 42.7 and 46.0 eV/ion pair, respectively, and by the deliberate addition of small amounts of contaminant gases showed that the low values obtained earlier were due to impurities.

Mixtures

It is sometimes necessary to employ a mixture of two gases to achieve a desired operating characteristic of an ionization chamber or proportional counter. In this case the interpretation of data may require a knowledge of the effective W for the mixture. It has been found that an

effective value, W_{ij}, can be calculated for mixtures of several pairs of molecular gases using the empical equation

$$W_{ij} = (W_i - W_j) Z_{ij} + W_j$$

where

$$Z_{ij} = \frac{P_i}{P_i + (\frac{f_j}{f_i})P_j}$$

Here W_i and W_j are the W-values of the pure constituent gases present in the mixture at partial pressures P_i and P_j, respectively. The quantities f_i and f_j are empirical constants tabulated in Table 4-1 for various gases.

TABLE 4-1

Constants for Calculation of W_{ij} for Certain Binary Mixtures of Gases

Gas	f_i or f_j	Gas	f_i or f_j
H_2	0.5	CH_4	1.8
N_2	1.0	C_2H_2	3.3
O_2	1.3	C_2H_4	3.4
CO_2	1.8	C_2H_6	3.5

DC Measurement of Ionization

Recombination and Electron Capture

The electrons and positive ions formed in a gas during ionization may be partially or totally lost to obsevation by recombining with each other. If the gas is electronegative or is a mixture containing electronegative components, recombination may be preceded by electron capture to form negative ions. One classification of the mechanisms by which recombination occurs is based on the possible schemes by which the excess energy of the system may be disposed of. Another classification is based on the past history of the ions:

(a) Preferential recombination between the positive ion and the negative ion (or electron) from which it was originally separeted.

(b) Columnar recombination between positive ions and negative ions (or electron) distributed along the track of the ionizing particle.

(c) Volume recombination between positive ions and negative ions (or electrons) from the tracks of different particles.

Preferential recombination in nonelectronegative gases results when the liberated electron suffers a collision very close to its point of liberation and is scattered to the neighborhood of the parent ion. In electronegative gases, the electron may be captured very close to its point of

liberation to form a negative ion which will then combine with the parent positive ion. Except in electronegative gases at high pressures, preferential recombination is quite improbable. Columnar recombination, on the other hand, is a common process and becomes particularly important in an ionization chamber containing electronegative gases. Volume recombination may be important in DC chambers operated in high intensity radiation fields.

Electrometer Response and Sensitivity

Information about the total amount of ionization produced in an ionization chamber can be obtained by DC measurements of the current resulting from the motion of the electrons and ions through the chamber gas under the action of the applied electric field. These small currents, typically from 10^{-14} to 10^{-8} amperes are most conveniently measured by electrometers of the vacuum tube, vibrating capacitor or quartz fiber types. The two methods of current measurement are known as the IR drop method and the rate of drift method.

In Figure 4-1, C includes the capacitance of the chamber, the connectors, and of any capacitor added to provide a more convenient operating range. The shorting switch, S_2, is used to protect the electrometer from surges due to the connection of the battery to the circuit and to discharge of C at the beginning of a measurement. When the applied potential is sufficient to collect the electrons and ions in the chamber, the magnitude of the resulting current I is proportional to the rate of ion production and, hence, to the intensity of the radiation field. When S_2 is open and S_1 closed, this current flows to the RC network resulting in a potential across the electrometer given by

$$V(t) = IR(1 - e^{-t/RC})$$

where t is the time measured from the moment of switching. The limiting, steady rate value of V(t) is

$$V = IR$$

If R is known, a measurement of V yields the value of the current I. If both S_1 and S_2 are opened at the start of a measurement, the flow of the constant current I into C results in a change of potential across the electrometer with time given by

$$\frac{\Delta V}{\Delta t} = \frac{I}{C}$$

In this rate of drift method, the current is determined from the measured value of $\frac{\Delta V}{\Delta t}$ and a knowledge of the value of C.

Most investigators prefer the rate of drift method because of the difficulty in making accurate determinations of the high values of R and the relatively long response time resulting from the use of high resistances in the measurements of small currents. This latter objection is overcome by the use of feedback circuits in most electrometers.

In many DC measurements involving ionization chambers, it is important only that the pressure of the chamber gas and the applied electric field remain constant in order that the measured current be proportional to the intensity of the radiation field. However, in laboratory

investigations, it is frequently necessary to know that the measured current accurately represents the total collection of all ions produced in the chamber. In nonelectronegative gases at relatively low pressures, this condition of saturation can be assured by increasing the applied field until the measured current becomes constant. However, in electronegative gases and in mixtures containing electronegative gases, and particularly at higher pressures, it is doubtful that true saturation is ever achieved, due to capture and recombination.

In recent years, improvements in design of vacuum tube electrometers make these the most convenient and satisfactory instruments for the measurement of currents in the range of 10^{-6} to 10^{-13} amperes. Below 10^{-13} amperes, the currents and the fluctuations in the currents that flow into or out of the grid of the input tube, even when no signal is present, limit their usefulness. Quartz-fiber and vibrating capacitor electrometers may have quite high sensitivities and are preferred for the measurement of currents below 10^{-13} amperes. These types have the added advantages of exceptional stability and freedom from drift, but suffer in comparison with the vacuum tube electrometers in most other respects

Chamber Design and Construction

Ionization chambers are of so many types, depending on the intended application, that only the most general design and construction features will be considered here. The simple parallel plate chamber shown in Figure 4 2 will be used to illustrate some of these features This chamber was designed for the measurement of W values, using an alpha particle ionization source.

The body of the chamber and the electrodes is made of stainless steel* with Heliarc welded joints. The electrodes are circular metal plates, and the collector electrode is surrounded with a guard-ring as is customary, to minimize edge effects. Neoprene and silicone O-rings are used as gaskets to seal the chamber cover and connector to the collector electrode. Fluorothene insulators support the collector electrodes, and teflon is used as an insulator in the high voltage connector assembly and in the connector to the collector plate. Both are excellent insulators, and fluorothene, because of its better mechanical properties, is preferable in applications requiring machining. The high voltage is connected through a modified porcelain stand-off insulator; Kovar glass and Kovar porcelain lead-throughs are frequently used. A smooth finish on all surfaces is desirable and is essential on the surfaces which will be at high voltages. Before assembly, all surfaces are thoroughly cleaned with dilute acids or other suitable agents, carefully rinsed with distilled water and acetone or alcohol, and then thoroughly dried

Commercial laboratory gases have been improved in purity sufficiently in recent years to make the problem of gas purification less serious than it was earlier. In chambers operated at high pressures, it is still important to insure the removal of electronegative contaminants such as oxygen; the removal of molecular gases from chamber filling of the noble gases is essential for reliable operation. Electronegative contaminants can be effectively removed from most gases by circulation through calcium tyrnings heated to 300°C or uranium turnings heated to 200°C**. Helium is purified by passage through a charcoal trap cooled to liquid nitrogen temperatures and molecular gases, as well as other noble gases, can be effectively removed from argon by multistage distillation using liquid-nitrogen cooled traps.

*Brass and aluminum are frequently used in the construction of these components.

**Special care must be exercised if hydrogen is circulated through heated uranium turnings because of the large quantities of heat liberated in the reaction.

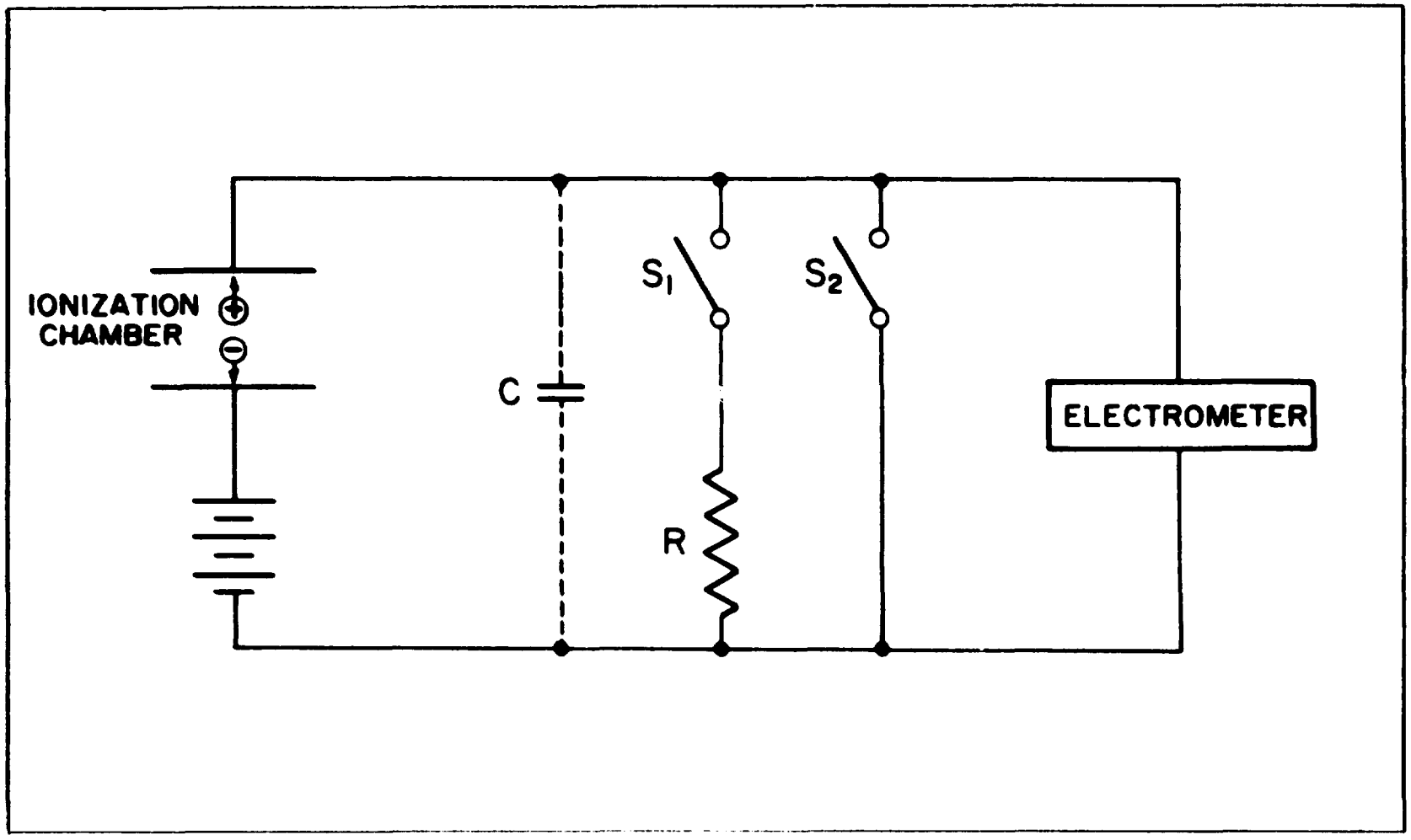

Figure 4-1

Ionization Chamber Connections to Illustrate the IR and Drift Methods of Measuring Current.

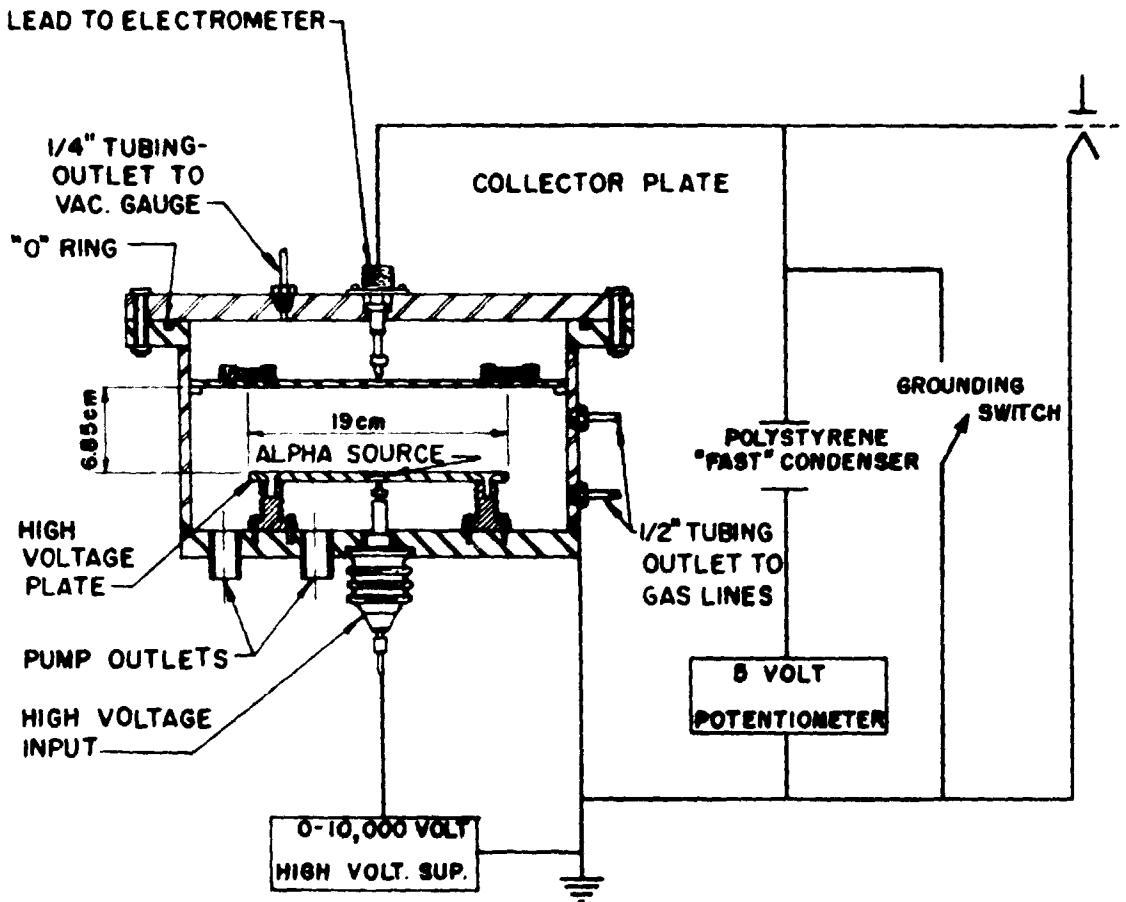

Figure 4 2

Ionization Chamber and Electrical Circuit for Measuring W for Alpha Particles

Pulse Ionization Chambers

Whereas DC measurements utilizing ionization chambers give information only about the total ionization produced in the chamber, pulse measurements permit the determinations of the disintegration rate and energy spectrum of the radiation source as well. However, proper interpretation of the results obtained from such measurements requires some understanding of the behavior of electrons and ions in gases, under the action of applied electric fields, and of the mechanism of pulse formation and amplication.

Proportional Counters

The Amplification Process

Proportional counters are usually made in the form of an outer cylinder of radius b with a thin coaxial center wire of radius a and filled with an appropriate gas to a pressure ranging from a few millimeters of mercury to a few atmospheres. In the most common mode of operation, the center wire is maintained at a positive potential with respect to the grounded outer cylinder. The ratio b/a might have a value from 50 to 1000. Since the electric field in such a cylindrical geometry is given by

$$E(r) = \frac{V_o}{r \ln (b/a)},$$

it is seen that the field in the vicinity of the center wire will become quite large. As a result, electrons moving toward the collector are able to acquire, between successive collisions with the gas molecules, an energy equal to or greater than the ionization potential of the gas. Each primary electron will then, in the course of its motion toward the collector, lead to an avalanche of charge as the secondary electrons, in turn, produce further ionization. Hence, if there are N_o ionization electron liberated by the ionizing particle, there will be a total of $2^n N_o$ electrons arriving at the collector, corresponding to n ionizing collisions in the cascade process for each primary electron. The factor 2^n is called the gas amplification. A true proportional counter will give an output voltage signal proportional to N_o, and there is a somewhat limited range of operating voltages for which any counter is truly proportional. If the gas amplification is less than about 10, the statistical variation in the sizes of the avalanches produced will lead to poor resolution. If the total ionization is sufficiently large, or sufficiently concentrated in space, that the avalanches from individual primary electrons interact appreciably with each other, true proportionality will be lost. Values of gas amplification up to 10^4 can be obtained in a properly designed counter without great difficulty.

Counter Construction

If proportional counters are to be used as spectrometers with good resolution, it is important to exercise special care in their construction. Since they are usually operated with static gas fillings, it is important to have high purity gas initially and to clean all surfaces carefully to avoid electronegative gas contaminants from outgassing in continued operation. The center wire should be as smooth as possible to avoid spurious discharges and should be carefully centered for improved resolution. Because of the small output signals, it is important

that insulators for the center wire and in the plugs of the high voltage connections be of high quality to avoid leakage noise in the amplified output. A special counter developed for application in fast neutron dosimetry will be discussed in a later lecture. However, a few words concerning the counter construction seem appropriate here. To make it satisfy the requirements of a Bragg Gray cavity, it is lined with polyethylene and filled with ethylene gas. An internal alpha particle source is provided for calibration. The high voltage lead is a Kovar metal-glass seal, and it is fitted with field tubes, after the manner of Cockcroft and Curran, to eliminate end effects and determine the active volume of the instrument. In this arrangement, the potential of the same field tube is adjusted to the potential of the same radial position in the gas at the center of the counter length resulting in radial electric field liner over the region of the counter between the ends of the field tubes. The large diameter of the field tubes prevents any gas multiplication resulting from radiation in the region from the end of the counter shell to the end of the field tube and thus defines the active volume of the counter.

Geiger-Müller Counters

If a gas filled counter is operated at voltages appreciably above those appropriate for the proportional mode of operation described in the previous section, the process of gas multiplication will proceed as before, but proportionality between promary ionization and amplitude of signal from the counter will be lost due to interactions between the avalanches from separate primary electrons. For operating voltages sufficient to produce gas amplifications above about 10^6, the mechanisms of avalanche formation and discharge termination lead to counter performance characterized as Geiger Müller operation. In this mode of operation, the initial avalanche due to even a single primary electron is followed by a succession of avalanches, propagated probably through photon emission by the excited atoms, molecules, and ions in the avalanche. In counters containing pure gases, the photons may produce photoelectrons at the counter wall to initiate further avalanches; in self quenching counters containing appropriate gas mixtures, the photoelectrons come principally from the gas. The result is a discharge which ultimately produces a positive ion sheath along the entire length of the collector. Multiple discharges due to the interaction of the positive ions with the counter wall are prevented in two general ways. In counters containing pure gases, the discharge is terminated by resistance or electronic quenching circuits which lower the applied potential below that necessary to sustain the discharge. In self-quenching counters containing mixtures of gases and organic vapors such as alcohol or ether, or one of the halogens, the discharge is quenched by the absorption of the excess energy in the dissociation of the molecules of the contaminant. In counters containing organic quenching agents, the dissociated molecules do not recombine, and the typical counter has a maximum lifetime of about 10^{10} counts corresponding to the depletion of the quenching agent. In halogen-quenched counters, there is appreciable recombination of the dissociated molecules resulting in much longer lifetimes.

The Geiger-Müller counter is used primarily to give a counting rate proportional to the intensity of the radiation field. In such application, the counting efficiency will depend on the counter construction and on the nature and energy of the radiation. However, it has several advantageous characteristics that will probably result in its continued use in survey monitoring applications. Since the output pulse of the counter is of the order of one volt, there is need for little, if any, amplification. The typically long plateau of 300 volts or more in which the counting rate is constant does not require great stability in the high voltage supply, and the high sensitivity, variety of chapes and windows, simplicity, and low cost all contribute to its

continued popularity.

By the proper choice of window or wall materials and thicknesses, uniqueness of response to a particular type or energy of radiation may be emphasized. Such a special arrangement is the Phil dosimeter developed at ORNL where a small halogen-quenched counter shielded with a lead and tin combination has been used to make an instrument which is energy independent for photon energy above 150 keV and which is insensitive to neutrons.

BIBLIOGRAPHY

1. K. Z. Morgan and J. E. Turner, *Principles of Radiation Protection,* John Wiley and Sons, Inc., New York, 1967.

2. W. J. Price, *Nuclear Radiation Detection,* McGraw-Hill Book Co., New York, 1964.

3. F. H. Attix and W. C. Roesch, *Radiation Dosimetry, Vol. II,* Instrumentation, Academic Press, New York, 1966.

LECTURE N° 5

MIXED RADIATION DOSIMETRY

Introduction

This chapter will not attempt to cover all methods of dosimetry based on the ionization method. Instead, a selected set of examples will be chosen, the choices being dictated by two criteria: (1) The methods chosen will be most representative of the fundamental approaches to the utilization of the ionization method to measure mixtures of neutrons and radiation, and (2) the methods chosen are those which find most general application to radiation shielding, radiation biology, and radiation protection. Methods which are restricted mainly to radiation protection work (e.g., survey meters and personnel monitors) will be discussed in a later lecture.

Ionization Methods

It was shown that ionization methods are well adapted to the problem of measuring the energy absorbed per gram of a material enclosing a sensitive volume. That is, the response, I, of a chamber in which the total amount of ionization is collected may be expressed as

$$I = \sum_{\ell} \int_{0}^{\infty} \frac{\epsilon_{\ell}}{W(\epsilon_{\ell})} \, n_{\ell\beta}(\epsilon_{\ell}, E) d\epsilon_{\ell} \tag{5-1}$$

where $W(\epsilon_{\ell})$ is the energy required for a particle of type ℓ at energy ϵ to produce a pair of ions and $n_{\ell\beta}(\epsilon_{\ell},E)d\epsilon_{\ell}$ is the number of interaction products of type ℓ which dissipate an amount of energy in the range of energies between ϵ_{ℓ} and $(\epsilon_{\ell} + d\epsilon_{\ell})$. It also has been assumed that all ion pairs are collected. To the extent that W is independent of particle type ℓ and energy loss ϵ_{ℓ}, the above equation may be writen as

$$I = \frac{\epsilon_T}{W} \tag{5-2}$$

where ϵ_T is the total energy absorbed in the gas. It is also known that W is a slowly varying function of particle type and energy. Therefore, the total ionization current provides a fairly accurate measurement of the energy absorbed in the gas.

The energy absorbed in the gas may be used to determine the energy absorbed per gram of the material surrounding the gas cavity provided that the conditions stated in connection with the Bragg-Gray principle hold. Such arrangements of gas and solid material usually result in a detector which is too large to serve as a radiation probe*. However, the use of such detectors leads to results which may be interpreted to obtain approximately the absorbed dose in some gases and approximately the first collision dose in other gases. In either case, an additional requirement must be imposed on the kind of materials making up the detector if it is desired to measure the dose in another medium (e.g., tissue) over a range of radiation energies. This requirement may be expressed in the mathematical form

$$\left[\frac{D_{1m}(E)}{D_{1d}(E)}\right]_{E_1}^{E_2} = a(1 \pm \Delta) \tag{5-3}$$

---

* A radiation probe is defined as a device which is small enough to measure the absorbed dose at an arbitrary point in a medium without perturbing the radiation field.

where $D_{1m}(E)$ and $D_{1d}(E)$ are the first collision doses in the medium of interest and in the detector materials, respectively; a is a constant of proportionality, and Δ is the error which may be tolerated over the energy range $E_1 \leq E \leq E_2$

Ionization Chambers for the Measurement of Gamma Radiation

An example of an ionization chamber designed to measure the dose due to gamma radiation is shown in Figure 5 1 The design follows the Bragg Gray principle; the sensitive volume (50 cm^3 in this case) is filled with CO_2 gas and is surrounded with graphite walls. The condition expressed by the above equation may be examined by calculating the first collision dose in carbon and in tissue as a function of photon energy Following the procedures outlined in Lecture 3, the dose curves for carbon and for tissue are obtained The ratio of first collision doses, evaluated from the curves in Figure 3 1, is

$$\left.\frac{D_{1t}}{D_{1c}}\right|_{\substack{E_2 = 5\ MeV \\ E_1 = 0\ 2\ MeV}} = 1\ 1\ (1 \pm 0\ 05) \qquad (5\ 4)$$

Thus, it is seen that for photons in the energy range from 0 2 MeV to 5 MeV carbon is 'tissue-equivalent' provided that an error of 5% can be tolerated

The approximate gamma ray sensitivity of the ionization chamber shown in Figure 5 1 can be calculated from the definition of the roentgen and a few simplifying assumptions. From the definition of the roentgen (r) (Lecture 2), it is known that 1r of x or gamma radiation will produce in 0 00129 gram of dry air 1 esu or $3\ 33 \times 10^{-10}$ coulomb of charge

We assume (a) that the actual chamber may be approximated by a continuous carbon medium, (b) that charged particle equilibrium can be established with negligible attenuation or scattering of primary radiation, and (c) that all the ion pairs are collected. Under these conditions, we may write

$$I = 3.33 \times 10^{-10} \frac{D_{1a}}{D_{1c}} \times \frac{W_a}{W_g} \times \frac{m_g}{0\ 00129}\, r \qquad (5\text{-}5)$$

where I is the ionization current in amperes D_{1a}/D_{1c} is the ratio of the first collision dose in air and in carbon, W_a and W_g are the W values (eV/ion pair) for electrons in air and in the gas, respectively, m_g is the mass of the gas (in grams) in the sensitive volume, and r is the dose rate in roentgens per second The ratio D_{1a}/D_{1c} may be calculated by the method given in Lecture 3 and the ratio W_a/W_g for various gases may be obtained from date given in a number of testbooks.

Evaluation of this equation shows that for a chamber with a volume of 100 cc, containing gas at atmospheric pressure, the ionization current corresponding to a dose rate of 1 r per hour is of the order of 10^{-11} amperes. Even simple electrometers, particularly when used as null indicators in a rate of drift method, can measure currents on the order of 10^{-14} amperes Thus, ionization chambers of reasonable volume can be used to measure dose rates as low as 0 1 mr/hr. Vibrating reed type electrometers may be used to increase the sensitivity by another factor of 10 to 100.

The most serious limitation of the carbon CO_2 chamber to the measurement of gamma dose arises out of its response to neutrons The walls and gases of ionization chambers suitable

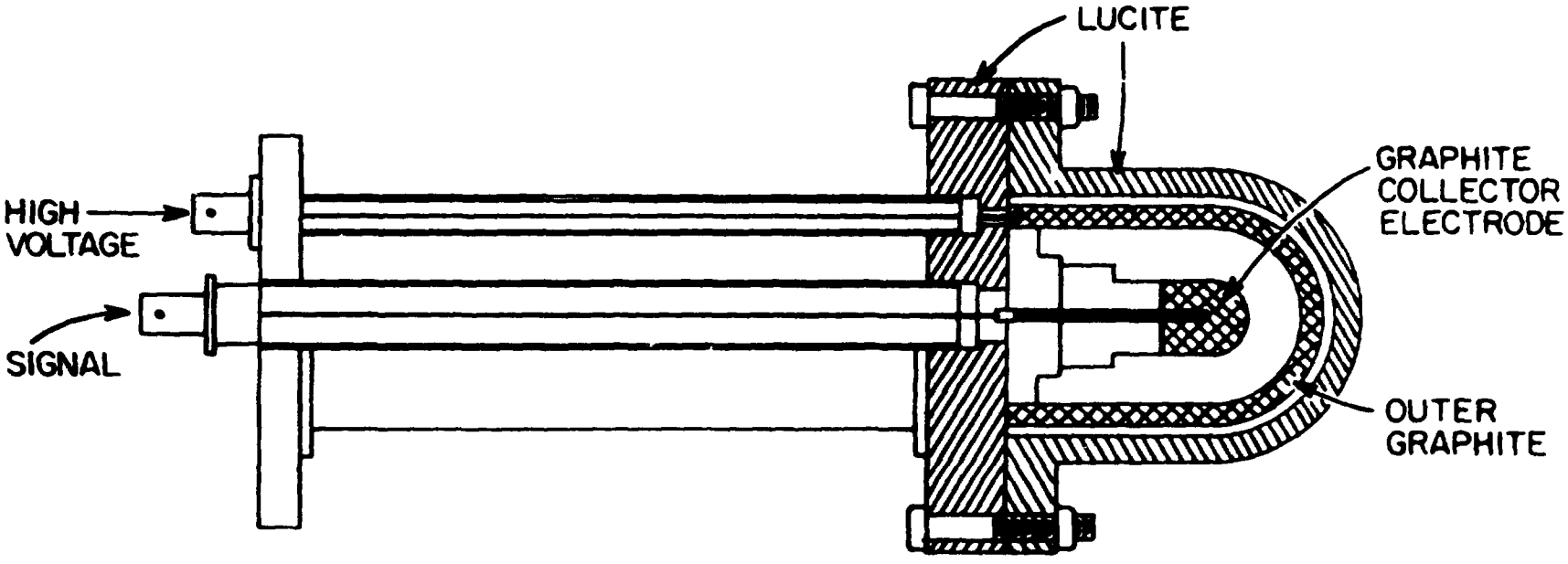

Figure 5-1

An Ionization Chamber for Gamma-Ray Dose Measurements

for dosimeters of X or gamma radiation must be made of materials having low atomic weights; otherwise, the conditions of Equation 5-4 would not hold over a wide range of energy. Fast neutrons, on colliding with low atomic weight materials, impart appreciable energy. It follows that the average fraction F_c of energy imparted per elastic collision, assuming isotropic center-of-mass scattering, is $2M/(M+1)^2$ where M is the atomic mass number of the recoil atom. For the purpose of illustration, we approximate the C-CO_2 with a carbon wall and a hypothetical carbon gas and calculate the neutron response of such a chamber. Let P(E) be the neutron response, defined as

$$P(E) = E_n/E_\gamma \tag{5-6}$$

where E_n is the amount of energy absorbed by 1 gram of carbon atoms for 1 tissue rad of incident fast neutrons, and E_γ is the amount of energy absorbed by 1 gram of carbon for 1 r of gamma radiation. The quantity E_n may be expressed as

$$E_n = n N_c \sigma_c(E) F_c E \tag{5-7}$$

where n is the number of neutrons per cm^2 in 1 tissue rad of fast neutrons, N_c is the number of carbon atoms in a gram, $\sigma_c(E)$ is the carbon scattering cross section for neutrons of energy E. Evaluation of P based on tabulated neutron cross sections gives the results shown in Table 5-1.

TABLE 5 - 1

Variation of P with Neutron Energy E

E(MeV)	P(%)
0.1	10.9
0.5	14.9
1.0	14.9
2.0	14.5
3.0	15.1
4.0	24.7
5.0	16.8
10.0	34.1
20.0	48.7

If the W value for carbon atoms in CO_2 were set equal to the W value for electrons in CO_2, the results in Table 5-1 would be satisfatory estimates of the neutron response of the C-CO_2 chamber. Actually W for carbon recoils is poorly known at present, and the results are perhaps too large by as much as a factor of 2 at some energies. However, it must be concluded that a C-CO_2 chamber may grossly overestimate the gamma dose when fast neutrons are present.

Tissue-Equivalent Ionization Chambers

Ionization chambers may be constructed such that the atomic composition of the materials making up the walls and gas of the chamber are essentially the same as the atomic composition of tissue. In this case, one expects that, except for possible differences in the W of

the gas for heavy particles compared to electrons, the ionization current will be proportional to the combined rate of energy absorption due to neutrons and gamma ray interactions with tissue.

For most applications, tissue can be approximated with a plastic having the following composition by weight: hydrogen (10.1%), nitrogen (3.5%), carbon and traces of oxygen (86.4%). This material differs in atomic composition from tissue mainly in that oxygen is replaced with carbon. In the energy range from 0.5 MeV to 14 MeV, the error in the neutron dose resulting from this substitution is less than 6%. A tissue equivalent gas mixture which is normally used with the above tissue equivalent plastic is, in terms of percentage partial pressure: methane (64.4), carbon dioxide (32.4), and nitrogen (3.2). If more precise results are required, it is possible to construct chambers lined with tissue-equivalent gels matching a tissue compositon ($C_5H_{40}O_{18}N$) exactly.

Figures 5-2 and 5-3 show two designs of tissue equivalent ionization chambers which have been put to extensive use throughout the word. Various other designs have been developed and altogether the tissue equivalent chamber is a very useful instrument which has found much application in radiobiology and radiation protection. The sensitivity considerations given for the gamma ionization chamber (Equation 5-5) apply with minor modification to the tissue equivalent ionization chambers.

Combined Chambers for the Dosimetry of Mixtures of Neutrons and Gamma Radiation

Consider now the simultaneous use of the tissue equivalent chamber and a teflon-CO_2 chamber in a radiation field consisting of neutrons and gamma radiation. When the tissue chamber is exposed to 1 r of hard X or gamma radiation, the absorbed dose is approximately 0.97 rad. A neutron dose of 1.03 rads in tissue will produce approximately the same amount of charge as the 1 r of gamma radiation, the larger neutron dose being due to the difference in W. The teflon CO_2 chamber absorbs about 0.97 rads for 1 r of gamma radiation, but when exposed to 1 tissue rad of neutrons, the reading, $\overline{K(E)}$, for a given neutron energy spectrum is much less than the reading produced by 1 r of gamma radiation. Thus, the readings of the tissue-equivalent chamber and the teflon CO_2 chamber, R_T and R_c, respectively, will be given by

$$R_T = \frac{D_n}{1.03} + \frac{D_\gamma}{0.97} = 0.97\, D_n + 1.03\, D_\gamma$$

$$R_c = \overline{K(E)}\, D_n + \frac{D_\gamma}{0.97} = \overline{K(E)}\, D_n + 1.03\, D_\gamma \qquad (5\text{-}8)$$

where D_n and D_γ are the neutron and gamma tissue doses in rads. The quantity $\overline{K(E)}$ may be calculated with equations analagous to Equations 5-6 and 5-7. Table 5-2 shows some values of K(E) as determined by calculation and by experiment.

Solution of Equation 5-8 gives the components D_n and D_γ provided that enough is known about the neutron energy spectrum to allow a reasonable average value, $\overline{K(E)}$, to be selected. If the neutron energy is not known, we may set $\overline{K(E)} = 0.16 \pm 0.08$ over the energy range from 0.5 MeV to 8 MeV. Lack of precise information on $\overline{K(E)}$ results in an error of the order of 10% in D_n, independent of R_T and R_c and, hence, independent of D_n/D_γ, but may

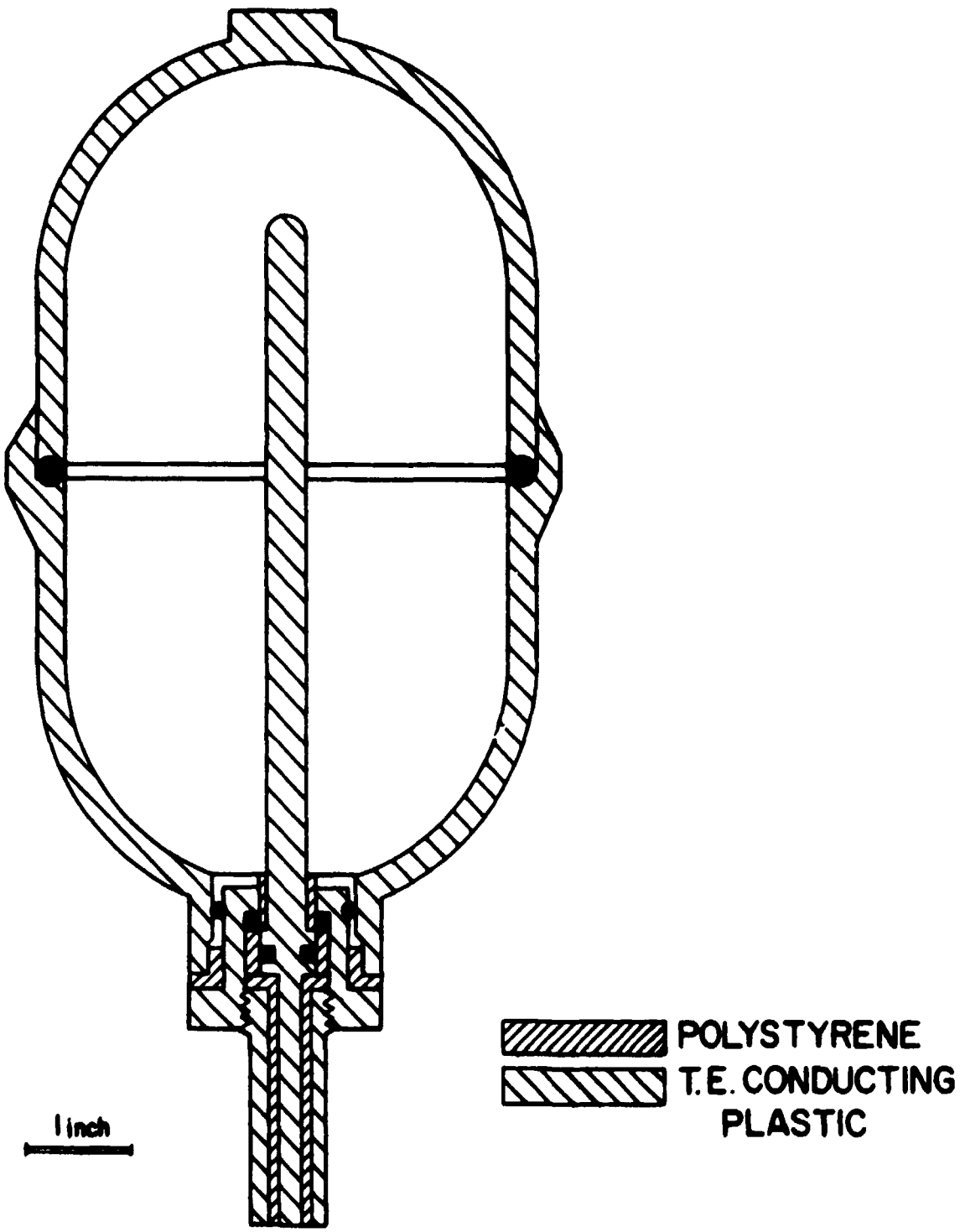

Figure 5-2

Cross Section of a Large Tissue Equivalent Ionization Chamber.

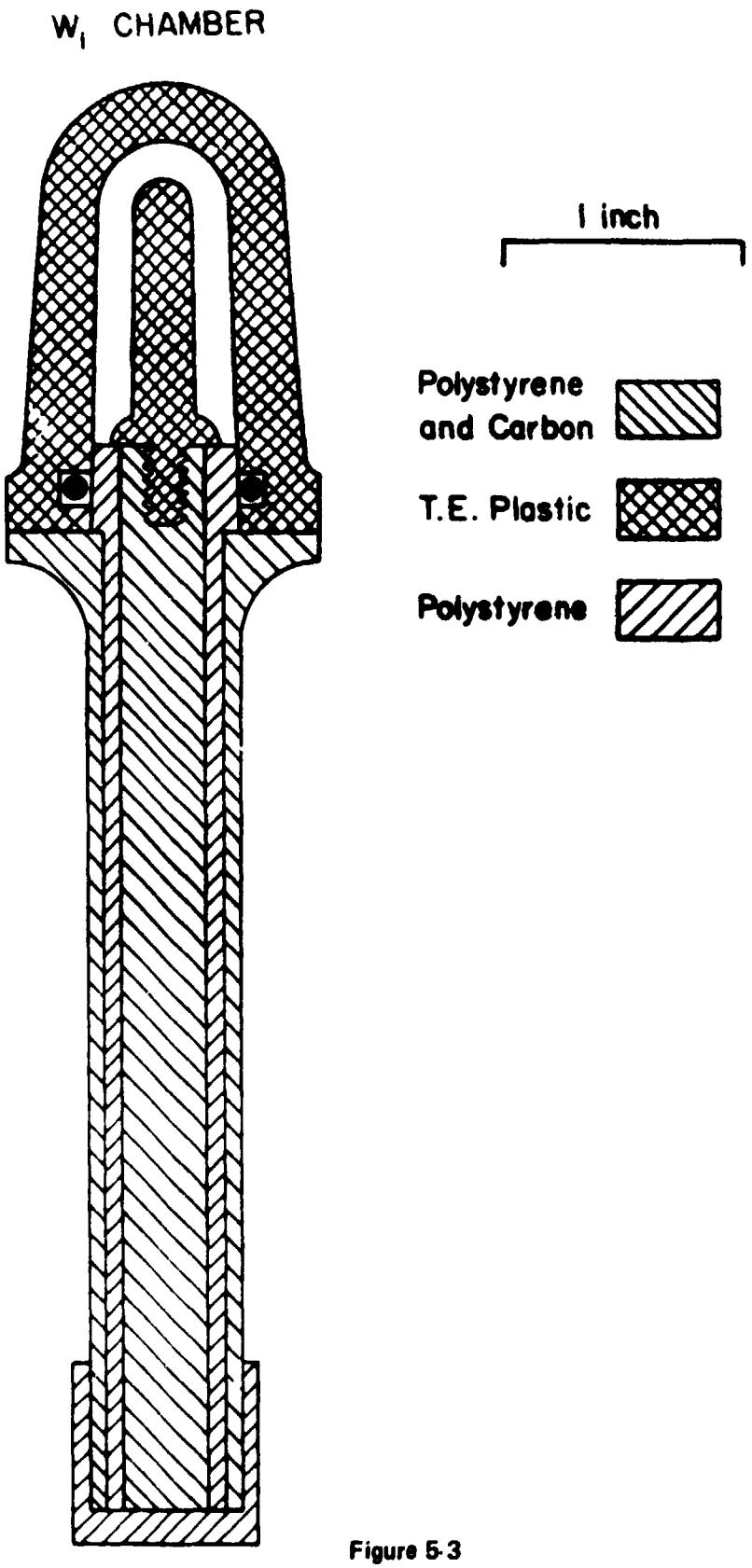

Figure 5-3

Cross Section of a Small Tissue Equivalent Ionization Chamber

lead to large errors in D_γ depending on D_n/D_γ. However, additional errors are introduced in D_n when $D_n/D_\gamma \ll 1$ due to the problem of subtracting two small numbers which are very nearly equal.

TABLE 5 - 2

Maximum K (E) (R/rad) for a Teflon-CO_2 Chamber

Neutron Energy (MeV)	Observed K(E) (R/rad)	Computed K (E) (R/rad)
0.5	0.08	0.11
1.0	0.08	0.18
2.0	0.09	0.13
3.0	0.12	0.10
4.0	0.15	0.15
6.0	0.20	0.16
8.0	0.24	0.20

Proportional Counter Methods of Neutron Dosimetry

Even when the response function is chosen to be the integral of the first moment of the energy loss distribution, considerable advantage ensues from the use of counting methods. In the case of ionization chambers, one can deal only with the total energy loss as expressed in Equations 5-1 and 5-2; in particular, the lower limit on the integral sign of Equation 5-1 must always be set equal to zero. With pulse counting techniques, on the other hand, we may employ a more general response function as follows:

$$R_c(E) = \int_B^\infty \epsilon\, n(\epsilon, E)\, d\epsilon \tag{5-9}$$

where B is the minimum energy loss which we wish to record. The advantage afforded by the choice of $B > 0$ is that a bias level B may be chosen such that neutrons may be counted even with much larger gamma-ray backgrounds. These statements will be illustrated first with the absolute proportional counter.

One design of the proportional counter is shown in Figure 5-4. The counter is completely lined with polyethylene, C_nH_{2n}, and is filled with ethylene, C_2H_4, at a pressure of 75 cm Hg or with cyclopropane, C_3H_6, at a pressure of 50 cm Hg. In either case, the walls and gas are matched in atomic compositon, which satisfies one of the requirements of the Bragg Gray principle. Thus, with a response function as specified by Equation 5-9, one can expect to measure approximately the energy absorbed per gram of ethylene. From this information, one may determine the energy absorbed per gram of tissue; as discussed in Lecture 3, one can show that

$$\left.\frac{D_{1E}}{D_{1T}}\right|_{E_1 = 0.01\ \text{MeV}}^{E_2 = 20\ \text{MeV}} = 1.45\,(1 \pm 0.10) \tag{5-10}$$

over an energy range from 0.01 MeV to 20 MeV.

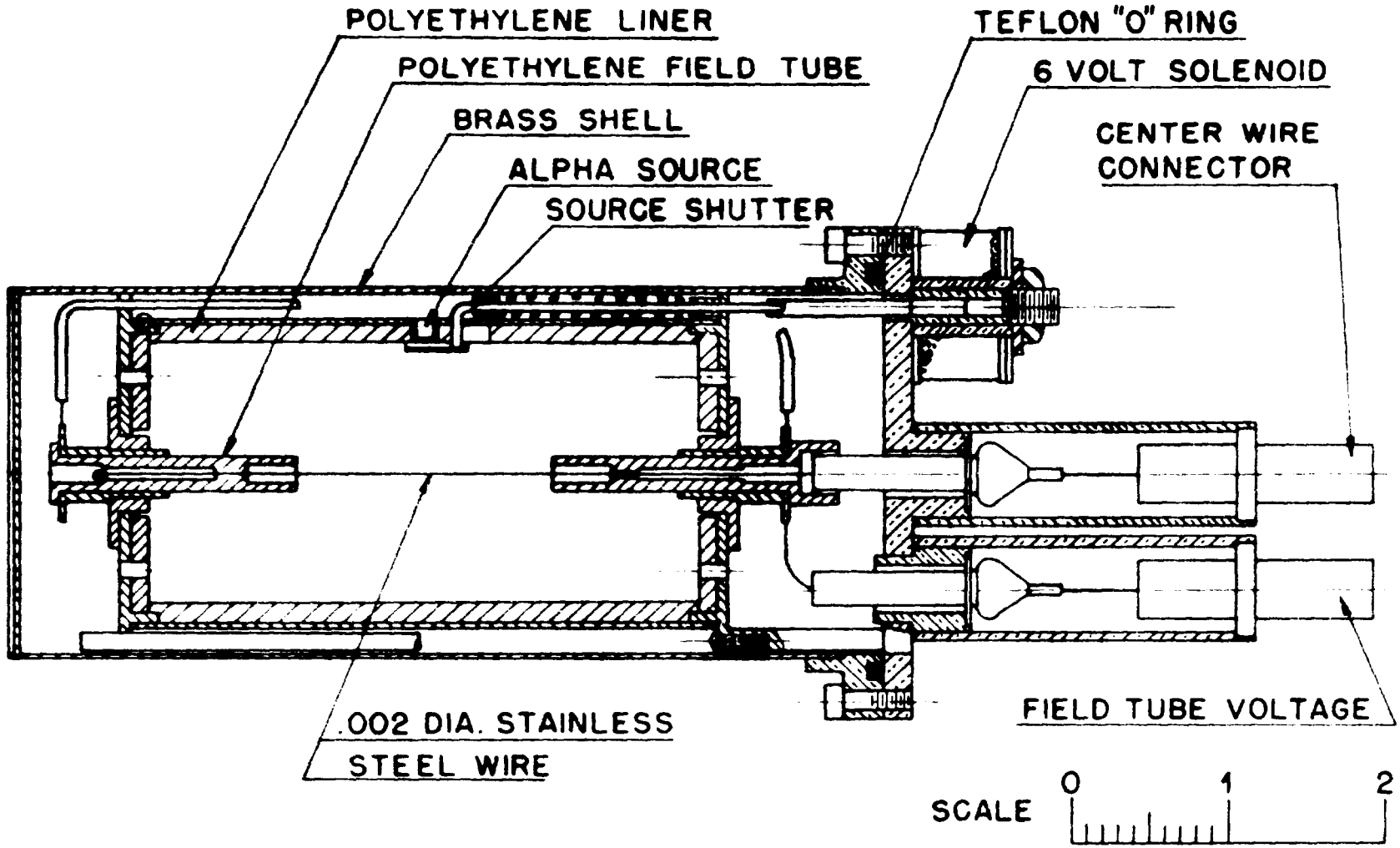

Figure 5-4

Cross Section of a Proportional Counter for Fast Neutron Dosimetry

From Figure 5-5, it is seen that gamma radiation, because of relatively low specific ionization by the secondary electrons, produces relatively small pulse heights. Therefore, it is easy to reject gamma radiation by pulse height selection. After gamma ray discrimination, the neutron pulses are added linearly to obtain the quantity $\epsilon_T(E)$ which is associated with the Bragg-Gray principle. In practice, gamma ray discrimination causes an amount of energy proportional to the area A_1 (Figure 5-5) to be lost under the bias, however, the relatively small fraction $f = A_1/(A_1 + A_2)$ can be estimated by a procedure discussed below.

The proportionality implied above between pulse height and the number of ion pairs in a single ionizing event depends on two conditions: (a) There must be no electron attachment, and (b) the height of the pulse at the output of the linear amplifier must not depend on track orientation. Condition (a) may be fulfilled only by rigorous exclusion from the counter of such gases as water vapor, oxygen, and some of the halogens, which have very large attachment cross sections. Condition (b) may be fulfilled by proper selection of the amplifier rise time and decay time. A variation of the angle between the ionizing particle's path and the center wire in a proportional counter causes a variation in the pulse profiles. However, it has been shown that if the rise time and decay time constants, assumed equal, as in many good pulse amplifiers, are greater than the collection time of electrons in the counter, then the pulse height at the output of the amplifier depends only slightly on the rise time of the proportional counter pulse.

If it is assumed that the pulse height is proportional to the number of ion pairs, absolute calibration of the neutron dose may be accomplished by means of an alpha source, provided that the sensitive volume of the counter is also known. Therefore, these two features, i.e., alpha calibration source and known sensitive volume, have been incorporated into the proportional counter desing in Figure 5-4. The sensitive volume is determined by means of "field tubes" held at the appropriate electrostatic potential. The neutron dose in ethylene is proportional to $A_1 + A_2$; this area may be expressed in MeV/sec by means of the ^{239}Pu alpha particle pulse height, Fig. 5-5. More specifically, the first collision dose rate in tissue, D_T, is given by

$$\dot{D}_T \quad (\text{MeV sec}^{-1}\ \text{gm}^{-1}) = \frac{1}{1.45}\left[\frac{A_1 + A_2}{A_c}\right] \times \frac{\dot{E}_c}{V\rho} \tag{5.11}$$

where $\dot{E}_c$ is the rate of energy absorption (MeV/sec) corresponding to the arbitrarily chosen calibration area A_c, V is the sensitive volume of the counter in cm^3, and ρ is the density of the C_nH_{2n} gas in gm/cm^3. The quantity $\dot{E}_c$ is determined directly from the alpha particle energy as follows:

$$\dot{E}_c = \dot{C}_o \times \frac{V_o}{V_\alpha} \quad E_\alpha \tag{5.12}$$

where $\dot{C}_o$ is the count rate and V_o is the pulse height for the arbitrarily chosen area A_c, and V_α is the pulse height produced by alpha particles of energy E_α.

When using the absolute proportional counter with conventional electronic apparatus, the value of B may be chosen to suit the particular experimental conditions. Factors governing the choice of B include the following: neutron energy, neutron intensity, gamma ray energy, and gamma-ray intensity. In any practical case, however, the discrimination level below which the results may be appreciably affected by gamma radiation may be determined directly for the particular set of experimental conditions. Figure 5-6 shows how this may be accomplished in a typical case. In this illustration, the integral count rate corresponding to just 1 mrad/hr of fast

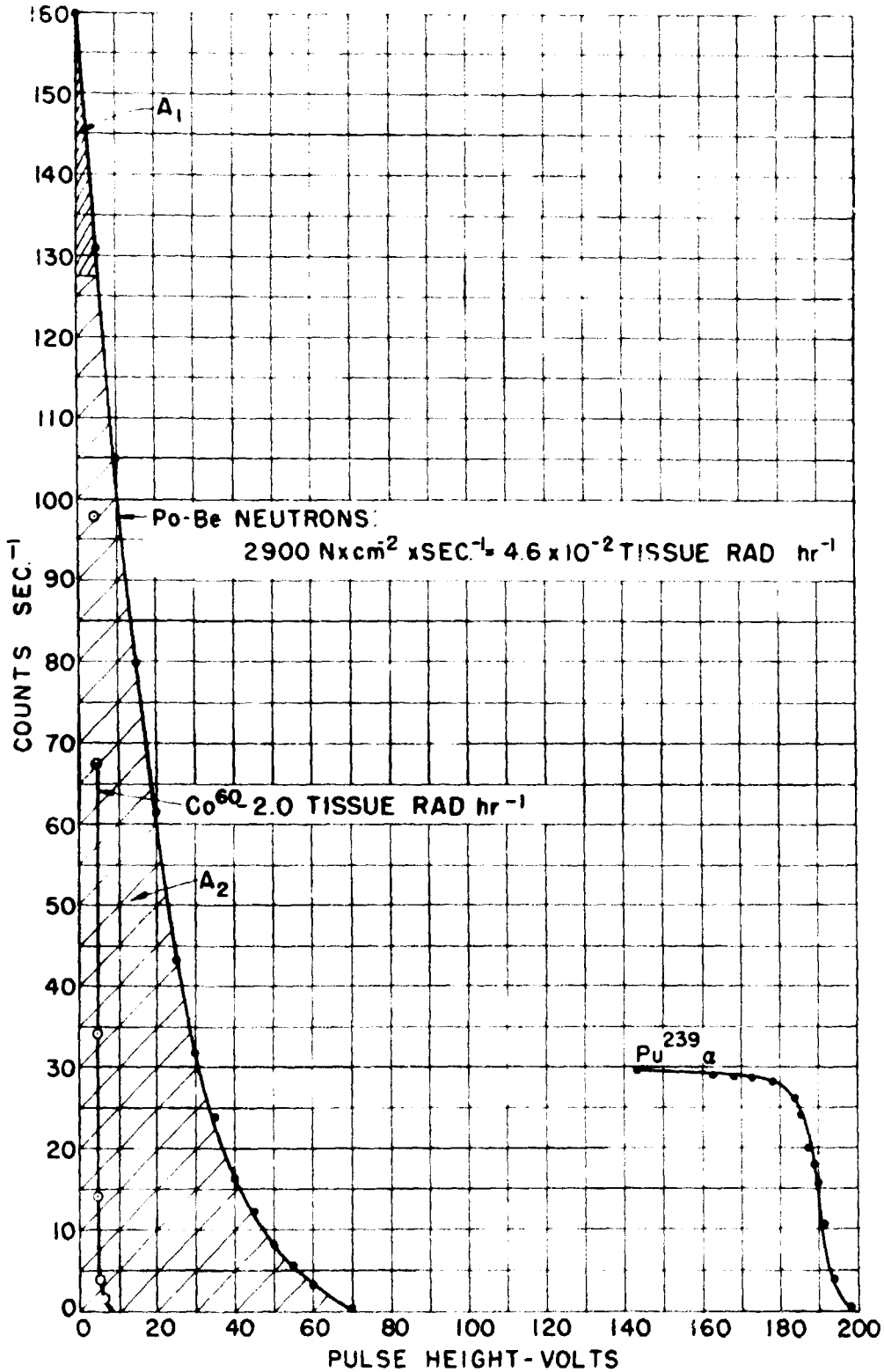

Figure 5 5

Integral Pulse Height Distribution for Po Be Neutrons
Pu α Particles and Co Gamma Radiation

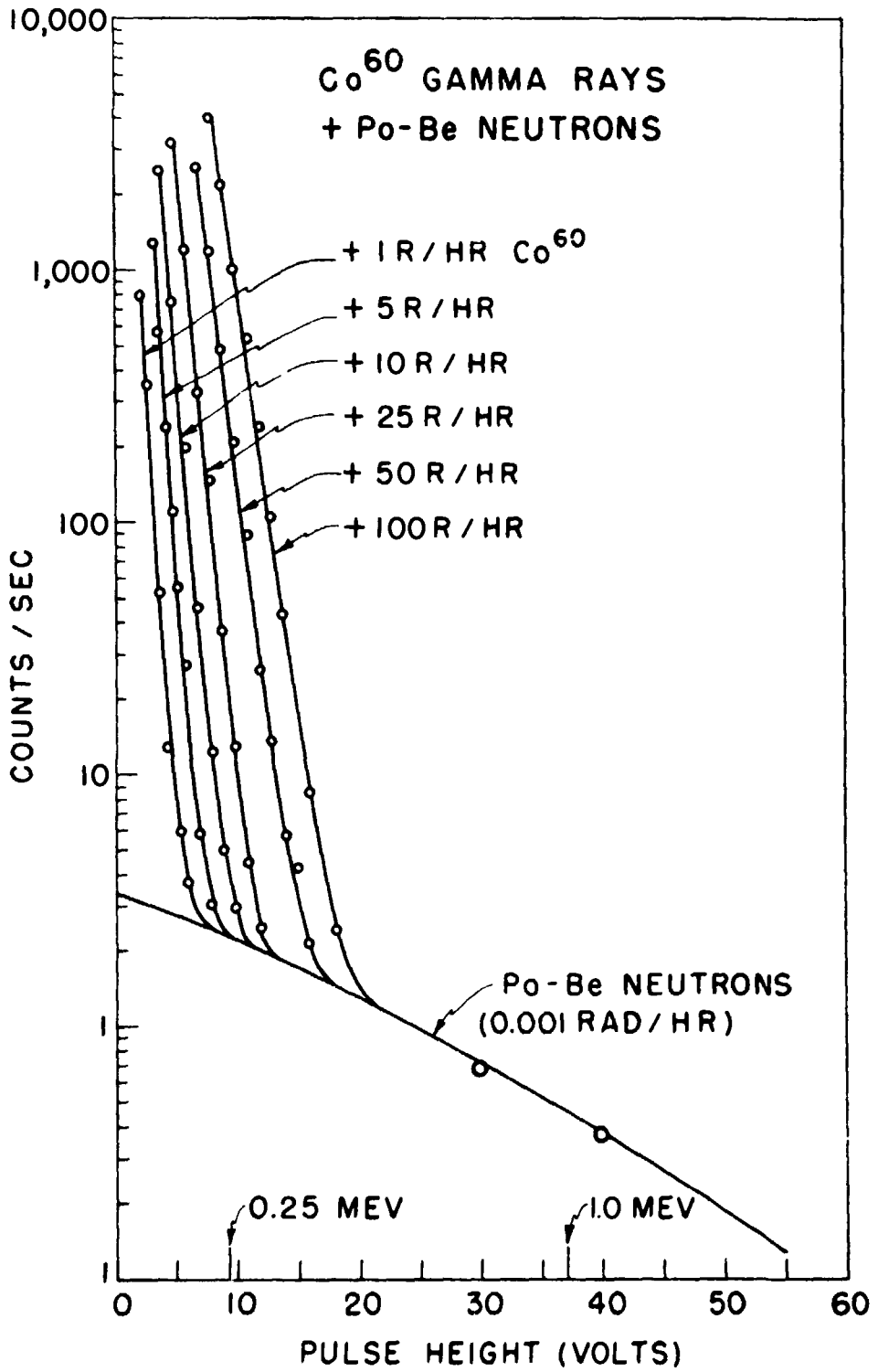

Figure 5 6

Integral Pulse Height Spectrum Produced in a Proportional Counter by Fast Neutrons and Gamma Radiation

neutrons (Po-Be) plus various gamma intensities ranging from 1 r/hr to 100 r/hr of ^{60}Co gamma radiation is plotted on a log scale as a function of pulse height. It is seen, for example, that for a gamma-ray dose rate of 1 r/hr, the bias level required to discriminate against gamma rays is about 0.20 MeV, and the absorbed neutron energy lost under the bias would be about 10% (see Table 5-3) On the other hand, if the gamma (^{60}Co) dose rate were increased to 25 r/hr, the bias level would have to be increased to about 0.36 MeV, and the neutron energy lost under the bias would be about 20% It should be noted that this energy lost may be estimated by plotting the data in the form illustrated in Figure 5-6, extrapolating the count-rate versus pulse-height curve for values of pulse height $\leq$ B, and then integrating the area under the entire curve. In other words, the values for f given in Table 5-3 do not necessarily represent errors in the measured dose, although they do represent the fraction of the total dose which must be approximated by an extrapolation procedure

In practice, it is convenient to integrate pulses automatically, thus eliminating the requirement for determining the area under the pulse height distributions Figure 5-7 shows schematically a very simple type of pulse integrator. At A, B, C, and D are discriminator tubes biased so that the pulse height required to make the tubes conduct are 5, 10, 20, and 40 volts, respectively. The discriminators feed into the 1, 2, 4, and 8 count stages of a usual binary-type scaling unit. Each time Tube A conducts because of the arrival of the 5-volt pulse, one count is added to the scaling unit. A 10-volt pulse causes both A and B to conduct thus adding three counts to the scaling unit if the N^{o} 1 indicator is not on. If the N^{o} 1 indicator is on, a net of only one count will be added to the system, because the pulse which was stored in the N^{o} 1 scaling position is lost in coincidence with the channel which is adding two pulses to the system. Thus the average is two counts for each 10 volt pulse. Similar arguments show that each 20-volt pulse gives an average of four counts while the 40-volt pulse gives an average of eight counts. Therefore, it is not necessary to use anticoincidence circuits to prevent the lower level discriminators from adding counts to the system From studies with monoenergetic neutrons, it is seen that the integrator reads to within ± 10% of the true area under the pulse height distribution curves when the neutron energy lies between 0.5 MeV and 14 MeV.

A convenient instrument utilizing the counter mentioned above and the 4-stage binary integrating circuit has been developed As shown by the block diagram of Figure 5-8, the output signals from the pulse height integrator are fed into an indicating system which uses decade scalers, preset timers, and lamps as decimal indicators, in such a way that the dose rate is indicated directly in mrad/hr.

A Geiger-Müller Tube as a Gamma-Ray Dosimeter

In this section, we will discuss a method of gamma ray dosimetry which uses commercially available halogen type Geiger-Müller (G M) counter as the detector. This ilustrates the case where the response of the system is simply the total number of interactions with the system A single ion detector has been developed for measurements of gamma dose in the presence of high neutron field. This counter has a negligible neutron response; however, like other instruments used for this purpose, it generally requires considerable electronic apparatus and operational skill. In the present work, we have shown that a small halogen-type G-M counter can be arranged with suitable shields to provide an instrument that is (a) energy independent for X or gamma radiation above about 150 keV, (b) insensitive to fast neutrons, and (c) insensitive to thermal neutrons.

TABLE 5 - 3

Fraction, f, of Energy Spent by Recoils Losing Less Than the Bias Energy, B, in the Counter

Bias		Fast Neutron Energies							
Energy MeV	PHS— Volts	0.5 MeV	1.0 MeV	2.0 MeV	3.5 MeV	4.8 MeV	14 MeV	Po-B	Po-Be
0.074	2.6	0.089	0.020	0.015	0.013	0.014	0.025	0.006	0.014
0.14	5.3	0.195	0.094	0.041	0.035	0.028	0.085	0.028	0.045
0.21	7.8	0.320	0.129	0.076	0.056	0.059	0.162	0.065	0.101
0.28	10.5	0.526	0.235	0.123	0.091	0.098	0.258	0.099	0.144
0.36	13.2	0.730	0.333	0.188	0.128	0.162	0.369	0.152	0.205

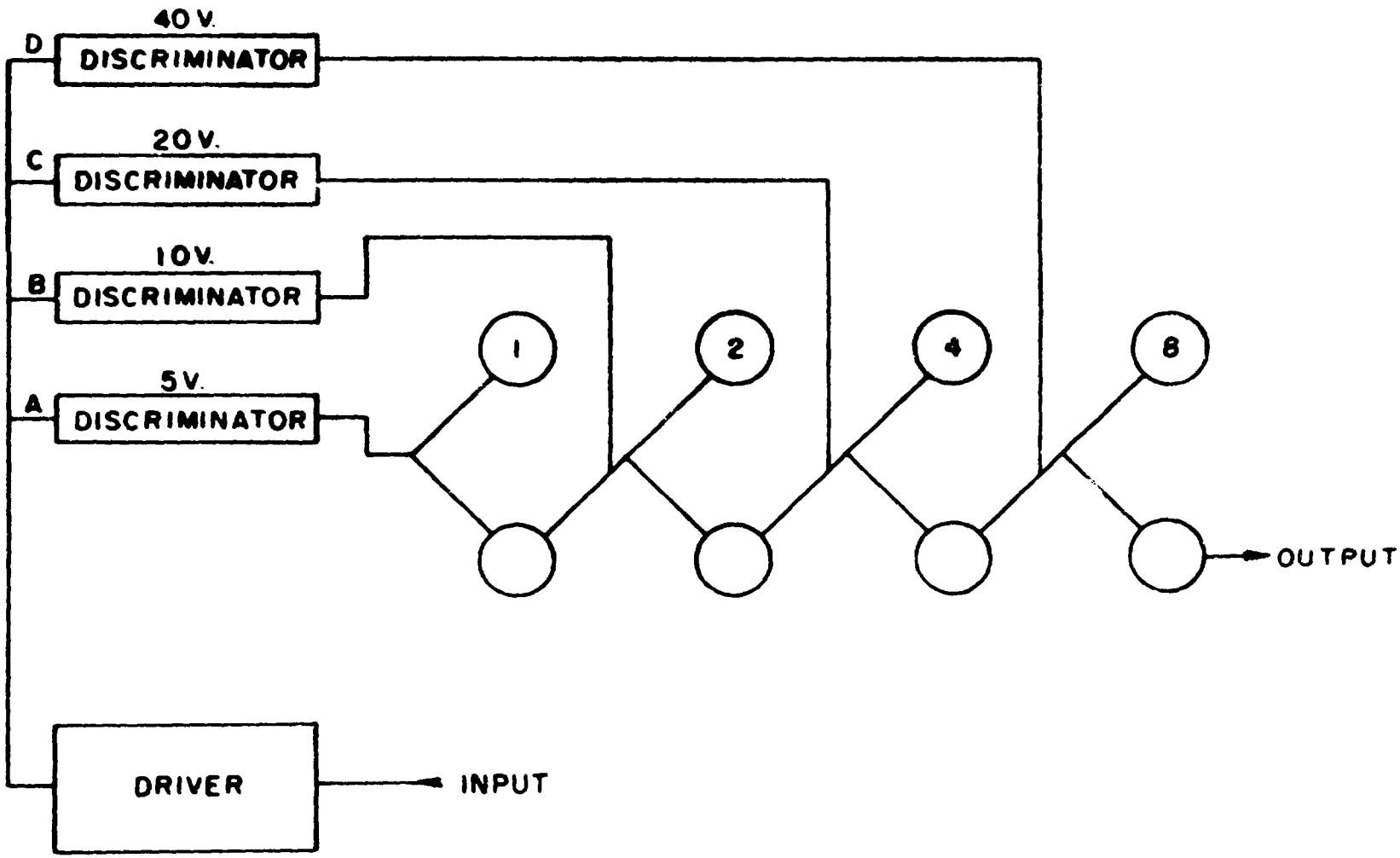

Figure 5 7

A Simple Method of Pulse Integration, Use a Binary Scaler

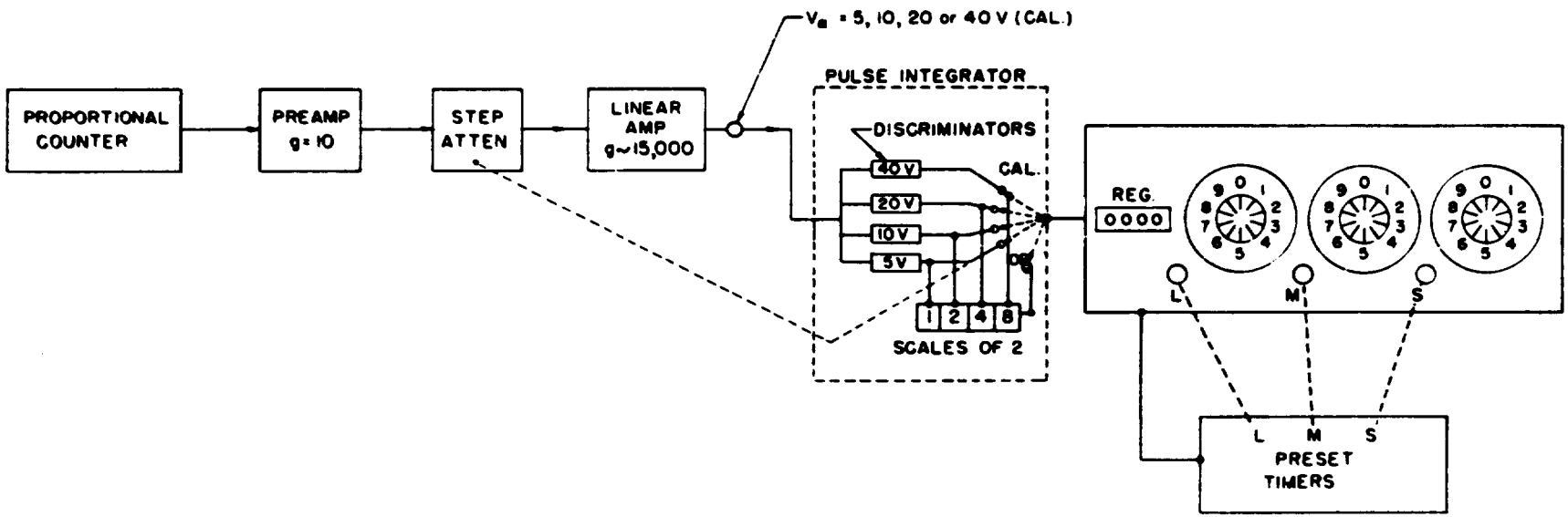

Figure 5-8

Block Diagram of a Fast Neutron Dosimeter (RADSAN)

The counter used is a Philips N^{o} 18509 micro G M counter filled with neon, argon, and a halogen quenching agent The cathode made of stainless steel has a wall thickness of 90 mg/cm^2 As shown by Figure 5 9, the unshielded counter has considerable energy dependence below 200 keV However, it can be made to furnish readings of exposure dose in r that are essentially independent of gamma ray energies down to 150 keV by shielding the counter with 0.053" tin plus 0 010" lead on the sides, and 0 022" tin plus 0 004" lead on the end (Figure 5-10). A drawing of the probe unit showing the arrangement together with a Li shield, which will be discussed later is shown in Fig 5-11 The response as a pulse device is essentially linear from 0.1 mr/hr to 5 r/hr, as shown by the curve in Figure 5 12

By calculation, it can be shown that the main contribution to the fast neutron response is due to inelastic collisions in the gamma energy correction shield and has a maximum at about 5.0 MeV neutron energy An upper limit to the neutron response at 5 MeV is 0.15% The assignment of a reasonably valid neutron response of the G M counter by experimental methods is not possible at present due to the unavailability of a facility having a radiation field with a sufficiently large neutron to gamma ratio Studies in which the G M counter was irradiated with monoenergetic neutrons in the energy range from 0.68 Mev to 4 2 MeV indicate that the response in this energy range is less than 0 5%

The response of the counter to thermal neutrons was determined experimentally, making use of the water thermal column at the Oak Ridge National Laboratory Graphite Reactor. It was concluded that the thermal neutron response of the probe unit is low, requiring about 5 x 10^9 neutrons/cm^2 to produce the same response as 1 r of gamma radiation Further, the thermal neutron response may be reduced by using the Li shield With the Li shield (Figure 5-11), about 1 5 x 10^{1} neutrons/cm^2 would be required to produce the same response as 1 r of gamma radiation

Special Counting Methods for Fast Neutron Dosimetry

A proton recoil proportional counter was designed such that the first collision tissue dose could be obtained simply by measuring the number of counts produced in the counter The energy response $n_T(B,E)$ of the counter is determined by three sources of recoil proton shown in Figure 5-13. Calculations were made of the probability that neutrons of energy E could cause a recoil proton to lose in the counting volume energy greater than a bias energy B, needed to discriminate against gamma radiation The energy responses (Figure 5 14) for the three sources of protons are such that when added in the illustrated proportions of hydrogenous materials, the tissue first collision dose curve is approximated (Figure 5 15) The response has been checked experimentally with monoenergetic neutrons and agrees well with theory. The chief disadvantage of this counter is the fact that the response is directional, and the energy response is correct only when a plane beam is normally incident to the end of the counter containing the plane radiators.

Dennis and Loosemore[2] have modified the above ideas to develop a proportional counter that is nondirectional in response In this case, the neutron energy response curve follows the recommendations of the International Commission on Radiological Protection as given in British Journal of Radiology Supplement N^{o} 6, 1955. At that time, the permissible level was stated in terms of the absorbed energy at a depth 2 cm below the surface of tissue. Skjöldebrand[4] has developed a spherical scintillation detector whose energy response is

adjusted to the multiple collision dose curve of Snyder and Neufeld. Thus, this instrument indicates the maximum absorbed dose that a man would receive if located in the radiation field.

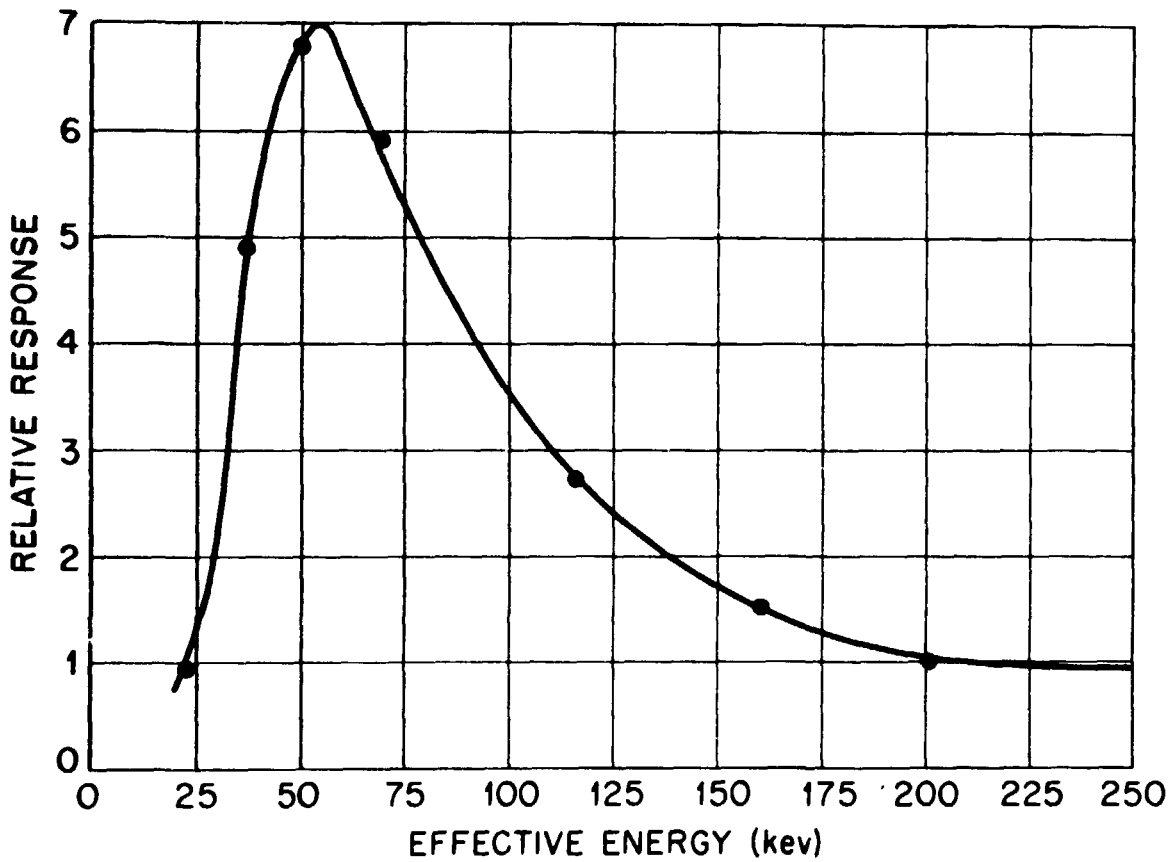

Figure 5-9

Energy Response of a Geiger-Müller Counter

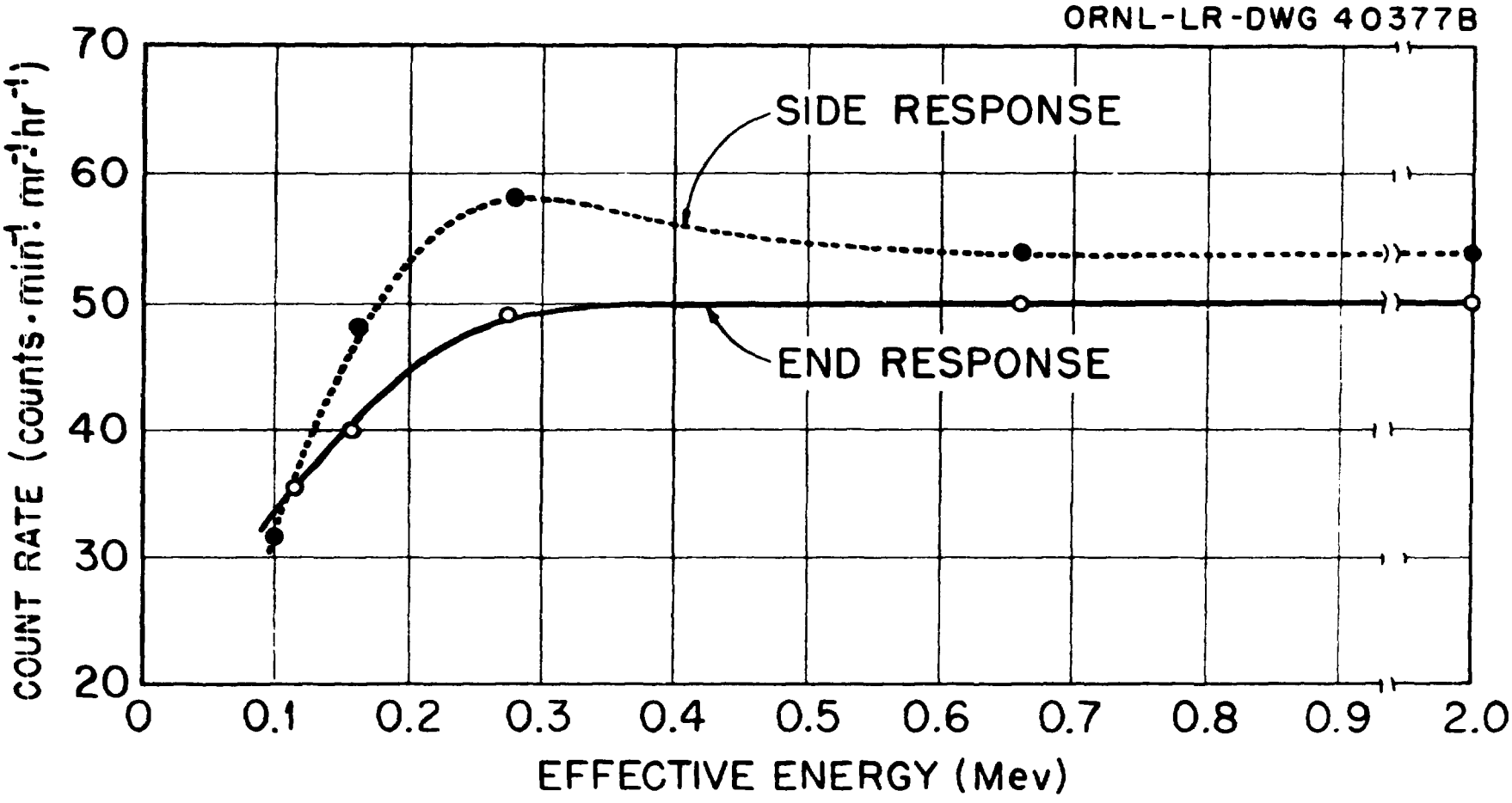

Figure 5-10

Energy Response of a Shielded Geiger Müller Counter

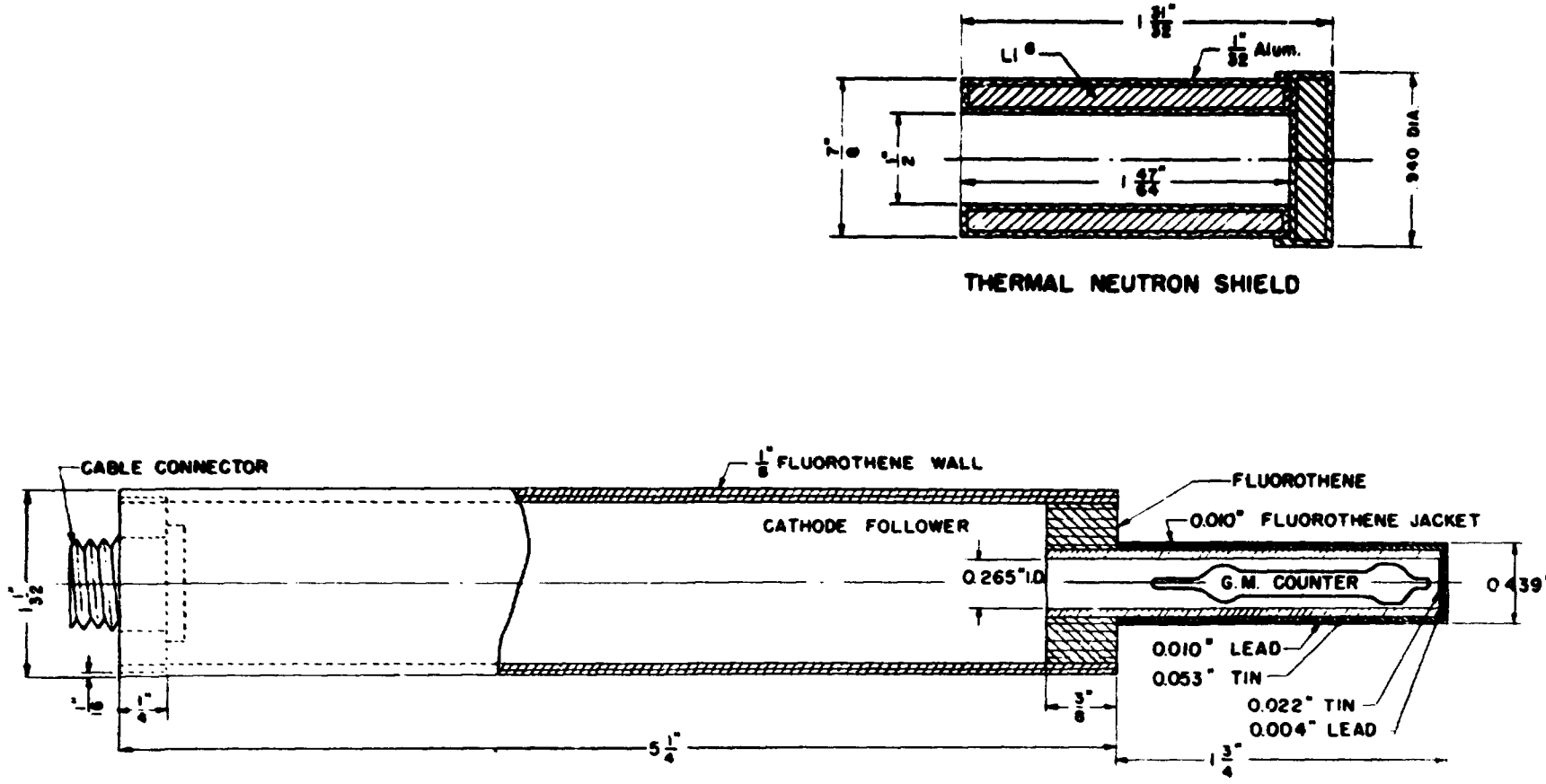

Figure 5-11

Probe Assembly of a Geiger-Müller Counter Showing Provision for Thermal Neutron Shielding.

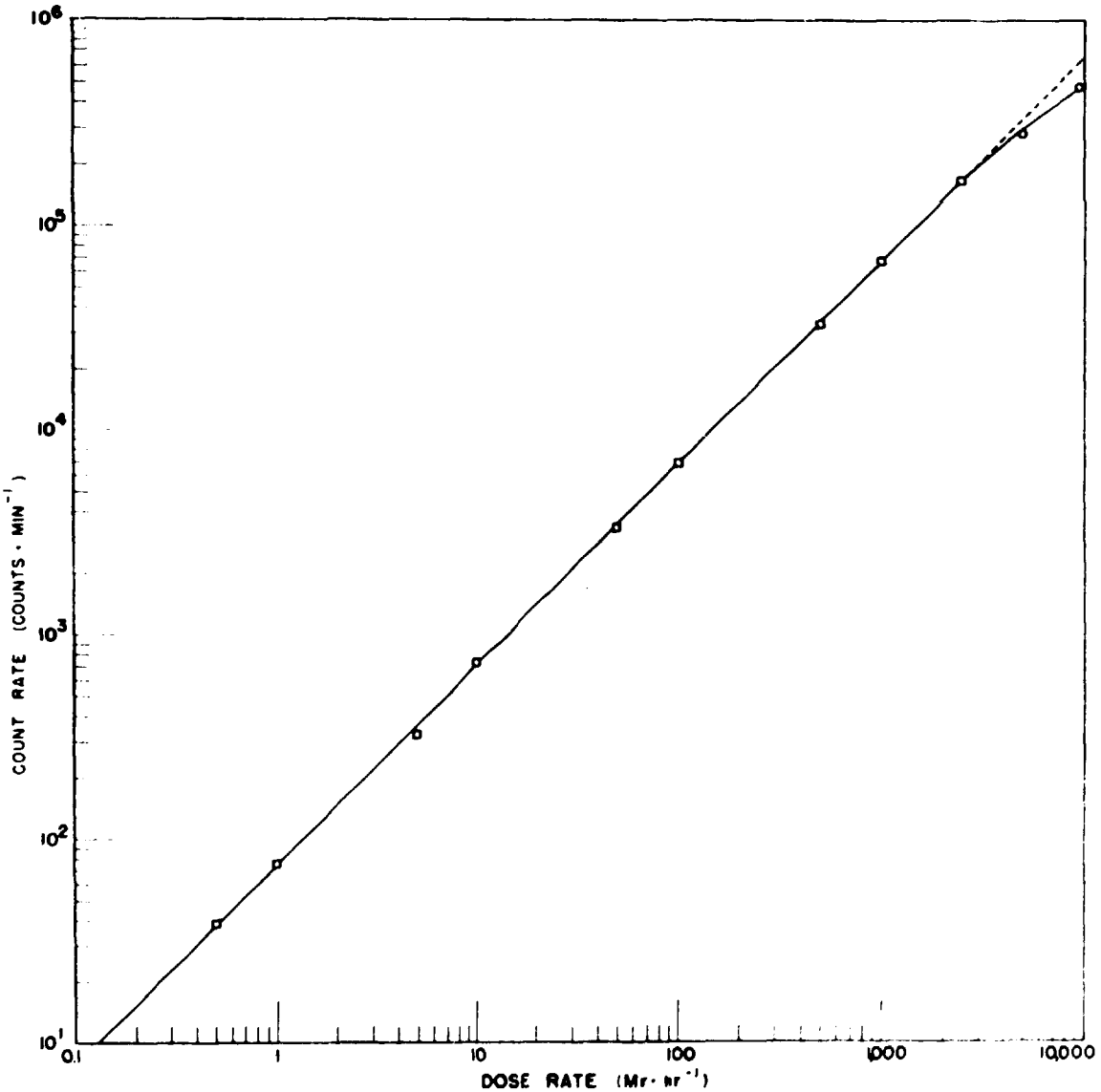

Figure 5-12

Intensity Response Curve for the Phillips Micro G M Counter

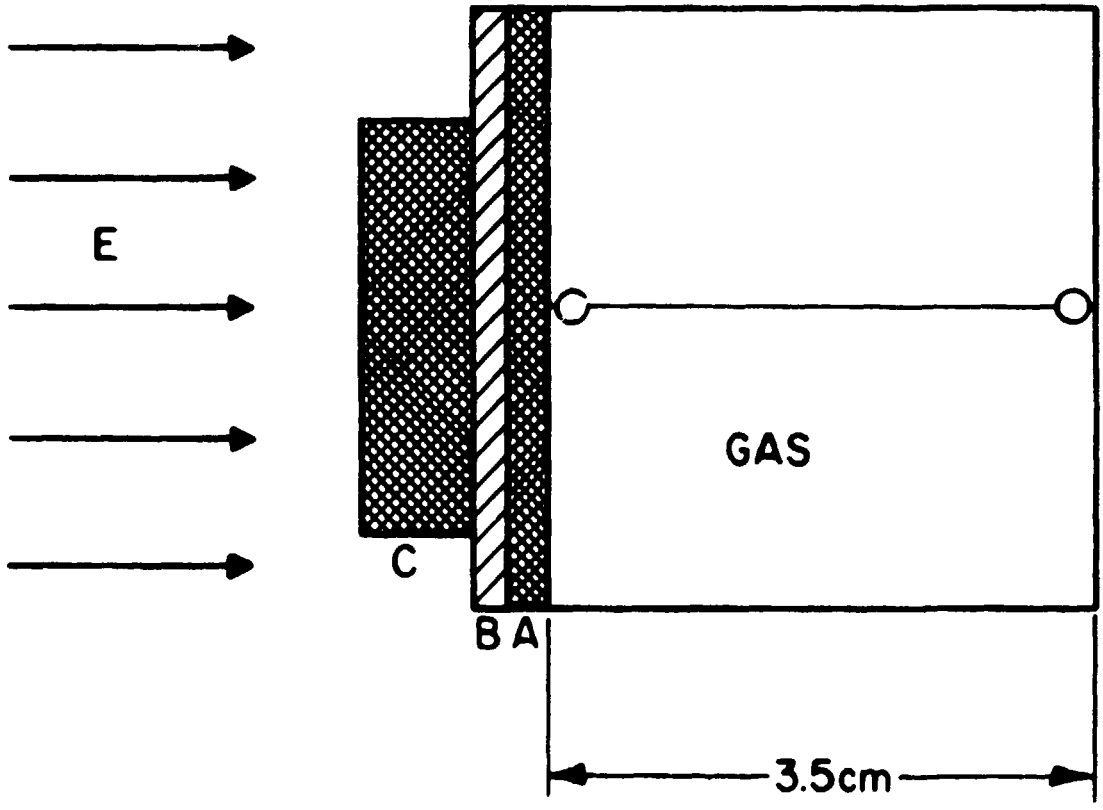

Figure 5-13

Schematic Representation of Count-Rate Dosimeter.
A - Paraffin (13 mg/cm^2), B - Aluminum (29 mg/cm^2), C - Paraffin (100 mg/cm^2).
Ratio of paraffin areas (A_1/A_3) = 2.9. The gas is methane at 30 cm Hg pressure.

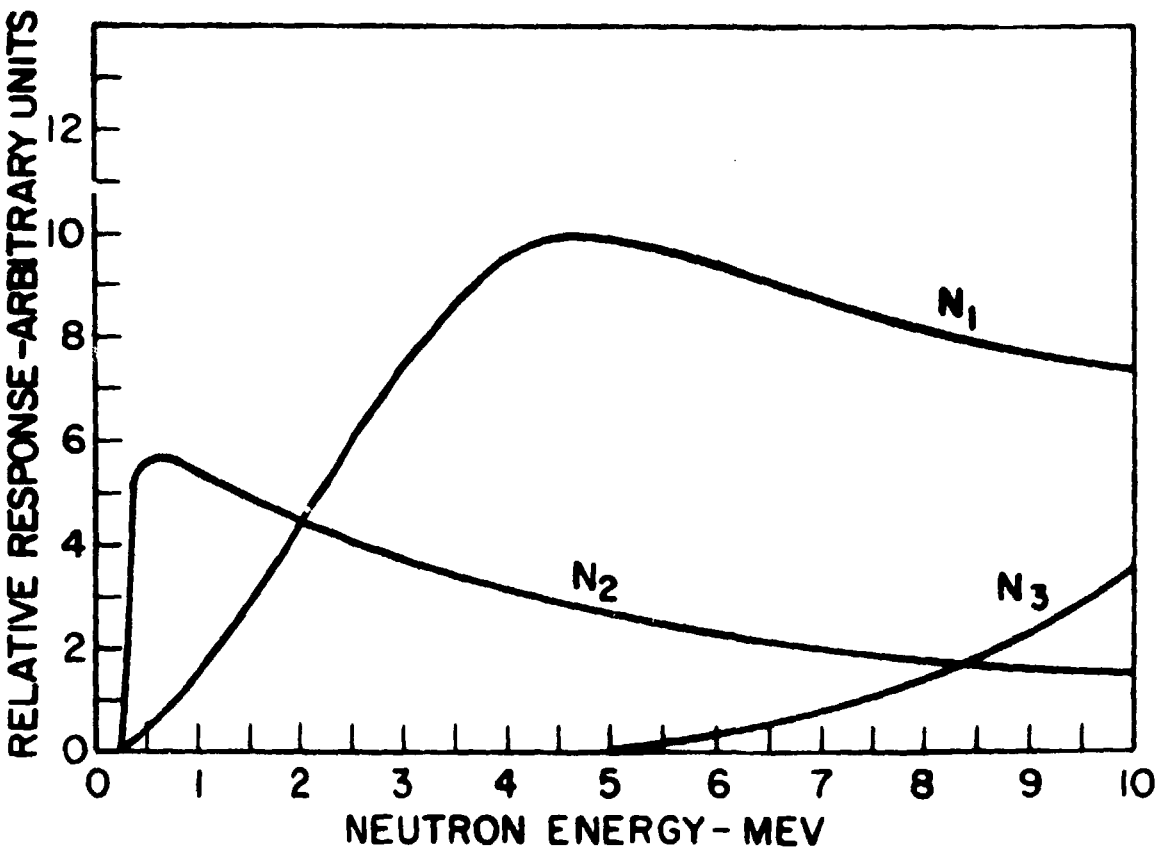

Figure 5 14

N_1 Response of Plane Slab of Paraffin, for which E_1 = 3 MeV and B = 0.2 MeV
N_2 Response of Hydrogenous Gas, where B = 0.2 MeV
N_3 Response of Thick Paraffin Slab, where E_1 = 5 MeV and B = 0.2 MeV.

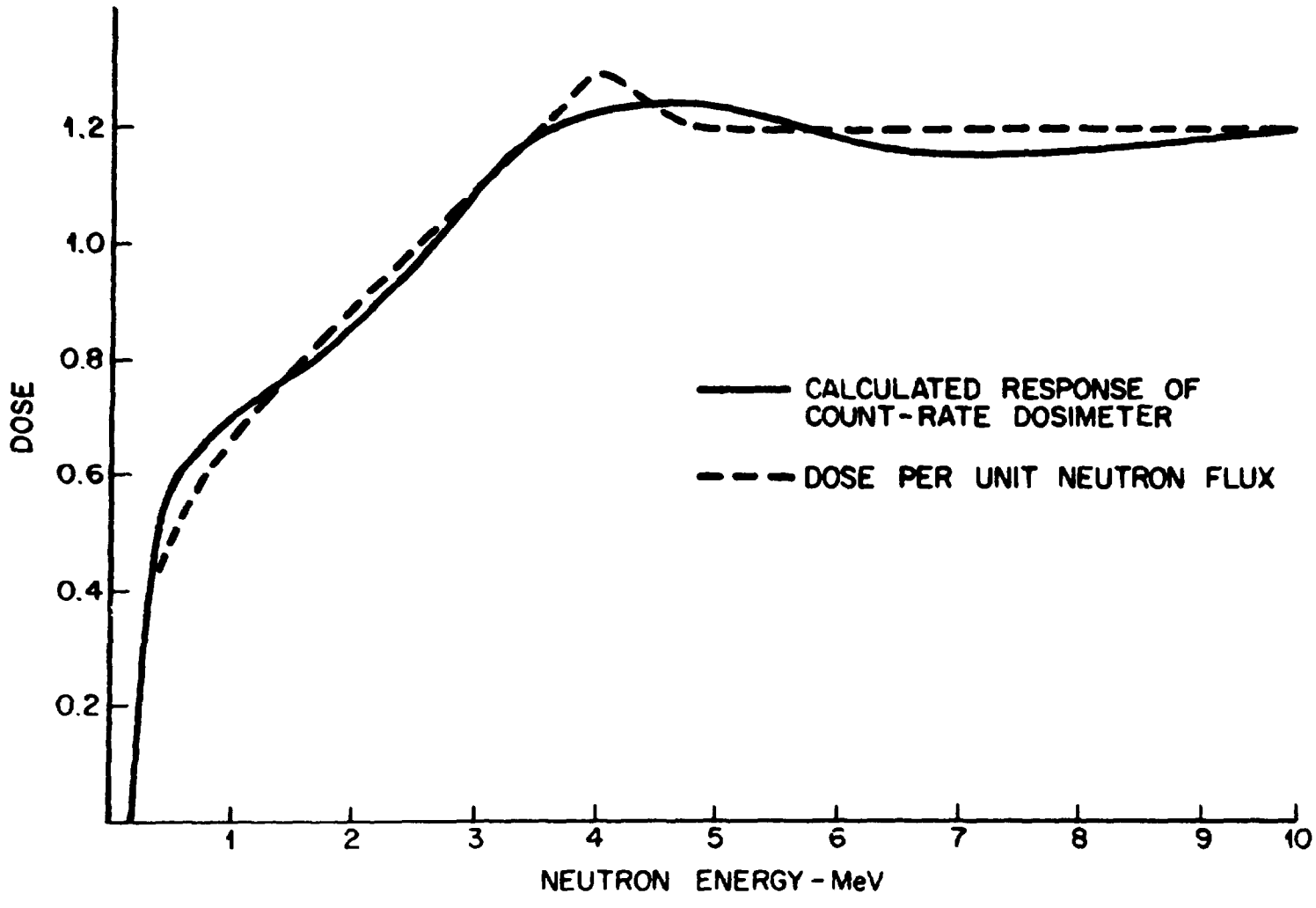

Figure 5-15

Energy Response of Count Rate Dosimeter.

BIBLIOGRAPHY

1. K. Z. Morgan and J. E. Turner, *Principles of Radiation Protection*, John Wiley and Sons, Inc., New York, 1967.

2. J. A. Dennis and W. R. Loosemore, *A Fast Neutron Counter for Dosimetry*, Atomic Energy Research Establishment Report EL/R 2149, Harwell, 1957.

3. H. H. Rossi and G. Failla, Nucleonic *14*, Nº 2, 32 (1956).

4. R. Skjöldebrand, J. Nucl. Energy *1*, 299 (1955).

LECTURE Nº 6

SPECIAL METHODS IN RADIATION DOSIMETRY

Introduction

Dosimetry is one of the most fundamental requirements in health physics and radiobiology. An understanding of the interactions of radiations with matter and the basic concepts of physical instrumentation are necessary to both the accurate measurement and interpretation of radiation exposures. This lecture purports to give a general introduction to dosimetry problems and examples of sistems which have been developed to solve them.

The ideal and complete dosimetry in a radiation field would include, at the point of interest in the medium, for each type of radiation present the following: (1) Total energy absorbed, (2) dE/dx (or LET) distribution, (3) angular distribution, (4) energy absorption rate, and (5) the energy spectrum. Seldom, if ever, is the ideal measurement possible. The most often measured quantities are exposure dose or dose rate for x or gamma rays and first collision dose (or kerma) for neutrons. In many cases, the measurements have been limited to total fluence or energy fluence measurements. Spectral distributions are sometimes determined for one or all types of radiation present, and occasionally the dE/dx or LET (Linear Energy Transfer) distributions are calculated. One instrument for measuring LET has been reported, and certain emulsions and cloud chambers may be used for measuring dE/dx in the constituent media.

In 1962, the ICRU introduced a new unit for "dose", i.e., kerma, which denotes "the sum of the initial kinetic energies of all the charged particles liberated by indirectly ionizing particles in a volume element of the specified material" (NB62). Because the term "first collision dose" had been interpreted in more than one way, the term kerma was intended to be more precise and less ambiguous. In general, it is equivalent to one of the widely accepted meanings of first collision dose, but it does not fill the need for a quantity for "secondary equilibrium" conditions. The units for kerma are ergs/gram. For gamma energies above 3 MeV and neutron energies above 15 MeV, the ratio of the energy liberated to that absorbed in a small mass of material becomes increasingly greater than unity.

The most widely used methods of "dosimetry" for indirectly ionizing radiation have been based on either (1) the measurement of the energy expended by secondary particles, or (2) the computation of dose from fluence measurements. The first case is typified by an ionization chamber having walls sufficiently thick to establish equilibrium between the indirectly ionizing radiation, e.g., gamma rays, and the primary ionizing radiation, e.g., Compton electrons. On the basis of the Bragg-Gray relationship, the energy deposited in the cavity, E_c, i.e., the product of the number of ion pairs per unit mass of gas, J, and the energy required to produce one pair, W_c, can be used to compute the energy deposited in the wall medium, E_s, by the relationship

$$E_s = SE_c = SW_cJ \qquad (6\,1)$$

where S is the ratio of the mass stopping power of the wall medium to that of the gas for the radiation of interest. The criteria for applying the Bragg-Gray principle were given in a previous lecture and in NBS Handbook 75, but it is essential that the ionizing particles be in equilibrium with the nonionizing rays and that the chamber be sufficiently small so as not to perturb the

incident radiation field.

The second approach to dosimetry is typified by the threshold detector technique. In this case, the fluence in various neutron energy increments is obtained by analyzing the reaction products in various detectors, e g , the fission product gamma rays from a ^{238}U foil which has an effective threshold for fission, when exposed to neutrons having a fission spectrum, of about 1.5 MeV and an approximately uniform cross section above that energy. From measurements of this type, the energy liberated (or absorbed, under equilibrium conditions) may be computed by the relationship

$$D(E) = 1\ 602 \times 10^{-8}\ E_n \sum_i N_i f_i \sigma_i \qquad (6\text{-}2)$$

where

$D(E)$ = neutron dose in rads/neutron/cm^2

E_n = the energy of the neutron (or average energy of the energy increments of neutrons)

N_i = number of atoms/gram of the ith species contained in the medium

f_i = average fraction of the energy of the neutron which is transferred to the interacting nucleus (in general, isotropic scattering in the center of mass system is assumed).

σ_i = elastic scattering cross section in barns (10^{-24} cm^2) for the ith species

It is not necessary to measure exposure dose with an "air wall" ionization chamber or absorbed dose with a chamber constructed of a tissue equivalent material In the strictest sense, all that is required is a detector with associated parameters which permit the response of the detector to be interpreted in terms of the quantities to be measured.

Photographic Film and Nuclear Emulsions

General Discussion of Response to Radiation

Photographic film was one of the first radiation detectors used after the discovery of x rays; in fact, natural radioactivity was first noted through this medium It is still the most widely used detector for personnel monitoring Photographic emulsions, usually on a plastic film base, are a very versatile medium whose sensitivity and other characteristics are largely controlled by their composition and processing during manufacture. Special techniques have been developed to adapt these emulsions to essentially all types of radiation measurements. The two major categories into which emulsions for radiation measurements are divided, according to intended use, are (1) x ray film, usually in dental packet size (1 1/4 x 1 3/4 in.), which can be calibrated for x- or γ-ray exposures in terms of blackening; and (2) nuclear emulsions on film or glass plates which are used in studying ionizing particle tracks.

The radiation sensing element in these emulsions is silver-halide, most often silver-bromide. Small crystals of the silver-bromide, ranging in size from less than 0.5 μ in nuclear emulsions to a few μ in the most sensitive x ray emulsions, are suspended in a gelatin which is generally deposited on a cellulose acetate film or on a glass plate The thickness of this

layer of emulsion ranges from a few μ for insensitive x ray film to the order of 2000 μ in the thicker particle detecting emulsions. Electrons traversing the emulsion become trapped in the crystal lattice causing the reduction of silver ions to atomic silver. These silver atoms, in turn, result in deeper traps, which capture electrons, reducing more silver ions, eventually forming microscopic aggregates of silver atoms which constitute the latent image. Upon development, silver-halide grains containing the latent images are reduced to metallic silver which appears to the eye as the blackening of x or gamma film or microscopic tracks in the nuclear emulsions. Underdeveloped silver halide grains are dissolved by the fixer.

Photographic Film as an X or γ-Ray dosimeter

There are many types of film commercially available and packaged in the small dental-type packet. Packets are available which contain more than one film type to increase the useful dose range of the packet. Table 6-1 lists some common types and their approximate ranges for γ rays of energy greater than about 300 keV. The exact range of a given type of film depends on exposure, storage, and development conditions.

A typical developing procedure, and that used at ORNL, is to develop in du Pont concentrated x ray developer, liquid mix, for 3 minutes at 68 ± 2°F, stop bath for 1 minute, fix for 10 minutes in du Pont x-ray fixer, quick rinse with agitation for 1 minute and wash for 20 minutes. The sensitivity of all emulsions can be varied by as much as an order of magnitude by varying the developer and procedures. Typically, films are processed in relatively large batches and a complete set of calibration film developed simultaneously. In addition to developing time and temperature for a given film and developer type, the dilution and deterioration of the developer by use and exposure to air also effect the blackening.

TABLE 6-1

Approximate Dose Ranges of Common Types of Film Using ORNL Processing Techniques

Type	Manufacturer	Description	Approximate Dose Range
508	Du Pont	Extra fast medical x ray film	0.03-6
1	Eastman	Single Emulsion	0.03-1
555	du Pont	Single Emulsion*	0.05-10
2	Eastman	Double Emulsion	0.03-1000
834	Eastman	Single Emulsion*	5-800
1290	du Pont	Single Emulsion	10-3000
548.0	Eastman	Spectroscopic	1000-30,000

* Used in 544 film packet

All photographic emulsions show a marked variation in response per roentgen as a function of photon energy. The major factor in this response function is the relatively high atomic number of silver, i.e., the photoeletric cross section for silver for photons of energy less than ~300 keV is large compared with the cross sections of the elements of which air is composed.

Beta Radiation Measurements

The response of film to electrons is an insensitive function of the electron energie comparing blackening to air ionization. This has been demonstrated for the energy region form 0.5 to 1.4 MeV for paper-wrapped film. Typical films exhibit about the same sensitivity to beta rays as to gamma rays, i.e., 1 rad of beta rays yields about the same film density as 1 r of gamma rays. A typical film will be surrounded by about 30 mg/cm^2 of paper. When calibrated in the usual manner, i.e., by laying the film packet flat on a slab of the beta-emitting material thicker than the maximum range of the beta particles in it, such film packets exhibit an energy dependence for beta rays. The shape of this curve is influenced by the tipe of emulsion and its wrapping.

Neutron Measurements

X ray film has a blackening response to fast neutrons about two orders of magnitude less than for gamma rays. Therefore, for most applications, a special class of emulsions has been developed. These fine grain emulsions are coated on the usual acetate film base or on glass plates. Table 6-2 shows some of the commercially available emulsions and their thicknesses and type of bases. In principle, neutron exposures can be determined by the number, length, and angular distribution of recoil proton tracks produced in the emulsion. In practice, neutron exposures can be estimated by simply counting tracks, provide that the emulsion is surrounded by the proper thickness of proton radiators. A track, viewed through a microscope, can be identified only if at least three grains have been developed, this corresponds to a length of about 3μ and a proton energy of 250 keV For unidirectional neutron beams, it is possible to use nuclear emulsions to determine fast neutron spectra (in principle, energies greater than 250 keV, but in practice, for energies greater than 500 keV). Special processing techniques must be applied to thick emulsions when used.

TABLE 6-2

Nuclear Emulsions for Particles Detection

Emulsion	Available Thickness**	Type of Base	Approximate Upper Energy Limit (MeV) for Particle Identification	
			Protons	Alpha
Eastman NTA*	25 1000	Glass or Plastic	3	10
Eastman NTB	50 and 100	Glass or Plastic	8	400
Ilford E1	To 400	Glass	20	250
Ilford G 5	To 2000	Glass	Very High	Very High

* Available with aluminum lamination as Kodak personnel neutron monitoring film, type B.

** Most emulsions are available in "pellets" without backing.

By "loading" the nuclear emulsion with boron, lithium, or other isotopes having large (n,α) or (n,p) cross sections, it is possible to use them as sensitive thermal neutron detectors. Because of the nitrogen already in the emulsions, thermal neutrons may also be estimated by covering a part of the emulsion with a thermal neutron shield, commonly 0.040 in. of cadmium, and observing the difference in the number of tracks in the shielded and unshielded areas caused by the $^{14}N(n,p)^{14}C$ reaction in the unshielded areas.

Advantages and Limitations of Film and Emulsion Techniques

The most outstanding advantages of film include the following: (1) Range of sizes down to the order of millimeters, (2) permanent record of measurement, (3) wide range of total exposures, (4) low weight for most application, (5) excellent spatial resolution, and (6) simultaneous recording of different radiations. Disadvantages of film include photon energy dependence, sensitivity to small changes in processing conditions, the quantity of processing time and equipment, latent image fading, sensitivity to temperature and humidity conditions for most applications, and the tedious effort and skill required for analyzing the nuclear emulsions. Film will be used for many applications in the future, but its role in personnel monitoring is expected to decrease as the use of solid-state devices, e.g., photoluminescent systems, increase.

Chemical Dosimetry

General Considerations of the Production of Radicals in Solutions by Radiation

Various chemical systems have been used to detect and measure radiation for many years. Those to be discussed briefly are solution types dependent upon the production of acids or free radicals by radiation. For example, acid generated in an organic solution containing an acidimetric dye produces a color change which can be related to dose qualitatively by inspection.

The detailed processes of irradiation produced effects in solutions is poorly understood even for water. Various reaction products are involved in further reactions and back reactions which rapidly become more complex as the number of reagents increases. However, for a given chemical system, the production of radicals to which the sensing element will respond can be empirically established and the system calibrated as a radiation detector.

The acid yield is generally specified in terms of "G" values, i.e., the number of acid radicals formed per 100 eV of energy absorbed in the medium. G values range from near unity to several thousand in various systems; yields higher than about 20 are indicative of chain reactions. In general, long chain reactions must be stabilized by such reagents as ethyl alcohol, resorcinol, etc., which render the system less sensitive and more stable than the unstabilized solution. A G value range of 15 to 30 covers most of the commonly used chemical dosimeter systems.

All sensitive chemical systems have one requirement in common; the reagents must be scrupulously pure. The best commercially available reagents must generally be repurified by multiple redistillation or recrystallization. Even slight traces of contaminants result in loss of stability and reproducibility. Containers must be nonreactive; a borosilicate glass, such as Pyrex

or neutraglas, ampole which has been steam cleaned and siliconed is best

Ferrous-Ferric System

The discussions of this dosimetry system are generally applicable to the ceric cerous system except for obvious differences. A solution of pure ferrous ammonium sulfate in 0.8 N sulfuric acid is the most commonly used ferrous ferric detector. Upon irradiation, ferrous ions are oxidized to ferric ions. The number of ions oxidized is directly related to energy absorbed from x or gamma radiation with the exceptions to be discussed. A spectrophotometer can be used to determine the amount of ferrous ion oxidized by measuring the absorption change at the 5100 Å peak or the ferric ion absorption change at the 3045 Å peak.

Because of the high effective atomic number (relative to air and tissue), the ferrous-ferric system exhibits a marked energy dependence for photons below several hundred keV. The exact height of the peak of the response curve, yield vs. photon energy, is a function of ampoule type and diameter. The most suitable range for the dosimeter is from about 5000 to 50,000 rads, and consequently the response as a function of fast neutron energy is not accurately known; the monoenergetic neutron sources most nearly free of gamma contamination, such as Van de Graaff generators, yield too low doses for most experimenters to conduct studies of response as a function of neutron energy. With proper control and calibration, the effects of room temperature, oxygen concentration, and dose rates on the system are usually negligible.

Chlorinated Hydrocarbon Chemical Dosimeters

Two types of chlorinated hydrocarbon dosimeters have been used frequently in the past. These are the "water equivalent single phase" dosimeter consisting of an aqueous dye solution saturated with the chlorinated hydrocarbon and the "two phase" dosimeter consisting of a chlorinated hydrocarbon overlayered with an aqueous dye solution.

The single phase dosimeter is a "short chain" type which is stable over periods up to a year and, with about 0.02% resorcinol, shows less dose rate and energy dependence effects than most chemical systems. Due to the hydrogen content, it is sensitive to fast neutrons. The chlorine renders the system sensitive to thermal neutrons. The G yield of the dosimeter is about 20.

A typical two-phase dosimeter consists of tetrachloroethylene with 0.1% resorcinol overlayered with about 25% by volume of water dye solution; a typical dye is chlorophenol red. The G yield of uninhibited C_2CL_4 may be as high as 6000, but in the stabilized dosimeter it is about 30. As the pH of the dye solution is changed from 6.0 to 5.0, the light transmission at 5800 Å increases, and the transmission at 4320 Å decreases. This corresponds to the usual operating range, and the color changes from red to yellow. The ratio of the transmission at the two wavelengths, 5800 Å and 4320 Å, is a monotonically increasing function of dose in this pH region as shown in Figure 6-1. This system exhibits a marked photon energy dependence of response below 500 keV unless filtered to "flatten" it, but is not rate dependent for dose rates at least as high as 4000 rads/min. It is temperature insensitive from about 5°C to 55°C, and the response is linear with total dose to greater than 100,000 rads. Thermal neutrons effect a large response (1 tissue rad n_t produces a response equal to about 5 tissue rads of gamma radiation), but 1 tissue rad of fast neutrons yields less than 5% of 1 tissue rad of gamma rays. These

dosimeters are stable over periods of years; an exception is the least inhibited, i.e., most sensitive ones for less than 50-rad exposures, which is stable for approximately 1 year.

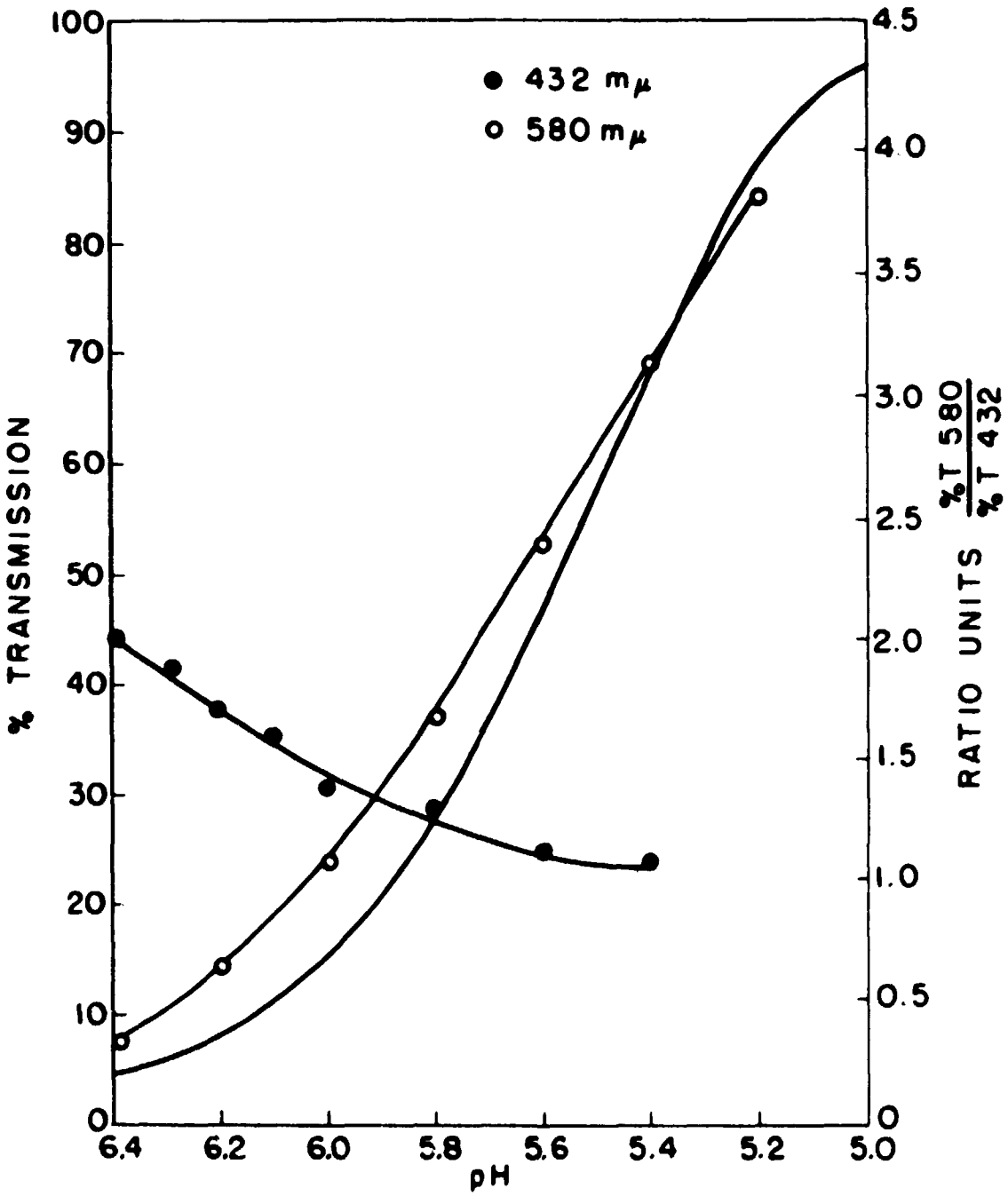

Figure 6-1

Percent Transmission at 580 mμ and 432 mμ (Left Scale) and the Ratio of Transmission 580/432 mμ as a Function of pH.

Advantages and Limitations of Chemical Dosimeters

Perhaps the greatest attribute of chemical dosimeters is the wide range of applications for which one type or another can be made They are economical when made in large numbers and they, like film, can be made in a great range of sizes For very high doses ($> 10^5$ rads), chemical systems are perhaps the most suitable integrating system available For lower dose (< 1000 rads), they are extremely sensitive to chemical and ampoule purity and require care and experience for stable reproducible dosimeters

Luminescence Dosimetry

Discussion of the Response to Radiation

Radiation-induced coloration and luminescence of crystals and glasses have been studied for many years. Commencing about 1950, a rapidly increasing number of studies of silver-bearing glass for dosimetry purposes was reported; much of the work was done at the U. S. Naval research Laboratories.

In general, many substances exhibit phosphorescence and coloration when exposed to radiation; in the gaseous state at sufficiently low pressure, the atoms of such substances exhibit resonance fluorescence, i.e., wavelenths characteristic of the atomic energy levels consisting of a spectrum of discrete lines. These lines represent the permitted transitions from various energy levels of electronic excitation to the ground state

In ideal crystals, there are forbidden energy zones between the permitted energy levels. Due to this periodic field of potential, irradiation in the ultraviolet absorption band has no permanent effect on the crystal. For example, an anion in an alkali-halide crystal loses an electron and is changed into a halogen atom or "positive hole". Such an electron immediately returns to its positive hole and there is no permanent effect on the crystal. The introduction of impurities or imperfections into the lattice structure disturb the periodicity of the lattice structure and produce localized energy levels which in ideal crystals would lie in the forbidden zone. The energy levels for ideal crystals and for real crystals having impurities are shown in Figure 6-2. Electrons raised to the conduction band can fall back into these defect levels and become bound to the defect. Hence, an impurity-bearing crystal may be changed by radiation and possess a changed absorption spectrum

When silver-bearing metaphosphate glass is exposed to radiation, two pronounced effects are observed: (1) The absorption peak shifts from 2400 Å to 3300 Å; (2) the emission spectrum peak shifts from 3700 Å to 6400 Å Either of these effects may be utilized for dosimetric purposes. The change in absorption at one peak or the ratio of absorption at both peaks can be related to x or gamma radiation dose, with the exceptions noted below. Also, the fluorescence at the 6400 Å emission peak may be excited by 3000 Å ultraviolet and related to x or gamma radiation dose. Schulman *et al.* have described this latter effect as "radiophotolumir.escence", a term defined by Przibram as "that phenomenon whereby a material, originally nonluminescent under uv or visible light, is made responsive to such excitation by pretreatment with gamma rays or x rays", with the further distinction that the newly created stable luminescent centers would not be destroyed by the uv radiation that is used to excite them. Studies of these two effects have centered chiefly on one type of glass, and development of dosimeters has followed similar

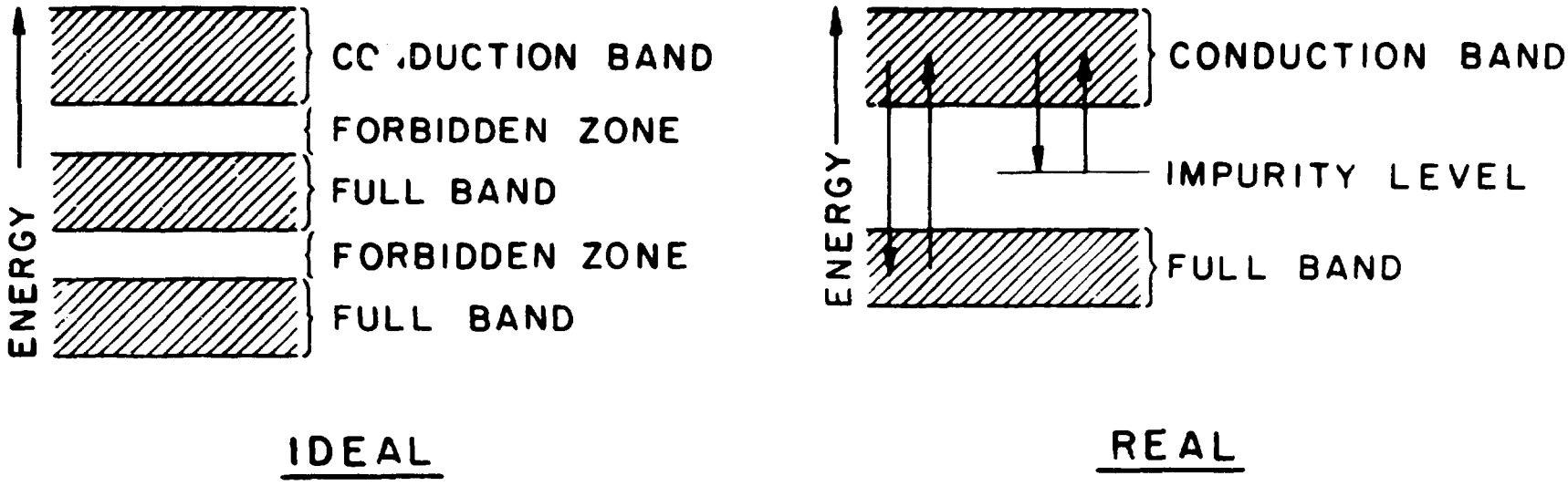

Figure 6-2

Energy Level Diagram for Real and Ideal Crystals.

lines, so the descussion below will be limeted to the radiophotoluminescence phenomenon and a metaphosphate glass, e.g , one comprised of 46% $Al(PO_3)_3$, 23% $Ba(PO_3)_2$, 23% KPO_3, and 8% $AgPO_3$, by weight.

When such glass is exposed to radiation, loosely bound electrons are released from the negative ions of the glass, and some of them are trapped by interstitial silver ions, forming a special type of F center, or 'luminescent center'. In the capture of liberated electrons, the Ag^+ ions are in competition with electron traps which arise from irregularities, i.e., impurities, in the molecular structure of the glass. The traps provide alternate energy levels which can be occupied by electrons. The distribution of electrons between Ag^+ ions, and other traps will control the relationship between electrons liberated in the glass by radiation and the fluorescence. When the Ag^0 atoms formed by electon capture (metastable) are exposed to uv light, they absorb energy and upon returning to ground state fluoresce with a peak at about 6400 Å.

Silver Metaphosphate Glass as a Gamma Dosimeter

In order to calculate the energy absorbed by a glass detector, assume that the response of the detector (or the Ag^0 atoms produced) is proporrional to the number of electrons freed in the detector. The spectrum of tertiary electron (the vast majority of the electrons formed by radiation are tertiaries) has been shown to be an insensitive function of photon energy. Then the glass response should be directly proportional to the energy deposited in it by ionizing electons, which, under electron equilibrium conditions, is equal to the energy deposited by the incident photons. Assume a uniform radiation field of photons of energy n(E) and a glass detector exposed in it under equilibrium conditions of such size as not to perturb the field significantly. Then the energy absorbed per cm^3 of glass can be written as

$$E_a = \Sigma\, nE\; e^{-[(\mu_i)\tau]/\rho} \qquad (6\text{-}3)$$

where nE_i is the fraction of photons of energy E_i, and μ_i = the average total mass absorption cross section (σ_T σ_C and σ_P, the photoelectric, Compton and pair production cross sections, respectively) for the elements in the glass for photons of energy E_i, τ is the thickness of the glass, and ρ the density.

A widely used detector composed of the metaphosphate glass described consists of a small glass rod 1 mm in diameter by 6 mm long. Although several varieties of glass are available commercially, that mentioned above, i.e., the 'high Z' glass, has been evaluated for the greatest variety of radiations and energies. The characteristics of the response of this detector are given in the paragraphs below.

Figure 6-3 shows the calculated response of the 'high Z' detector as a function of photon energy. Also, the figure shows a typical measured response curve for various x-ray spectra as a function of 'effective' energy. 'Effective' energy is defined as the energy of a monochromatic beam which has the same absorption coefficient as the given beam in an incremental thickness of standard filter material. Of course, many of the photons lie well above and below the effective energy causing the peak of the curve to be reduced in height and width. A third curve in this figure represents the response calculated by utilizing Villforth's calculation of Kramer's energy distribution of filtered x rays; the agreement of these values and the

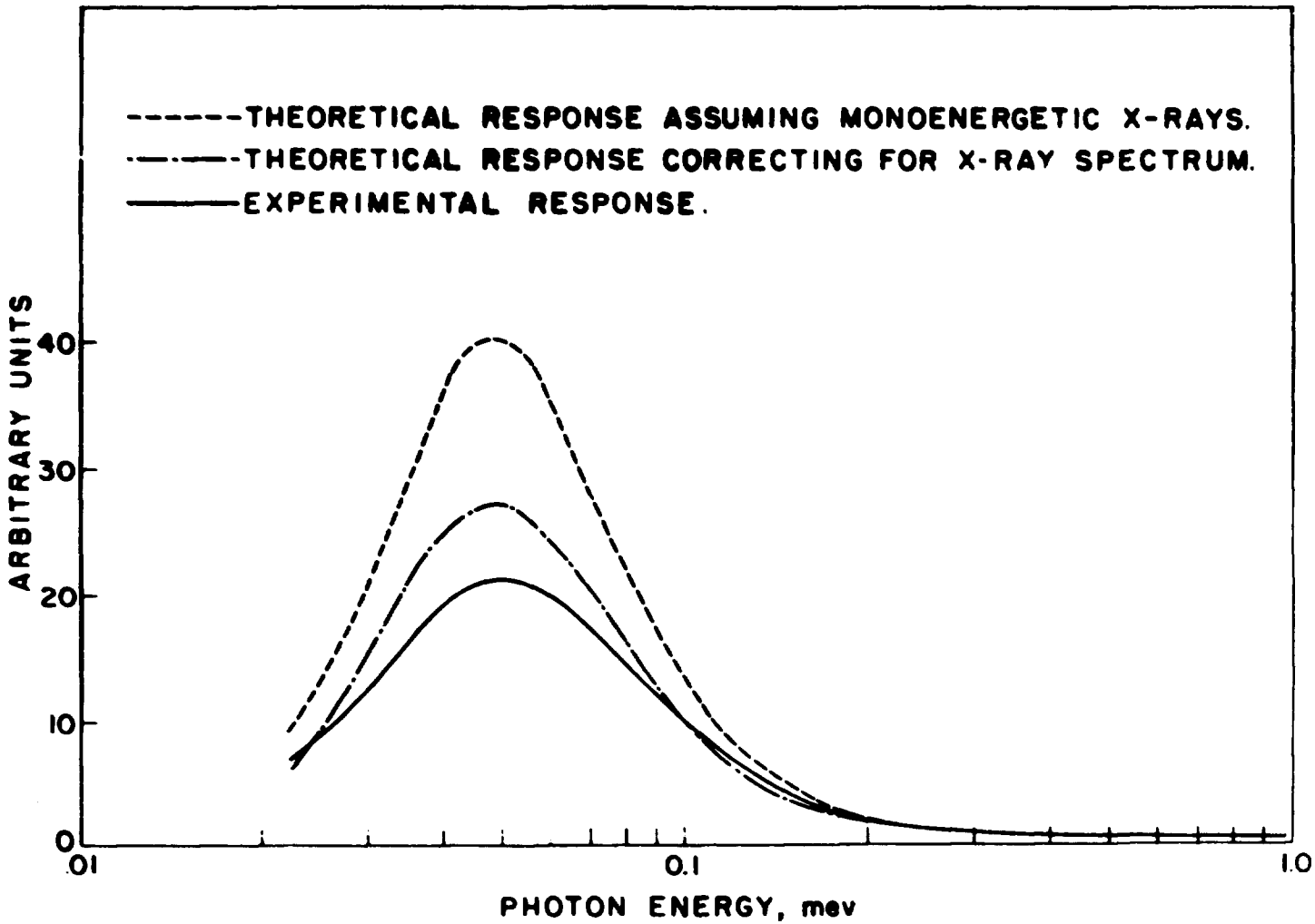

Figure 6-3

Comparison of the Theoretical and Experimental Photon Response of the Unshielded Glass.

experimental ones are good considering the many approximations used Figure 6-4 shows the effectiveness of some typical encapsulation techiques for flattening the peak in the response vs. photon energy curve. For photons greater than 300 keV, the effective dose range of these detectors is linear from about 5 to about 10,000 rads Such detectors have little or no dose rate dependence, but the long range fading characteristics are not as good as those of the "low Z" glass developed more recently. Cheka has examined the glass characteristics with a view to adapting the detector for personnel monitoring It appears to be suitable for most applications including those requiring frequent reading, as it may be read at intervals without affecting the integrated response.

Response of the Metaphosphate Glass to Neutrons

The principal thermal neutron absorber in the glass is silver, ^{107}Ag and ^{109}Ag, with cross sections of 30 and 84 barns respectively As both ^{108}Ag and ^{110}Ag are beta gamma emitters with short half lives (2 4 min and 24 sec, respectively), there is no prolonged buildup after exposure. Because of the small size of the detectors, the beta particles contribute most of the response. The measurement of gamma dose in a field of coexistent thermal neutrons and gamma rays may be accomplished by encasing the rods in a neutron absorber that does not emit beta or gamma rays Lithium 6 with an (n,α) cross section of 945 barns is commonly used.

Although the energy deposited in the glass by fast neutrons as a function of neutron energy may be calculated, the effectiveness of the ionization produced by the recoil ions cannot be assumed to be the same as for the fast electrons, i.e., 'columnar' recombination along the path of such a particle might remove many of the electrons before they could migrate to silver ions. Evidence has indeed been found that heavy particles are less effective in producing fluorescent response.

An experimental determination of the response of the glass to fast neutrons has been reported for a limited energy range, and others have reported measurements at 14 MeV. Figure 6-5 shows the response for neutrons of 0.5 to 1 5 MeV exposed in a fluoroethene capsule and uncorrected for the low gamma radiation background in the Van de Graaff target room. The data are sufficient to indicate the low sensitivity to fast neutrons

Advantages and Limitations of the Metaphosphate Glass Dosimeter

The commercially available system offers a reliable, economical, and fast neutron insensitive method for gamma radiation dosimetry For many applications, such as tissue implantation, the small size is of most importance As repeated readings can be made without destroying the fluorescence, the detector offers the possibility of a "life time" integrated reading. The marked dependence of the response on photon energy in the photoelectric region and the sensitivity to thermal neutrons are the greatest limitations of the unencapsulated glass. For the most accurate work, prereadings are required on all dosimeter, and care must be taken to clean the glass thoroughly before evaluation of the fluorescence is attempted.

New types of glass and new readers are being produced more and more frequently. The new "low Z" glasses available in West Germany and Japan make possible measurements of total exposure as low as 10 to 20 mR with a precision of about ± 30% They also have exhibited

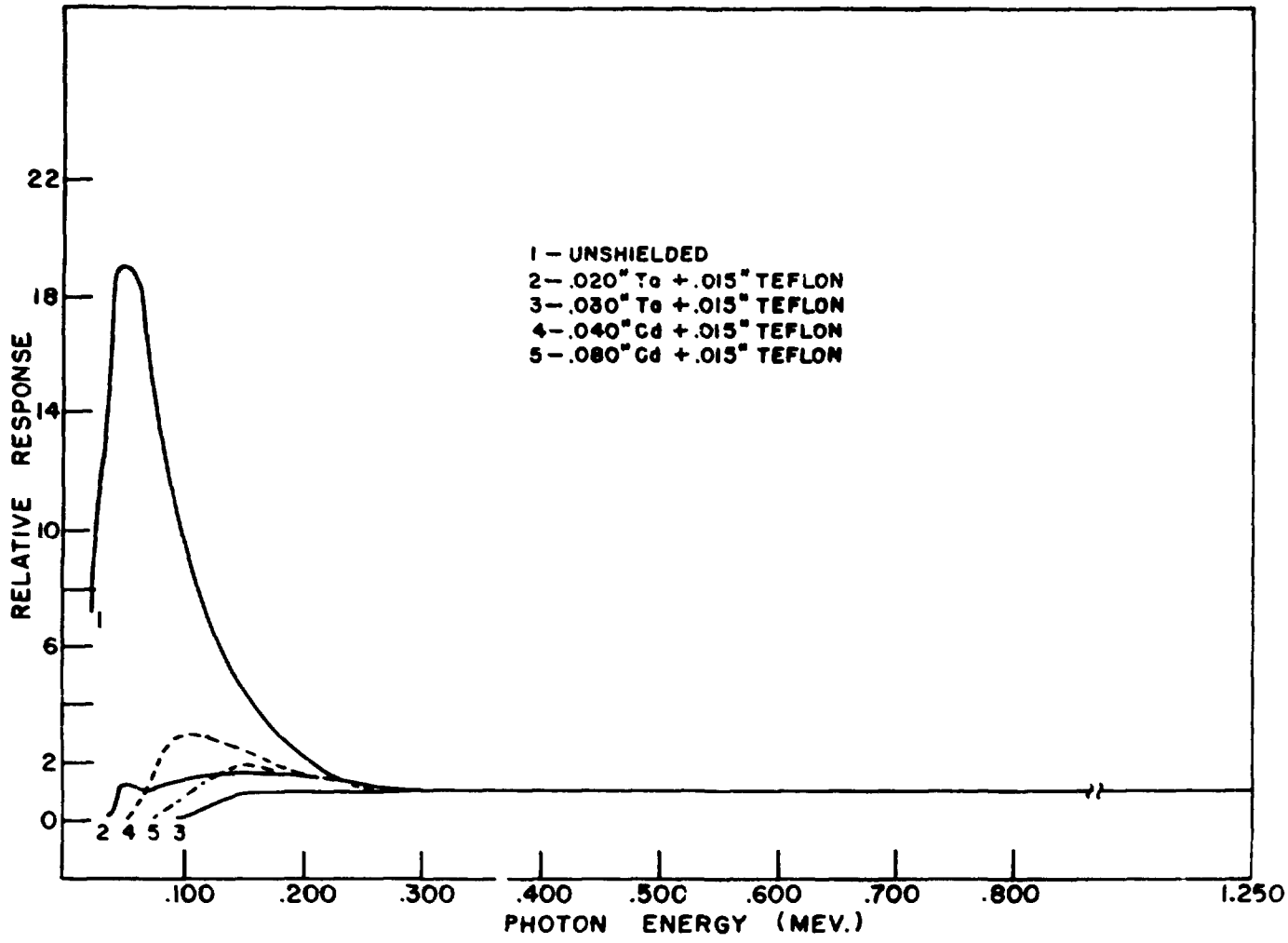

Figure 6-4

Luminescent Response of Glass Rods as a Function of Photon Energy for Various Shields.

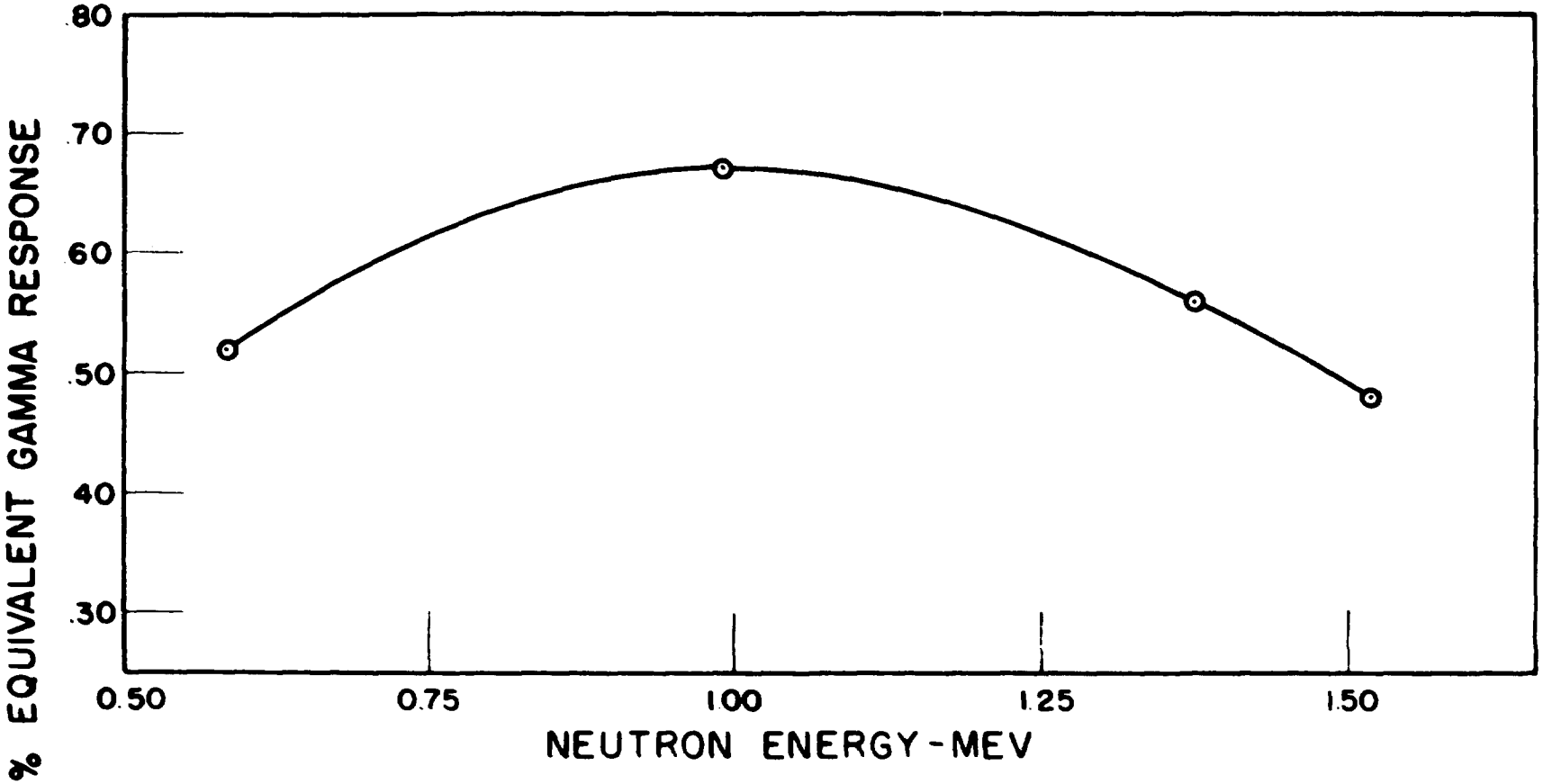

Figure 6-5

Neutron Response of Glass Relative to ^{60}Co Gamma Response

markedly less dependence of response per unit exposure as a function of photon energy as they are composed of $LiPO_3$ with just a few percent of Li_3PO_4

Thermoluminescence Dosimetry

Much of the preceding discussion can be applied to thermoluminescence, the process by which a substance, not normally luminescent when heated to temperatures below its thermally luminescent threshold (optical), can be made to luminesce at these temperatures by pretreatment with ionizing radiation The chief chemicals used for this application are CaF and LiF, the former being more sensitive and the latter exhibiting less "energy dependence" The thermoluminescent systems are suitable for the same applications, in general, as the photoluminescent systems, but there are a few differences which may be noteworthy The thermoluminescent systems are more sensitive, and exposures of the order of 1 mR have been detected with CaF This system of dosimetry is less dependent in response on photon energy than the photoluminescent system if LiF is used, but it is also more sensitive to neutrons which hamper its use in coexistent neutron photon fields The thermoluminescent system is also, in general, somewhat less convenient to use than the photoluminescent system because of the dry powder form in which the fluoride is used More convenient forms of thermoluminescent detectors have recently been developed and have come into wide use Many laboratories are using thermoluminescent dosimeters for personnel monitoring

A second feature of the thermoluminescent system is the erasure of the response during reading If repeated use of the detector for unrelated measurements is desired, this feature is an advantage; if long term accumulation of exposure with intermediate readings is desired this feature is a disadvantage The latter disadvantage can be overcome in many instances by utilizing several detectors simultaneously at the point of interest with sequential removal for evaluation

Thermally Stimulated Exoelectron Emission (TSEE)

Another method of dosimetry which is very similar to thermoluminescence involves a phenomenon called thermally stimulated exoelectron emission (TSEE) Although TSEE has been demonstrated for over forty years, the major portion of work in this area has been accomplished in the past ten years Basically, the quantitative measurement of thermally stimulated emission of low energy electrons from the surface of irradiated ionic crystals can be used as a method of integrating radiation dosimetry A very large amount of effort has gone into TSEE research The most promising material in use is a ceramic BeO, although other metallic oxides are coming under investigation Despite some difficulties in the interpretation of results, it seems safe to assume that the obvious similarities of thermoluminescence and TSEE indicate a similar basic mechanism

General Discussion of Scintillators

The modern scintillation counting system consists of a scintillator, a photomultiplier tube with a magnetic shield, and the associated electronics to amplify, analyze, and display the output In general, there is radiation shielding for the detector assembly Two types of associated electronics are common, pulse amplification and pulse height analysis and current amplification and display

Scintillation detectors, phosphors, of many types are available for many applications. The phosphors include organic solids, organic phosphors in plastic solids, organic solutions, inorganic solids, and inorganic gases.

Much of the discussion of luminescent centers and the excitation of metastable states given in the preceding section parallel the theory of phosphors; a major difference is the decay time of excited states. In the crystalline detectors such as NaI (Tl), the thallium activation or impurity centers are the luminescent centers as well; the impurity center absorbs some of the excitation energy of the atoms of the crystal and emits photons in the wave-length region typical of the NaI (Tl) scintillator. The amount of impurity is small, usually within the limits of 0.01% to 1%. In the various noncrystalline scintillators, some of the excitation energy in the medium, e.g., the solvent, is absorbed by the organic molecule which undergoes de-excitation in the wave-lengths characteristic of the phosphor.

Table 6-3 lists some typical, commonly used scintillators and some of their characteristics. The values are taken from several of the general references, and some values are averages of reported values.

TABLE 6 · 3

Some of the Characteristics of a Few Typical Scintillators

Name and Composition of Scintillator	Density g/cm^2	Peak Emission Wave Lenght Å	Scintillation Yield Relative to Anthracene*	Pulse Decay Time μ/sec
Organic				
Anthracene $C_{14}H_{10}$	1.25	4450	1.0	0.03
Stilbene $C_{14}H_{12}$	1.16	4100	0.7	0.007
P-Terphenyl in Xylene C_8H_{10}	0.86	4100	0.2	0.008
Inorganic				
Zinc Sulfide Zns	4.1	4500	1 to 2*	∼10
Sodium Iodide NaI (Tl)	3.67	4100	∼2	0.025
Calcium Tungstate $CaWO_4$	6.06	4300	∼0.75	∼1

* Zinc sulfide scintillations (yield and decay) are sensitive to the crystas' history e.g., quenching.

Once the scintillations are produced, the photons must reach the photocathode of the photomultiplier to produce a response. Typically, solid scintillators are surrounded, except on the phototube side, with thin reflectors of materials such as MgO or Al_2O_3, and the scintillator with a light pipe and phototube joined either directly or with silicone grease (or a similar viscous liquid) between the faces. In either case, Lucite is a common light pipe which transmits a high fraction of the light, and, in addition, is frequently used to avoid having surfaces with large differences in refractive index directly coupled; large differences cause greater reflection losses.

Photons that pass to the photocathode surface eject electrons from it. These electrons are focused by electric fields to the first of several successive multiplying electrodes or "dynodes", at which each electron will, typically, cause the ejection of about four others. As phototubes generally have 8 to 11 such dynodes, the overall multiplication is of the order of 10^6. A large variety of tubes are available. The range of photocathode sizes is from less than a square inch to hundreds of square inches of area. The peak response wave lengths for the more common tubes range from less than 4000 Å to greater than 5000 Å. Although most photomultipliers have circular end windows and photocathodes, a few are available with a side window and photocathode. The output of the phototube may be fed into one of a large variety of electronic systems. The electronics systems for application in scintillation work comprises an extensive field, and the reader is referred to many comprehensive works on that subject.

Scintillation Counters for Beta-Gamma Dosimetry

The scintillation produced by a fast electron in the scintillator is directly proportional to the energy absorbed over a wide energy range. Consequently, in "thick" detectors (thickness greater than the path length of the most energetic electrons), the energy distribution may be determined by pulse height analysis. For beta particle and fast electron counting, anthracene is commonly used. Inorganic phosphors, e.g., NaI (Tl), are widely used in gamma-ray spectroscopy. The relatively high Z of these phosphors and consequently their high photoelectric cross sections make possible the total absorption of many photons even in relatively small crystals, e.g., 2 in. x 2 in. cylinders. An incident photon of 1 MeV, for example can undergo a Compton interaction in the crystal and impart some fraction of its energy to an electron resulting in a scintillation; the scattered photon can then interact in the photoelectric region which, of course, results in all the remaining energy causing a scintillation which is simultaneous, in the time scale of the apparatus, with that of the Compton electron. The output pulse is then proportional to the total energy of the incident gamma ray.

Scintillation Counters for Neutron Dosimetry

Typically, organic phosphors having a large hydrogen content are used in scintillation counters for neutron measurements. In principle, neutrons collide elastically with the hydrogen nuclei; these recoil protons then expend their energy in the phosphor producing a pulse which is directly proportional to the energy absorbed provided the crystal is large relative to the proton path lengths of interest. If the phosphor is "tissue equivalent", or nearly so, the scintillation output is equal to absorbed tissue dose for a specimen of the size of the detector; for typical detectors, this is equivalent to first collision tissue dose.

However, there are no pure neutron fields, the gamma radiation in the field will also react

with the phosphor complicating the measurement Many devices and techniques have been developed to desensitize effectively the detector to gamma rays It is beyond the scope and space of this chapter to list and discuss these techniques of such a rapidly changing field It is suggested that the reader refer to the large volume of material published monthly on neutron spectroscopy by scintillation techniques

Thermal neutron and slow neutrons are frequently detected by using phosphors containing atoms having a large cross section for (n_t,P) or (n_t,α) reactions such as the ${}^{6}_{3}Li(n_t,\alpha){}^{3}_{1}H$ reaction

Advantages and Limitations of the Scintillation Sistem

Perhaps the greatest advantage of the scintillation detector is its high sensitivity Another feature, also related to the relatively high density, is the applicability to spectroscopy The wide range of sizes and shapes of the various phosphors is a distinct advantage as is the great resolution of events in time and the range of elemental composition (especially hydrogen) The complexity of associated equipment necessary for many applications is frequently a disadvantage Sensitivity to electric and magnetic fields is often the limiting factor in the use of scintillation equipment In general, scintillation detectors have low sensitivity to low energy radiation because of the bias against 'noise' and poor energy resolution compared with, for example, proportional counters

Calorimetry

In principle, calorimetric determination of the energy absorbed by the medium of interest from the radiation beam of interest represents the ideal measurement of that one parameter, i.e. absorbed dose This assumes that all of the energy absorbed is converted to heat If one were interested in the energy that a certain x ray beam would impart to a cm^3 of H_2O, one would simply place the water in the beam in a well insulated container and measure the temperature rise as a function of time

The most limiting factor in calorimetric dosimetry has been for many years the inadequacy of thermometry systems The temperature changes to be measured are generally small relative to those that can be measured accurately by resistance changes, the thermoelectric effect, or the physical expansion of the absorber However, since about 1945, a more sensitive temperature detecting element has been available; this is the "thermistor". Thermistors are metallic oxide semiconductors which have high negative temperature coefficients A typical thermistor is the type 12A Western Electric which exhibits a negative temperature coefficient of 3.9% per degree centigrade at 20°C

The resistance change of the thermistor can be readily measured with a Wheatstone bridge and a galvanometer; most researchers use a dc amplifier and a recording galvanometer Figure 6-6 shows a temperature vs resistance plot for a thermistor

The two most frequently used calorimeter systems are the total absorption and the low perturbation types Calorimeters of the total absorption type have been reported in which sensibly all of the incident radiation is absorbed For determining the first-collision energy absorption, a low perturbation calorimeter is necessary, i e , one which does not significantly alter the radiation field

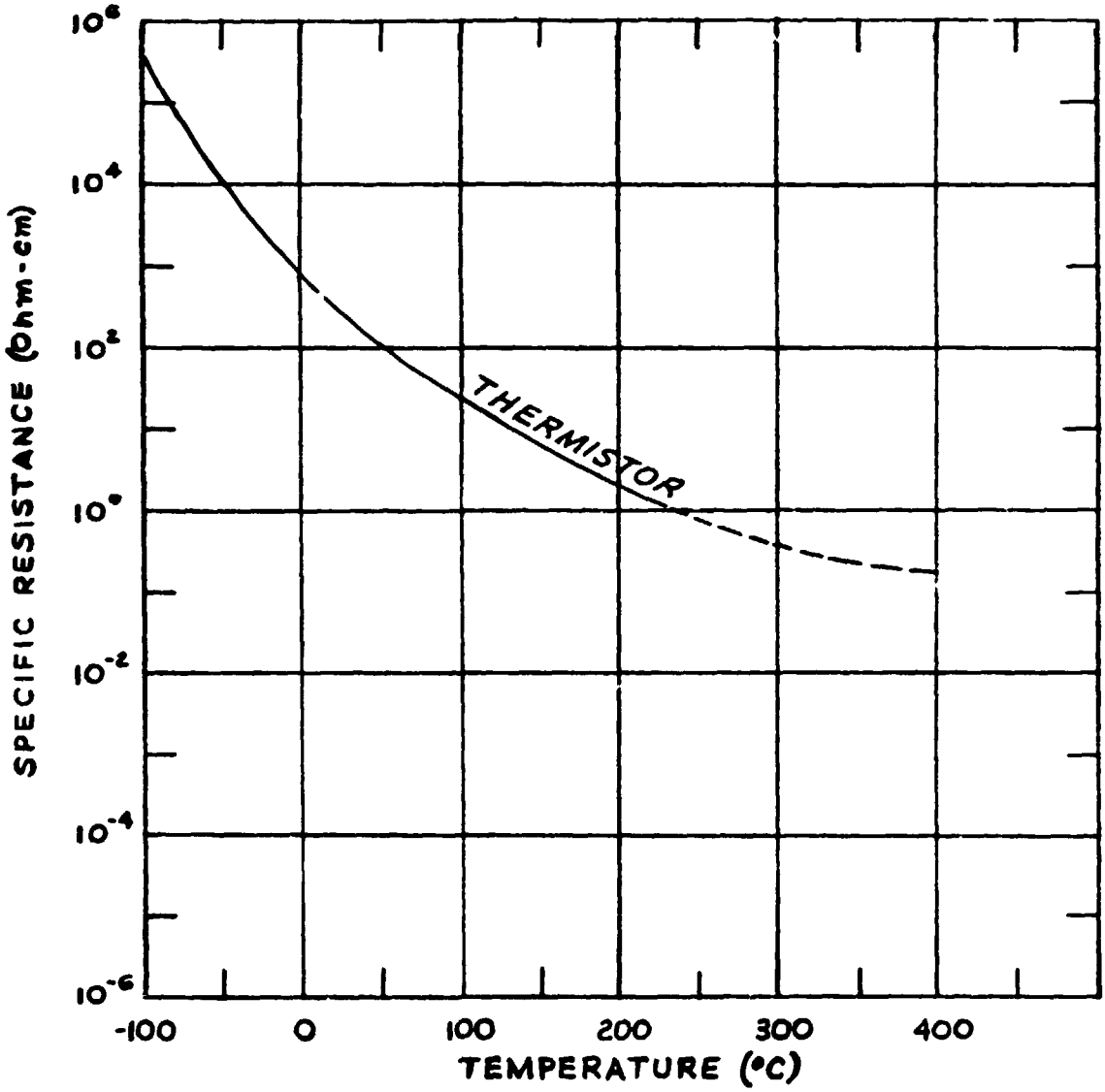

Figure 6-6

Logarithm of the Specific Resistance vs. Temperature of Thermistors Composed of the Oxides of Manganese, Nickel, and Cobalt

Total Absorption Calorimeter

For some applications, the total energy flux in a beam of radiation is desirable, e.g., in teletherapy. For measurements of this type Laughlin *et al.* designed a total absorption calorimeter. Basically, a lead cylinder exposed end-on to a collimated beam was used as the total absorber. The 6.2-cm-diameter by 3.4-cm long lead-filled cylinder, containing a small heating element and a thermistor, was suspended in an evacuated calorimeter box having thin-walled apertures for the radiation beam entrance; the box was then surrounded by a controlled-temperature oil bath, except at the radiation entrance ports. The thermistor was incorporated in a Wheatstone bridge circuit, the output of which was connected to a dc amplifier which was followed by a recording potentiometer. Calibration was based on absolute energy input by the heating coil. Measurements of intensity of x rays (400 kV self rectifying with 1.75 mm total equivalent filtration) gave excellent agreement with theory and with measurements utilizing ionization chambers.

Low-Perturbation Calorimeters

An example of a low-perturbation calorimeter is that used by Kalil *et al.* to measure electron stopping power of foils. In this case, foils of the order of 100 micrograms per cm^2 were the absorbing layer and caused little perturbation of a fast electron beam. For x- or gamma-ray measurement, thicker absorbers could be used.

The major components of the calorimeter used by Kalil included the foil, a low-mass mounting ring for the foils and thermocouples, two sets of six each copper-constantan thermocouples and a massive aluminum heat sink inside which the other parts were mounted. These parts were then assembled inside an accelerator tube, and the thermocouple leads connected to one of two circuits, those for six thermocouples to a "cooling circuit" and those for the other six to the monitoring circuit. A potential could be applied to the thermocouples in one of the thermopiles so that by the Peltier effect, the foil could be heated or cooled; these two effects are reversible. The heat generated in or absorbed by the junction is equal to the product of its thermoelectric power, the absolute temperature, and the current flow through it. Consequently, the calorimeter had a built-in absolute calibration device, assuming appropriate circuitry. For low absorption measurements, e.g., first-collision dose, such calorimeters hold considerable promise.

Advantages and Limitations of Calorimetric Techniques

Assuredly, the greatest advantage of calorimetry is that it yields energy absorption in absolute units. For facilities where it can be used for routine work, it offers a reliable and reproducible standard. In general, the limiting parameter is relatively low sensitivity and the size and complexity of the apparatus. Calorimetric measurements frequently require more time and analysis than other systems.

Threshold Detectors

General Discussion of the Method

For measuring high neutron dose rates, such as from critical assemblies, the range of

proportional counters or other rate-type dosimeters is frequently exceeded. A desirable neutron dosimeter feature for these high rates would be that it store a latent image, i.e., exhibit a reaction effect such as the film, glass, or chemicals do for gamma radiation. An obvious conclusion is that the neutron reaction products in various elements might be made to suffice. One approach might be to observe neutron reactions that exhibit energy thresholds, e.g., the $^{32}S(n,p)^{32}P$ reaction which has a threshold at about 2 MeV and a reaction product which may be analyzed readily by means of the hard beta ray. By utilizing several threshold reactions, the neutron flux as a function of energy may be determined approximatly, and the tissue (or other) dose calculated.

The ORNL Threshold Detector System

Hurst *et al.* and Reinhardt and Davis have utilized four threshold detectors, plus the gold and gold shielded by cadmium detector for thermal neutrons, to measure neutron spectrum and dose. The fast neutron detectors are ^{239}Pu, ^{237}Np, and ^{238}U fission foils and ^{32}S. The ^{239}Pu is exposed in a ^{10}B shield to effect a threshold at about 4 keV. Figure 6-7 shows the cross section curves of the detectors to an energy of 6 MeV. Table 6.4 shows the effective cross sections and thresholds of the detectors and gives an indication of the sensitivity; the fission foils are commonly evaluated by using 2 NaI (Tl) 4-in. scintillators, 4-in. diameter and 2-in. thick, one on each side of the foil. The half-life of the ^{32}P from the $^{32}S(n,p)^{32}P$ reaction is 14.3 days and the beta-ray energy is 1.71 MeV. However, the delayed fission gamma rays from the fission foils exhibit a rapidly changing half life; Figure 6-8 shows the decay curves for these gamma rays. A typical flux histogram determined by the Hurst system of threshold detectors is shown in Figure 6-9.

Advantages and Limitations of Threshold Detectors

The major advantages of threshold detectors include the extremely high dose rates and integrated dose at which they can be used and the insensitivity to gamma radiation (negligible response to gamma rays of less than about 20 MeV). It is also advantageous to have an indication of neutron spectrum in addition to dose.

The most serious limitations of most threshold detectors result from the rapid decay of the reaction products (fission-product gamma rays) and the relatively complex and expensive equipment for evaluation. Except for installations equipped for automatic or semiautomatic reduction of count rate to flux and dose, these evaluations are somewhat time consuming.

Recent improvements in this system include the introduction of track-etch techniques which essentially eliminate the disadvantage of the rapid decay of the reaction products.

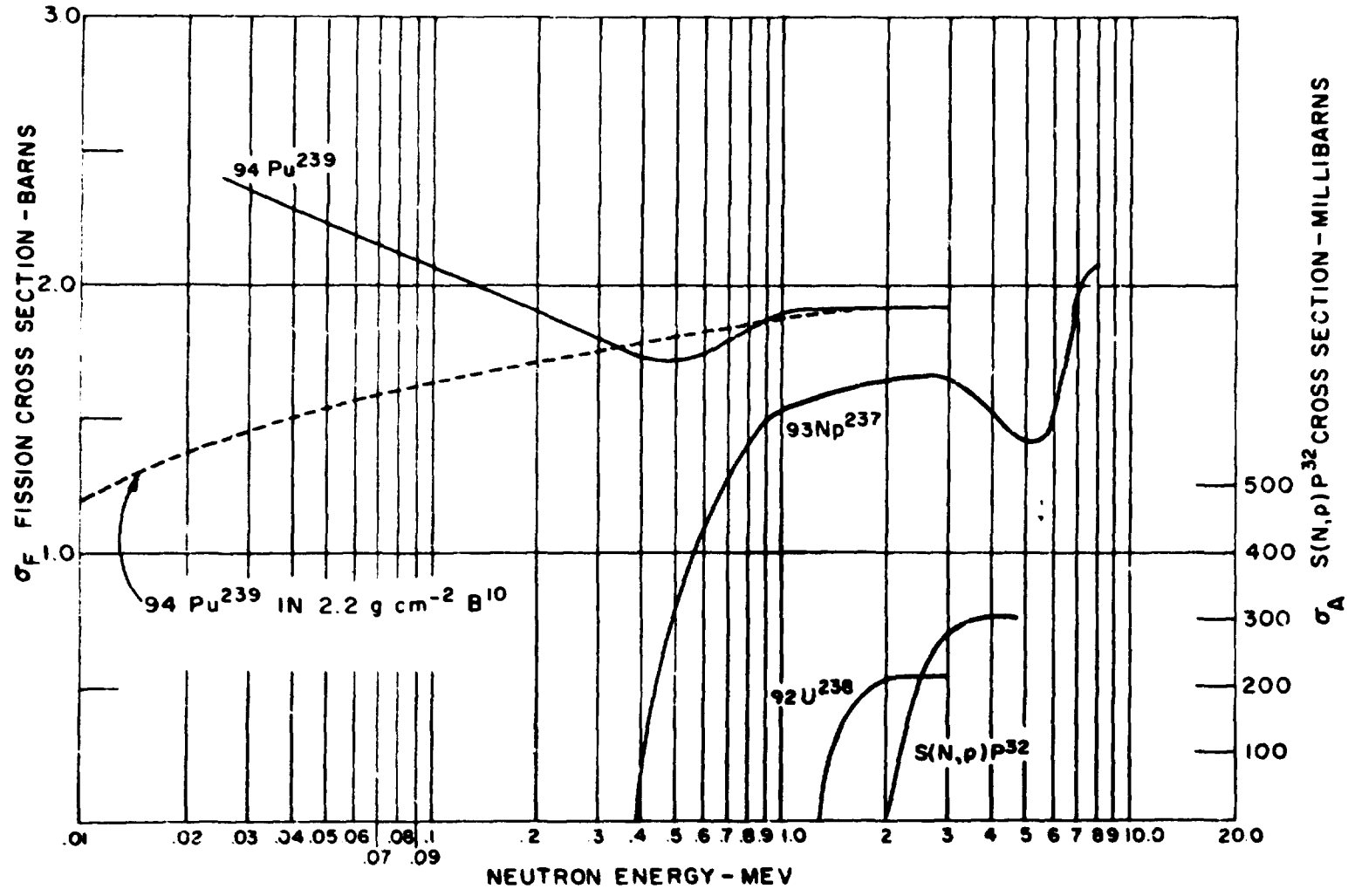

Figure 6-7

Fission Cross Section (Left Scale) and Activation Cross Section (Right Scale) of Threshold Detectors.

TABLE 6-4

Effective Thresholds and Cross Sections for the Foils Used in the Hurst Threshold Detector System

Detector	Threshold	Cross Section	Background		10 rad Neutron** 1 hr Post Exposure (c/m/g)
			Counter* (c/m)	Foil (c/m/g)	
^{239}Pu	∿ 1 keV	2.0×10^{-24} cm^2	280	970	1900
^{237}Np	0.75 MeV	1.6×10^{-24} cm^2	280	0	1440
^{238}U	1.5 MeV	0.55×10^{-24} cm^2	280	80	2520
S	2.5 MeV	0.224×10^{-24} cm^2	22	0	54
Au and Au + Cd	Thermal	Direct Calibration	50	0	†

*Fission foils "counted" by placing between two 4-in.-diameter by 2-in.-thick NaI (Tl) crystals. Sulfur samples "counted by placing on a 1 1/2-in.-diameter by 1/8-in.-thick plastic scintillator. Au samples "counted" by placing on a 1 1/2-in. by 1-in. NaI (Tl) crystal.

**Exposed to Godiva II at Los Alamos Scientific Laboratory. This neutron spectrum from this reactor is a somewhat softened fission spectrum.

†Of the order of several hundred c/m, but sensitive to the exposure environment due to scattering in walls, floors, etc.

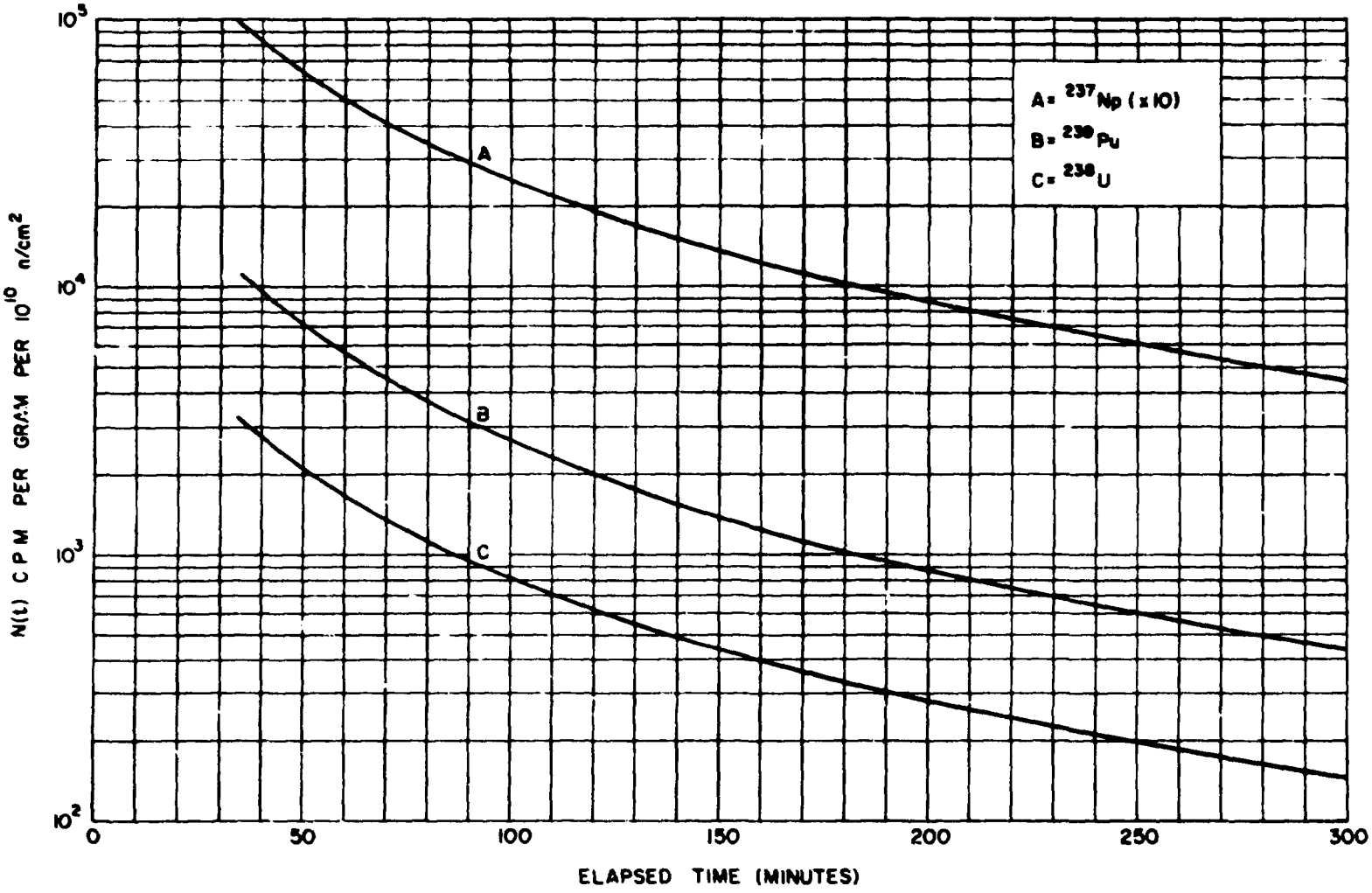

Figure 6-8

N(t) as a Function of Elapsed Time for ^{239}Pu, ^{238}U, and ^{237}Np.

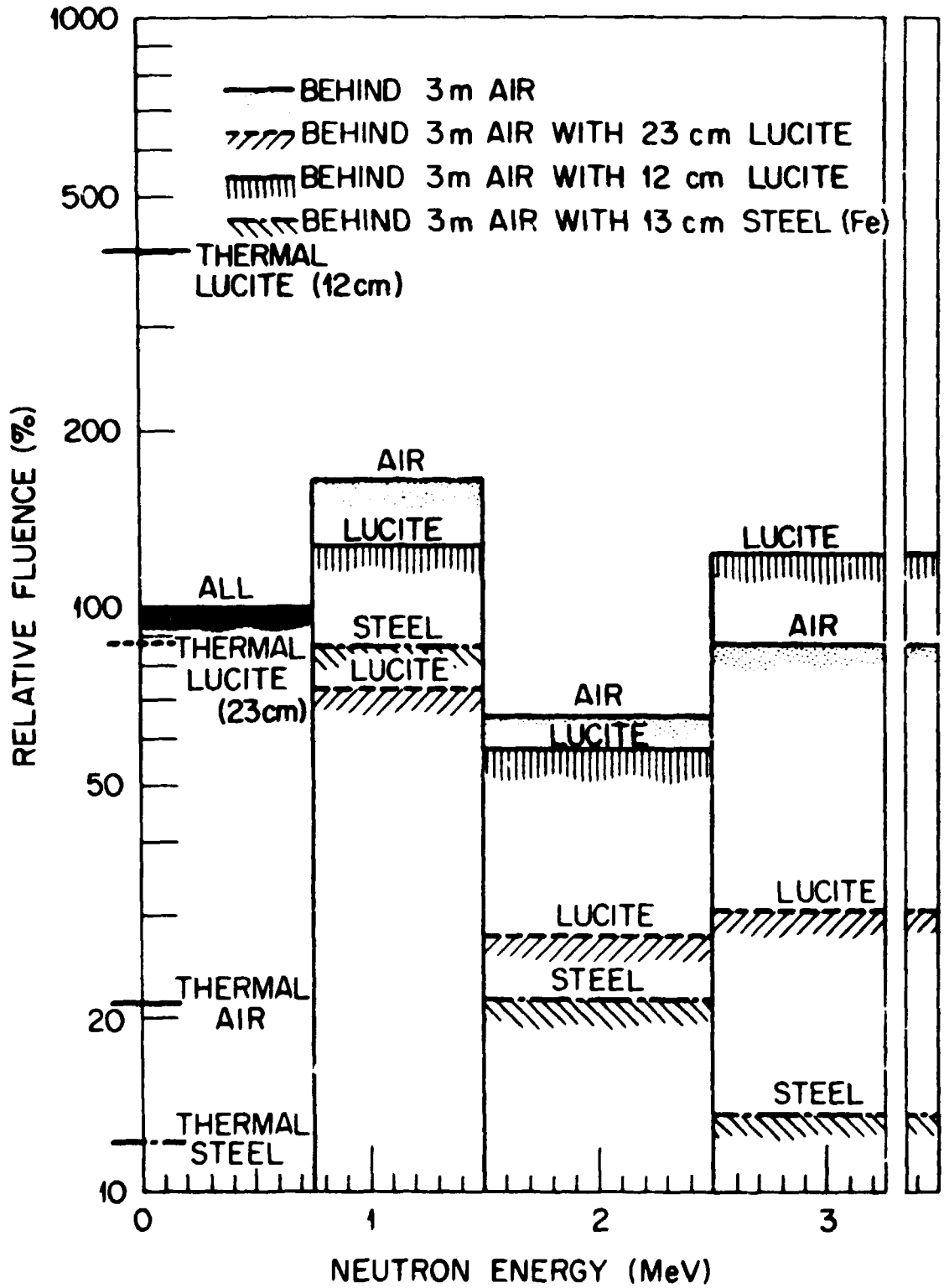

Figure 6 9

Health Physics Research Reactor (HPRR) Neutron Fluence Spectra

BIBLIOGRAPHY

1. K. Z. Morgan and J. E. Turner, *Principles of Radiation Protection*, John Wiley and Sons, Inc., New York, 1967.

2. G. S. Hurst and R. H. Ritchie, editors, *Radiation Accidents. Dosimetric Aspects of Neutron and Gamma Ray Expossures*, ORNL 2748, Part A, May, 1961.

3. *Measurement of Absorbed Dose of Neutrons, and of Mixtures of Neutrons and Gamma Rays*, National Bureau of Standards, Handbook 75, February, 1961.

4. J. A. Auxier, K. Becker and E. M. Robinson, editors, *Proceedings of Second International Conference on Luminescence Dosimetry*, CONF 680920, September, 1968.

5. F. Kalil, et al., *Stopping Power of Thin Aluminum Foils for 12 to 127 keV Electrons*, ORNL 2731, September 3, 1959.

6. J. S. Laughlin, et al., Am. J. Roentgenol., Radium Therapy and Nucl Med., *LXX*, 294 (1953).

LECTURE Nº 7

DOSE FROM ELECTRONS AND BETA RAYS

Introduction

When radiation strikes a medium, it causes ionization; associated with each ionization is an electron which may have an energy from a fraction of an eV to many keV. The more energetic electrons move about in the medium and cause still further ionization with the release of more electrons. It is apparent that the study of the energy distribution of electrons appearing in matter as a consequence of irradiation will provid information on the damage by the incident radiation. The field of electron spectroscopy differs from other spectroscopies in at least one interesting way in that there are few electron spectrometers available commercially. Spectrometers are almost always made to special designs to perform certain special tasks.

The field of electron spectroscopy is a large field which has grown up over many years. There are many hundreds of different types of spectrometers and many thousands of papers have been written concerning their use. It is not possible in a short lecture to go into great detail. In addition, it will be necessary to generalize in order to make a coherent presentation on such a large subject. There is an excellent reference by K. Siegbahn entitled "Alpha, Beta, and Gamma Ray Spectroscopy", which should be studied by anyone who wishes further information in this field.

Electron Spectrometers

Electron spectrometers may be classified by the energy differentiating mechanism as magnetic, electrostatic, scintillation, proportional counter or semiconductor. Each type offers particular combinations of transmission, resolution, and energy acceptance from 0.01 to 100 percent, 0.001 to 25 percent, and 1 eV to many Mev, respectively. Solid sources are usually employed which may range in diameter from a fraction of a mm to 10 cm. Energy calibration is usually accomplished by using internal conversion electrons or an electron gun or accelerator. Measurement of transmission is made by noting deviation, if any, from a Fermi plot of an experimental β spectrum from an allowed transition. Uses in health physics include measurements of: shapes of β-spectra which determine shapes of β-absorption curves, branching ratios, and average energies per disintegration, all of which are used in internal dose calculations; electron stopping powers, straggling distributions and W values are used in Bragg-Gray calculations; cross-sections for electron-electron interactions in solids and gases; slowing down spectra of β-rays, Compton and photoelectrons in solids; β-spectra from unknown emitters for identification. As monochromators, they select a narrow energy band from a β-ray continuum which may be used to measure efficiency of scintillators and energy dependence of β-ray dosimeters.

The pertinent energy-momentum and energy-velocity relationships for electrons are:

$$E = \sqrt{p^2c^2 + m_o^2c^4} - m_oc^2 \longrightarrow \frac{p^2}{2m_o} \text{ (low energy only)} \qquad (7\text{-}1)$$

$$= \frac{m_oc^2}{\sqrt{1 - v^2/c^2}} - m_oc^2 \longrightarrow \frac{1}{2} m_o v^2 \text{ (low energy only)} \qquad (7\text{-}2)$$

where E = electron kinetic energy
p = momentum
v = velocity
m_o = electron rest mass
c = velocity of light

It should be noted that the kinetic energy, E, is related to the momentum, p, by Equation 7-1, and that this relationship reduces to the familiar nonrelativistic form $E = p^2/2m_o$ only for low energy electrons, i.e., for electrons of less than about 25 keV. The alternative expression for the electron kinetic energy in terms of the velocity given by the second expression approaches $1/2\, m_o v^2$ also only for low energies. These expressions are rather tedious to compute; fortunately, this is now unnecessary by the excellent table giving the electron momentum and velocity as a function of energy from 0.2 eV to 3.3×10^{12} eV (U. S. Department of Commerce, National bureau of Standards Circular 571).

Principles of Magnetic Spectroscopy

An electron with momentum p perpendicular to a uniform magnetic field moves in a circular orbit of radius ρ. The relation connecting these quantities found by equating the product of the centripetal acceleration and electron mass to the magnetic force on a moving charge, is given in the first of Equation 7-3.

$$\begin{aligned} p &= He\rho \\ \frac{\Delta p}{p} &= \text{const} \\ N_1(p) &= \frac{cpm}{\Delta p} \\ &\approx \frac{cpm}{p} \approx \frac{cpm}{H\rho} \end{aligned} \tag{7-3}$$

and this equation is valid both relativistically and nonrelativistically. A differential in p is proportional to a differential in ρ and this equation implies that, if a group of electrons moving in a constant magnetic field is selected by a slit of width $\Delta\rho$ a band of momentum with width Δp, given above, will pass through this slit. Thus if $\Delta\rho/\rho$ is fixed geometrically, $\Delta p/p$ will be fixed at a constant value also, and the momentum resolution $\Delta p/p$ is a constant as indicated in the second of Equation 7-3.

A counter that counts the particles that move through a slit measures the number of counts per minute which lie between p and $p + \Delta p$. The ratio of counts per minute to Δp is the number of electrons per unit momentum which is defined as the momentum distribution $N_1(p)$. Thus $N_1(p)$ is given by the third of Equation 7-3 as $cpm/\Delta p$, or a proportional number, cpm/p, or $cpm/H\rho$. We frequently find the label $cpm/H\rho$ in the literature along the ordinate of a β ray spectrum. In this instance the ordinate represents the true momentum distribution of the electrons.

Principles of Electrostatic Spectroscopy

If electrostatic rather than magnetic deflection is employed in a spectrometer, the

governing relationship equivalent to Equation 7 3 is given in Equation 7-4

$$T = KV$$

$$\frac{\Delta T}{T} = \text{const} \tag{7-4}$$

$$\therefore N_2(T) = \frac{\text{cpm}}{T} \approx \frac{\text{cpm}}{T} \approx \frac{\text{cpm}}{V}$$

which states that the electron energy T being observed is proportional to the voltage V applied to the deflecting elements. By reasoning similar to that employed in Equation 7-3, it may be shown that the energy resolution $\Delta T/T$ is a constant in this case. Thus the energy distribution $N_2(T)$ is given by cpm/ΔT; or (counts per minute)/T; or cpm/V. Electrostatic spectrographs for β ray spectroscopy are rarely used because the relationships of Equation 7-4 are not valid for relativistic electrons. However, they will probably find increasing use in the future, particularly in the low energy region, because of their simplicity as well as their resolution and transmission characteristics.

Spectroscopy by Total Energy Absorption

In another class of spectrometers, the energy of an electron is measured by completely absorbing the electron in a scintillating material, a gaseous material, or a semiconductor. The size of the electric pulse in the photomultiplier or other associated circuitry generated by the absorption of the particle is proportional to the energy of the particle, and the distribution of pulse heights gives the energy distribution of the electrons. The resolution of such devices is given by a constant divided by the square root of the energy. This relation results from the fact that the statistical variation is the number of events associated with the absorption of a single electron is governed by a Gaussian distribution of pulses for absorptions of the same amount of energy.

In the scintillation spectrometer, the variation occurs primarily in the number of photoelectrons emitted at the cathode of the photomultiplier which views the light from a scintillating crystal. In the gaseous or proportional counter spectrometer, the variation occurs in the number of ion pairs created in the gas of the counter. In the solid-state spectrometer, the variation is in the number of electron-hole pairs which are formed. In all three spectrometers, the apparent energy spread may be calculated by first dividing the amount of energy absorbed by the amount required to produce one event, that is, about 1000 eV in a crystal, 30 eV in a gas (the W value of the gas), or 3 eV in the semiconductor. The number of events then has a deviation equal to the square root of this number, and this deviation multiplied by 1000, 30, or 3 gives the apparent energy spread. Although the energy resolution varies as the reciprocal of the square root of the energy, the energy distribution is given directly by the counts per minute observed because the resolution is entirely statistical in nature. These relations are shown in Equation 7-5.

$$\Delta T = \text{const}\sqrt{T}$$

$$\therefore \frac{\Delta T}{T} = \frac{\text{const}}{\sqrt{T}} \tag{7-5}$$

but

$$N_2(T) \approx \text{cpm}$$

Conversion of a Momentum distribution to an Energy Distribution

It is often useful to convert a momentum distribution into an energy distribution or vice versa. Equation 7 6 states the underlying

$$N_1(p)dp = N_2(T)dT$$

$$N_2(T) = N_1(p)\frac{dp}{dT} \qquad (7\ 6)$$

$$= \frac{N_1(p)}{v}$$

relationship between the two distributions; the number of particles $N_1(p)dp$, having momenta between p and $(p + dp)$ must equal the number of particles $N_2(T)dT$, which have energy between T and $(T + dT)$. If, for example, the momentum distribution $N_1(p)$ is known, the energy distribution $N_2(T)$ may be obtained by dividing $N_1(p)$ by the electron velocity, as shown in the third of Equation 7 6.

The Extrapolation Chamber

The extrapolation ionization chamber is often employed in a routine manner in β dosimetry. In the Bragg-Gray theory of the cavity ionization chamber, the size of the cavity was assumed to be such that the secondary ionizing particles lost only a small fraction of their energy in crossing it. The severity of this restriction, even for measurements of medium energy x-rays, has already been pointed out, and it is usually difficult, and often impossible, to design a chamber in which this condition is obviously satisfied. Some experimental check on the validity of the theory is therefore necessary when cavity chambers of larger size are used, and one such check is to measure the ionization per unit mass of air as the pressure is reduced. If this tends to a constant value, the latter may be taken as the value which would be obtained in an infinitesimally small cavity.

Another method is to vary the size of the chamber and plot the ionization per unit mass of air as a function of chamber size. The value for a vanishingly small cavity is then obtained by extrapolating the observations down to zero chamber size. The correction for wall absorption can be eliminated in a similar manner by taking observations for several wall thicknesses and extrapolating to zero thickness. A chamber was devised for this purpose by Failla and was called by him an *extrapolation chamber*. It consists of a parallel plate chamber with variable plate spacing, the volume from which ionization is collected being a small coin shaped region at the center of the plates, surrounded by a wide guard ring. With appropriate modification, this type of chamber has been used for various specially difficult dosimetric problems, e.g., the estimation of the dose due to a radioactive isotope uniformly distributed in tissue, the dosimetry of β-ray sources, and the measurement of dose rate in electron beams. In the last two instances, the ionizing particles are themselves the primary radiation and are not isotropically produced secondaries as the Bragg-Gray theory requires. The introduction of any finite cavity into a medium irradiated by a *directed* beam of ionizing particles will always disturb locally the particle flux, and only a technique which employs some of extrapolation chamber can give reliable information about the dose distribution in the medium.

In order to determine accurately the very small electrode spacings which may be

necessary in an extrapolation chamber, it is often best to measure the electrical capacity of the collecting electrode with respect to the opposite plate and to deduce the spacing from this and the area of the collector. As a rule, the collector is separated from the guard ring by a very narrow insulation gap, and its effective area can be determined accurately.

Ionization Chambers for Fast Electron Dosimetry

A parallel-plate ionization chamber having thin foil electrodes is suitable for monitoring or for dose measurements in a fast electron beam. The plates are very thin foils of aluminum or copper or of graphited mica or polystyrene. The central foil is the collector, and the two outers are at ground potential. The volume from which ionization is collected may be defined by letting the electron beam enter the chamber through a diaphragm of known diameter.

Alternatively, if a mica or polystyrene foil is used, a small collecting area may be isolated from the rest of the central foil by a scratch through the graphite, and a connection from this brought out through a long screened "panhandle". Foils of polystyrene, mica, or aluminum of thickness half to one thousandth of an inch are very suitable: copper foil of thickness 0.00012 in. can be obtained, which is quite strong enough for small diameter chambers.

When a beam-defining diaphragm is used, the *active volume* of the ionization chamber is the coin-shaped region between the outer foils which is traversed by the beam. With an isolated collecting area on the central foil, the active volume is the coin-shaped region lying between this collecting area and the grounded foil above it. The ratio of active to inactive volume should be kept as large as possible, and this is best achieved by avoiding complicated designs. The foils can readily be cemented to their supporting rings. If this is done at about 100 to 200°C and if the material of the rings has a slightly smaller expansion coefficient than the foil, the latter will remain tightly stretched, and therefore plane, as the ring cools.

To determine a superficial dose rate, the chamber should be brought as close as possible to the surface of the irradiated material in order that the full backscatter may be included in the measured ionization. Some electrons are scattered back from the foils themselves, but this error can usually be kept quite small with thin foils of low atomic number. For accurate work, the foil spacing must be adjustable, and the extrapolation chamber technique must be employed to determine the true superficial dose rate.

BIBLIOGRAPHY

1. K. Siegbahn, editor, *Alpha, Beta, and Gamma Spectroscopy,* North Holland Publishing Company, Amsterdam, 1965.

2. K. Z. Morgan and J. E. Turner, *Principles of Radiation Protection*, John Wiley and Sons, Inc., New York, 1967.

3. L. Marton, C. Marton, and W. G. Hall, *Electron Physics Tables*, National Bureau of Standards Circular 571 (1956).

4. R. D. Birkhoff, *Electron Spectroscopy in Health Physics Research*, Health Physics *9*, 973-986 (1963).

5. G. Failla, Radiology *29*, 202 (1937).

LECTURE N° 8

INTRODUCTION TO RADIATION BIOLOGY

Introduction

It would be impossible to present in one lecture all pertinent aspects of the effects of radiation on biological systems. However, this lecture is intended to present a few of the basic interaction processes, introduce several of the observed effects at the cellular level due to radiation, and then extend the discussion to include the effects of radiation on the total organism (namely, man). The latter discussion will present both immediate lethal effects and late effects of irradiation.

Action of Radiations in Aqueous Systems

As you know, ionization produced by radiation is a random process. If a complex system (one consisting of more than one kind of molecule) is irradiated with an ionizing radiation, ionization will occur in all the different kinds of molecules present in the system in the proportion in which the molecules are present. Unless a dose large enough to ionize every molecule in the mixture is delivered, some molecules of each type will be ionized, and some of every type will be left intact. This does not mean that all the intact molecules will scape radiation-related change. If it is possible for changes to be brought about in these intact molecules by the irradiation products of the ionized molecule the energy of an ionizing particle must be transferred to one of the intact, un-ionized molecules from a molecule that has been "hit" (ionized).

Thus, there are two, quite different mechanisms by which chemical changes in molecules may be brought about by ionizing radiation. One is **direc action**, i.e., a molecule is ionized or excited by the passage of an ionizing particle. The other is **indirect action**; the changed molecule has not itself been ionized or excited by a particle. However, the molecule is changed, because it has received the energy of an ionizing particle by transfer from another molecule which has been ionized through the direct action of radiation.

It should be kept in mind that cells (and, therefore, living systems) are extremely complex mixtures or solutions. Water is the solvent, and the chemical reactions which make up the process called "metabolism" take place in it. The cell molecules (proteins, carbohydrates, nucleic acids, inorganic substances) are either dissolved in or suspended in a watery medium. When cells or tissues are irradiated, most of the energy transfer goes on in water, because the water presents the largest number of "targets" for the radiation. Solute molecules, because they are relatively scarce, will be acted upon infrequently. However, chemical changes can be brought about in the solute molecules if the energy of the ionizing particles is transferred to them from the ionized water. It is apparent, with respect to changes brought about in the molecules of which cellular constituents are composed, that the interaction of ionizing radiation and water, and the chemistry of irradiated water is very important.

Water, as any other material, is ionized when irradiated. An electron is removed from the molecule leaving behind an ionized water molecule.

$$H_2O \xrightarrow{\text{radiation}} H_2O^+ + e^- \qquad (8\text{-}1)$$

$$H_2O + e^- \longrightarrow H_2O^-$$

Equation 8 2 depicts the ejection of an electron from a water molecule. The molecule is now positively charged, and the electron, which has to be ejected, is traveling with some discrete energy through the medium. The reaction shown in Equation 8-2 typically follows that in Equation 8 1. An un-ionized water molecule captures an electron (set free in Equation 8-1). The result is another ion, a water molecule endowed with a negative charge. Thus a pair of ions (H_2O^+ and H_2O^-) has been formed.

The above reactions represent only a first step in a series of reactions, because the final products of irradiated water are H, OH, H_2O_2, and HO_2. It is clear that none of these is formed as an immediate result of the passage of ionizing radiation through a water molecule.

The ions H_2O^+ and H_2O^- are not stable and dissociate almost immediately into free radicals. Free radicals are distinguished by the presence of a single, unpaired electron (unpaired from the point of view of direction of spin on the electron's own axis). The outer electron orbits of H_2O^+ and H_2O^- may be represented in the following manner:

$$H_2O^+ = H^{\cdot}\ \cdot\ddot{O}\cdot\ {}^{\cdot}H$$

$$H_2O^- = H^{\cdot}\ :\ddot{O}:\ {}^{\cdot}H$$

As previously stated, these ions almost immediately dissociate into two subunits:

$$H_2O^+ \longrightarrow H^+ + OH^{\cdot}$$

$$H_2O^- \longrightarrow H^{\cdot} + OH^-$$

In this case, the dot symbolizes the unpaired electron. Free radicals thus formed are responsible for the indirect action of radiation, since they are extremely reactive (in pure water they ordinarily react within 10^{-5} seconds). Reactions of free radicals are reasonably indiscriminate; a free radical may interact with another free radical, with a molecule already "damaged" by radiation or with an intact molecule.

The reactions of free radicals can be subdivided into five general categories.

A. Commonly, there will be a number of reactions among the free radicals themselves.

1. $H^{\cdot} + OH^{\cdot} \longrightarrow H_2O$
2. $H + H \longrightarrow H_2$
3. $OH^{\cdot} + OH^{\cdot} \longrightarrow H_2O_2$

B. Free radicals may react with the water in which they are formed.

1. $H^{\cdot} + H_2O \longrightarrow H_2O + OH^{\cdot}$

C Free radicals may react with their own reaction products

1 $H_2O + OH \longrightarrow H_2O + H$

2 $H_2O_2 + OH \longrightarrow HO_2 + H_2O$

3 $HO_2 + HO_2 \longrightarrow H_2O_2 + O_2$

4 $HO_2 + OH \longrightarrow H_2O + O_2$

D Free radicals may react with oxygen

$$O_2 \xrightarrow{H} HO_2 \xrightarrow{H} H_2O_2 \longrightarrow OH + H_2O \xrightarrow{H} 2H_2O$$

The hydrogen free radical reacts with oxygen to give HO_2 (the hyperoxal radical) an important product which further reacts to produce the potent poison, hydrogen peroxide (H_2O_2) The presence of oxygen in cells and tissue at the time of irradiation increases the magnitude of the effects of radiation, irrespective of the end point under observation This interaction between oxygen and radiation is known as "the oxygen effect"

E Finally, and most importantly, free radicals may interact with organic molecules (the molecules of which cells and tissues are built) and change them When these interactions take place, the indirect action of radiation has occurred

the following equations illustrate how these interactions may come about:

1 $HO_2 + RH \longrightarrow R + H_2O_2$

2 $RH + HO_2 \longrightarrow RO + H_2O$

If RH in either of these cases is a fundamental organic molecule, important to the metabolism of the cell, then an upset in the chemistry (metabolism) is expected In addition, H_2O_2 (hydrogen peroxide) is a cell poison and, if present in sufficient quantities, can materially interfere with metabolism

As we have seen, not all products of free radical interactions are harmful to living systems (water and molecular hydrogen) Some of the products of such reactions are poisons; still others are free radicals themselves capable of further reaction and transfer of the energy of the ionizing particle. Organic free radicals may represent not only changed molecular constituents of the cell, but also substances that are free to attack other such constituents and spread molecular change still further. However, one concludes from the previous discussion that indirect action primarily, but not exclusively, occurs from water derived free radicals

Target Theory

The various molecular species of which cells are composed have specific functions The labors of the cell as a whole are divided among its various components and the components function in cellular activity in harmony with each other Every component of the cell is important, perhaps indispensable, for the maintenance of normal metabolism and for viability, because each has a special role to play in normal metabolism However, the number of

molecules that makes up each type or species varies; some species are present in excess while others are present in limited numbers. The loss of the molecular species present in limited numbers can seriously affect metabolism. Among the nucleic acids, deoxyribonucleic acid (DNA) is the most important in this respect. DNA is the rarest species of molecules in the cell and plays the widest, most critical role in metabolism.

The existence of such a hierarchy of functions, and of the molecules which perform them, has led to the supposition that there may be critical or "key" molecules in the cell. The alteration of these molecules could result in the loss of vital functions and even the death of the cells of which these molecules are components. This supposition has led to evolution of the concept of "target theory". This theory has been used to interpret radiation results in both living and non-living systems. Target theory demands that, for serious change in function of an organism or molecule to be brought about by radiation, the initial transfer of energy (ionization) must occur within a limited vital or sensitive volume. Consequently, the application of target theory must be restricted to cases in which direct action is the sole, or at least the predominant, mechanism for producing molecular changes. Target theory has had its greatest success when its use has been restricted to experimental systems in which indirect action is ruled out (i.e., dried, crystallized viruses). Remember that nearly all biologic systems are composed of large amonts of water and that indirect action is by far the predominant mode through which changes in the molecules which comprise a cell are brought about.

In order for target theory to apply, the following requirements must be met:

1. Survival of function following varying doses of radiation must be exponentially related to increasing dose.

2. The process must be independent of dose rate.

3. The dose of different types of radiations required to produce a given biologic effect must increase in order of gamma rays, hard x rays, soft x rays, neutrons, beta and alpha particles (an order of increasing LET).

The fact that target theory cannot be directly applied to all living systems does not destroy the concept of the key molecule. Some functions will be sensitive to inactivation by smaller amounts of radiation energy than other. This will be due mainly to a difference in the number of agents which control the function. For example, a change in one molecule can result in the loss of function (inactivation of some viruses). But life (vital function) in more complex structures such as cells is not dependent upon one molecule but upon many, so that several, at the least, must be changed before inactivation (death) occurs.

The inactivation of an enzyme is a good illustration of single hit phenomenon. One hit or change in an enzyme molecule is all that is thought necessary to inactivate these molecules. If one plots the fraction of enzyme molecules surviving irradiation as a function of the dose, a curve similar to that shown in Figure 8-1 is produced.We see immediately that the inactivation efficiency decreases with increasing dose and inactivation expressed as a function of increasing dose falls off exponentially.

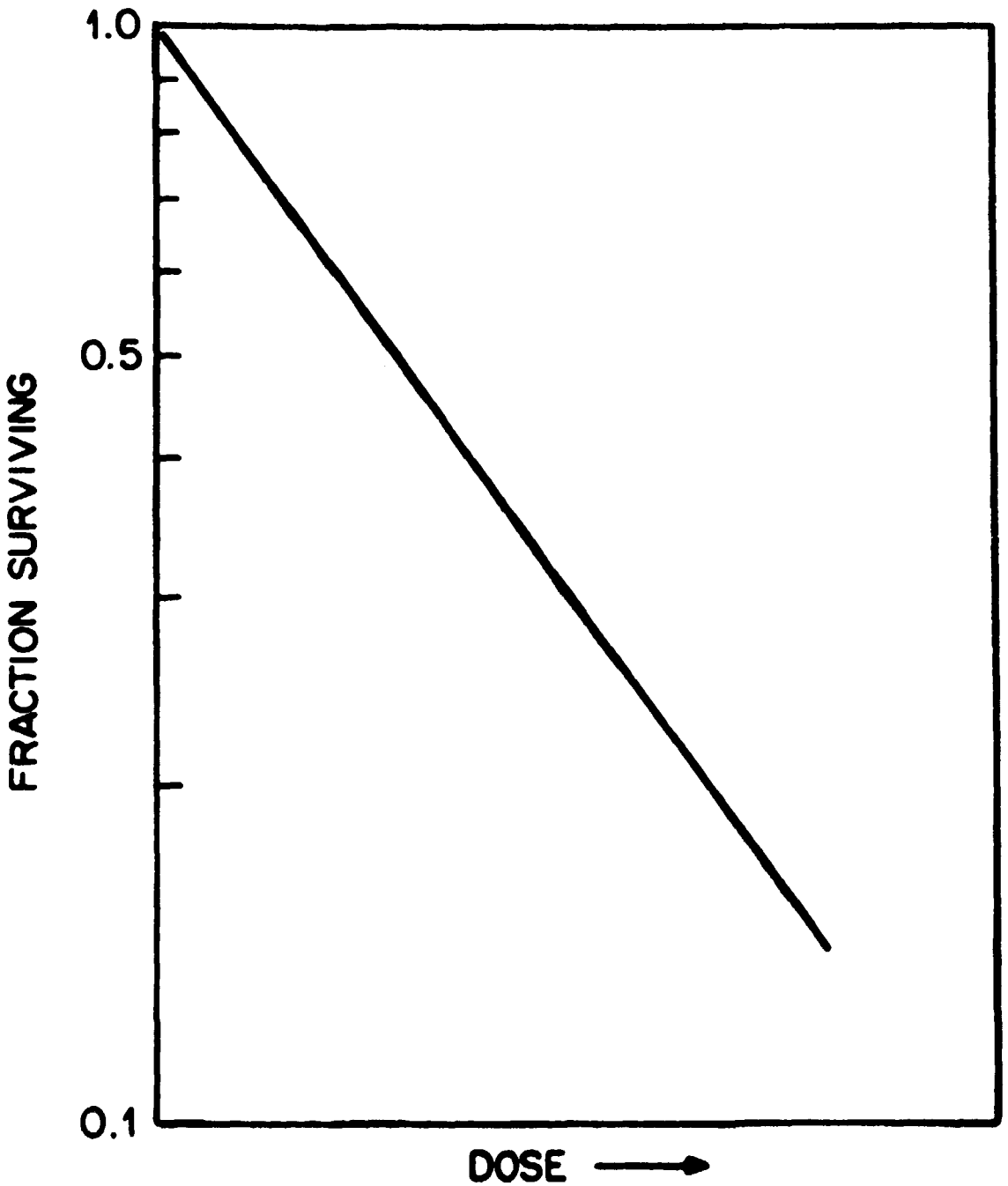

Figure 8 1

Typical Dose Response Curve

Higher on the scale of life, organisms become increasingly complex There are often several different structures which may control the same function. The multiplicity of "targets" makes inactivation of the organisms as a whole, by a single hit, highly unlikely The more targets there are per organism, the less efficient any given dose of radiation will be for inactivating them However, survival data for these "multi-hit" cases is presented in the same manner (Figure 8-2). When the linear part of these curves is extrapolated beyond the initial threshold value to zero dose, the point of intercept on the y axis is said to be numerically related to the average number of targets or key molecules per organism. That is, the intercept at zero for $N = 1$ is taken to mean that only one key molecule exists in these organisms. On the same basis, an intercept of the y-axis at points greater than one is taken to indicate more than one target per organism.

Effects in the Total Organism

Lethal Effects

The principal effect of exposure of the whole body to penetrating, ionizing radiation is the shortening of the life of the exposed organism. The length of time live is shortened is dependent on the dose level to which the organism is exposed (it will also depend upon various other factors) It is possible that there are very low doses of total-body radiation which do not elicit the earlier death of the irradiated animal. But this has not been proved; most evidence tends to indicate that if such a threshold does exist, it will be very low

Total-body irradiation of mammals with rather large doses of ionizing radiation ($\sim$ 300 rad or more) causes death of the organism more or less "immediately" Doses of radiation which bring death with about 30 days are referred to as "immediately lethal", and the action of the radiation is said to have been "acute". Immediately lethal is a relative term; animals may not die immediately after exposure to radiation, but they have not escaped its effects The effects are manifested later in their lives; in contrast to immediate effects, these are called "late effects". The immediately lethal effects are generally called somatic effects, whereas the late effects comprise the genetic and late somatic effects of radiation

The observed response to single exposures of ionizing radiation given uniformly over the total body is primarily dependent upon dose. For any similar group of mammals, exposure to increasing doses results in the appearance of a growing number of signs indicating that response to radiation is occurring. Ultimately, a dose-level is attained at which, in addition to the above signs, some of the animals begin to die As the dose is increased beyond that which begins to kill some of the irradiated animals, more animals will die, and survival time of the animals that die grows shorter. When mean survival times are computed for each dose of radiation greater than that which begings to cause death, a pattern, consistent for nearly all species of mammals studied, emerges. This pattern is illustrated in Figure 8-3. The graph shows three clearly distinguishable components First, over the dose-range of 200 or 300 rad to about 1000 rad, the response is dose dependent. As the dose is increased, the mean survival time decreases from weeks to days. The second phase extends over a very wide range ($\sim$ 1000 to 10,000 rads), but is independent of dose. The mean survival time at any point on this plateau region is about 3 5 days The last component of the pattern is also dose-dependent. In this case, as the dose increases, the mean survival time decreases from days to hours and even to minutes

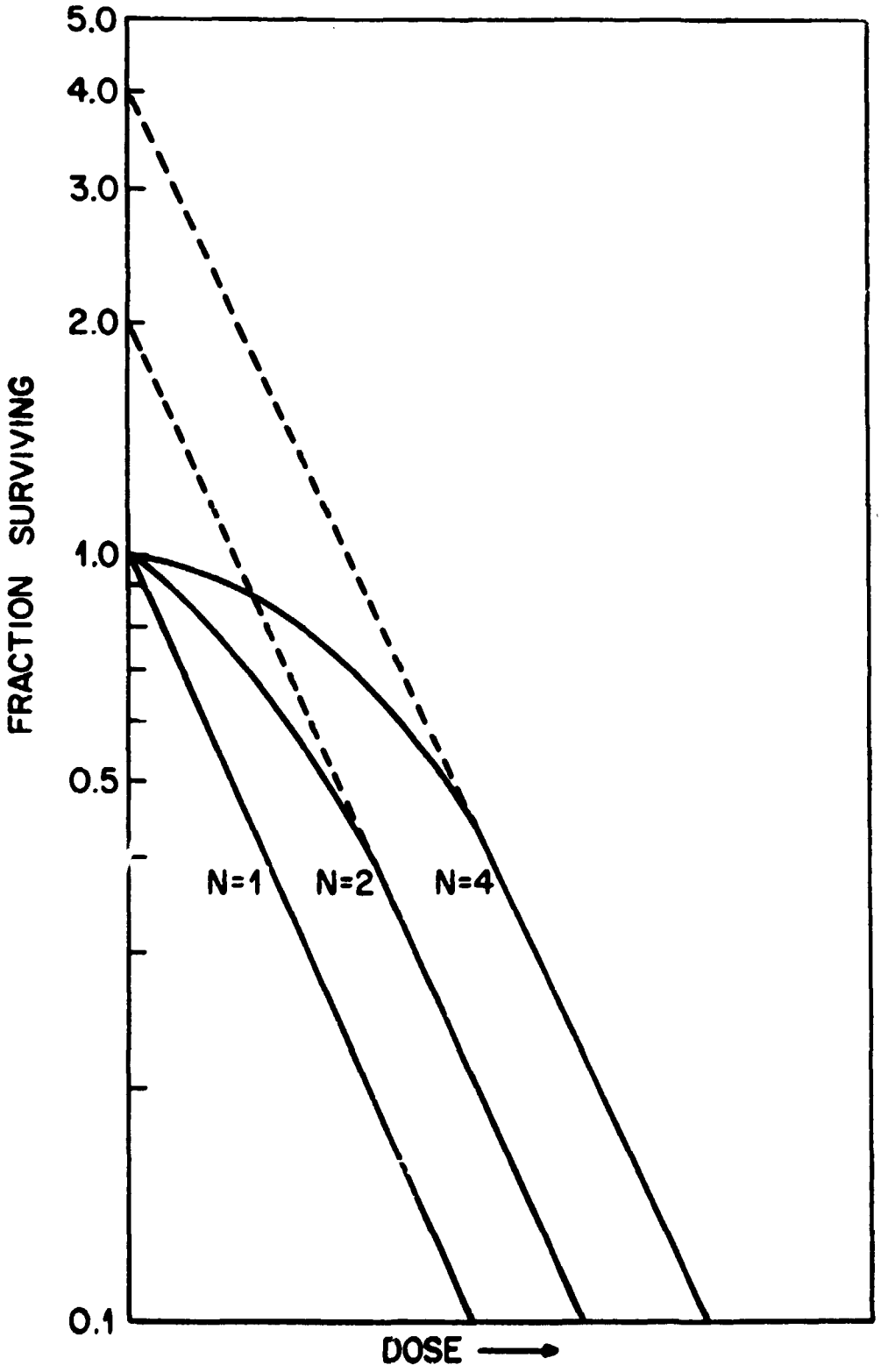

Figure 8-2

Dose Response Curves Illustrating Multihit Relations

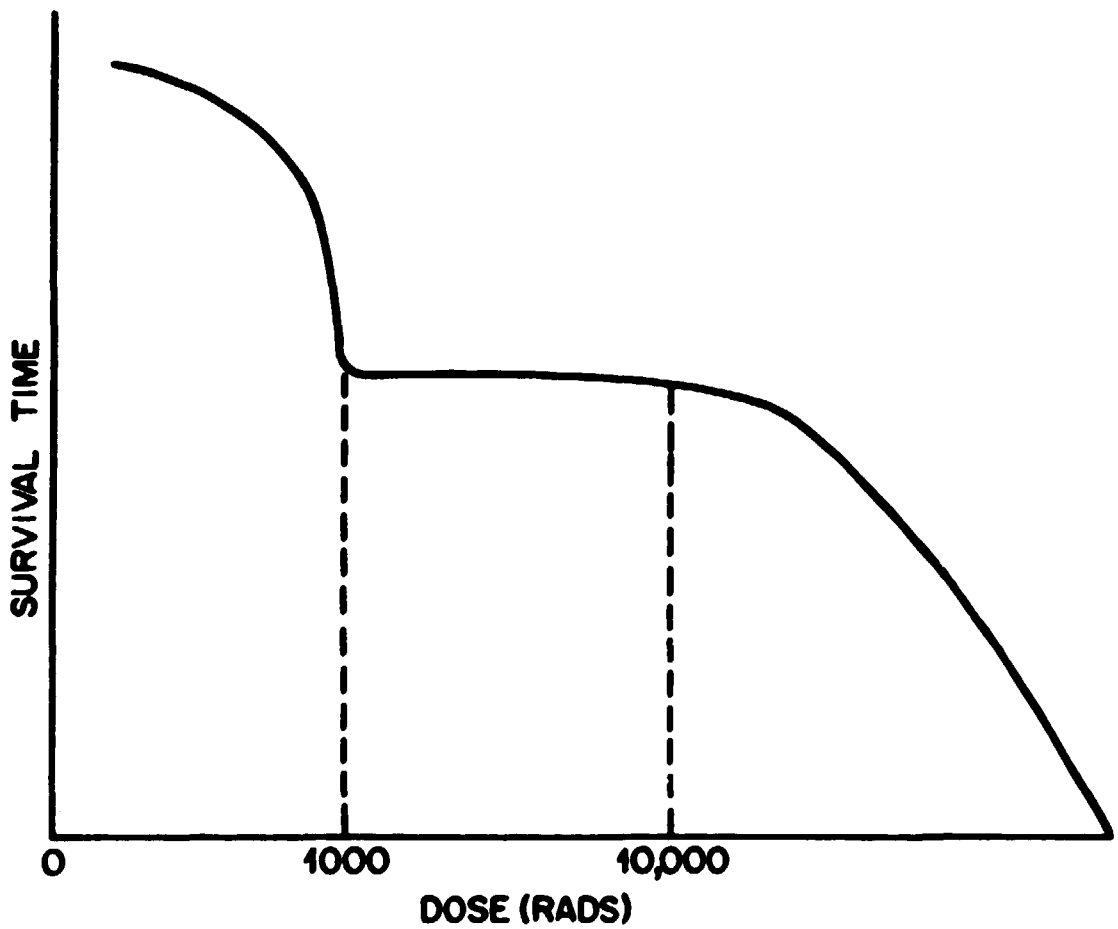

Figure 8.3

Mean Survival Time for Mammals Following a Single Dose of Radiation to the Total Body.

The three regions of the dose response curve are widely believed to reflect damage to and failure of three different organ systems. In the first region, where death may occur within weeks to days, the effects are thought to be due to the radiation damage to and the failure of the hemopoietic system. This organ system is responsible for the manufacture of the corpuscular elements of the blood. Do not be confused; other organ systems are damaged by the total body irradiation. However, in this case, the hemopoietic system is the radiosensitive system whose failure brings death. These comments can also be extended to the two regions of response discussed below.

A dose range is finally reached in which large numbers of cells of the gastrointestinal tract are badly damaged. When enough cells are damaged, death of the irradiated animals will occur principally as the result of damage to and the failure of the gastrointestinal system to function properly. This is a region of dose independence, and mean survival time for most mammals will be about three to four days.

As the region of dose dependence is reached at the higher dose levels, we find that death is due primarily to the failure of the central nervous system. As before, death is due to the failure of the central nervous system, but all other organ systems will be seriously damaged. The gastrointestinal and the hemopoietic systems will both be severely damaged and will fail, just as they do at lower doses. However, the failure of the central nervous system brings death very quickly so that the consequences of the failure of other systems do not have time to express themselves.

The sensitivity of various tissues and organs to radiation is dependent upon the rapidity with which their mature, functional cells die out and are replaced by new cells. These new cells are a result of cell division among undifferentiated (immature, unspecialized) cells in the tissue. This relationship was put into the form of a law by Bergonié and Tribondeau. The law states that radiosensitivity of tissues depends upon the number of undifferentiated cells which the tissue contains, the degree of mitotic activity (cell division) in the tissue, and the length of time that cells of the tissue stay in active proliferation (i.e., the number of cell divisions between the earliest, immature state of a cell and its final mature, functional state).

In all tissues of the body, mature functional cells wear out, become defective or inefficient, and are replaced. They are replaced by cells which differentiate (or specialize), but which are themselves immature and unspecialized. An undifferentiated cell in the tissue or organ will divide. One of the daughters will differentiate and replace a worn out cell while the other daughter remains undifferentiated and 'replaces' the undifferentated cell from which both daughters arose. In this way, tissues remain in a steady state with respect to numbers of cells. The total number of cells does not change; sufficient mature, functional cells are always present to carry out the functions of the tissue or organ because the rate of reproduction and replacement is always equal to the rate of cell loss.

Some tissues have a high rate of cell renewal (bone marrow and gastrointestinal tissue are good examples) so that, at any time, relatively large numbers of their cells are dividing and differentiating. It is widely known that the division cycle is a singularly radiosensitive phase of cell life. Radiation interferes with cell division through its effects upon the chromosomes in the nucleus of the cell. If a tissue has a high rate of mitotic activity, it is reasonable to expect it to be radiosensitive. A somewhat arbitrary listing of the radiosensitivity of systems and organs can

be constructed simply upon what we know concerning the mitotic activity of the system. In a general sense, mammalian tissues can be arranged in the following order of increasing resistance to radiation:

1. Spermatogonia.
2. Lymphocytes.
3. Erythroblasts
4. The rest of the classical hemopoietic tissues.
5. Lining of the small intestinal tract
6. Stomach.
7. Colon.
8. Skin.
9. Central nervous system
10. Muscle.
11. Bone.
12. Collagen.

A close inspection of this listing can explain in very simple terms the effects discussed earlier and illustrated in Figure 8-3.

In following sections, a summary will be presented which will describe the major syndromes of the immediately lethal effects of total body irradiation

Bone Marrow Syndrome

Total body radiation, if given in sufficiently high, single exposures, brings death within a few weeks. While many organs and tissues are damaged, and death is due to damage in all of them, death will come about principally as a result of damage to the bone marrow

The time course of survival and the signs and symptoms that accompany it are called the "bone-marrow syndrome" In the initial phases, the obvious manifestation is nausea, sometimes accompanied by vomiting (called the prodromal period). It is at this time that the lethal effects are begining, and undifferentiated stem cells in bone marrow start to die. New cells for the circulating blood are no longer produced. The next major manifestation is a period of apparent well being (called the latent period). During this period, more precursor cells in the bone marrow die, and the marrow spaces become nearly cell free. Since circulating cells are not renewed, a drop in blood count is observed. At the same time, a period of severe gastrointestinal disturbance begins (diarrhea, later becoming bloody) resulting from radiation damage to the gastrointestinal tract. Hemorrhage into tissue, fluid imbalance, serious infection, and, ultimately, death follow. Death is the result of failure of the bone marrow and the body systems which fight infection.

Gastrointestinal Syndrome

The full gastrointestinal syndrome is brought about only by total body exposure. Death is the result of damage to many tissues, but the most important are the gastrointestinal epithelium and the renewal systems of the bone marrow. Death itself is due to fluid and electrolyte loss, infection, and nutritional impairment. The irradiated animal dies in shock

Central Nervous System Syndrome

Mean survival time for the central nervous system is dose dependent However, there appears to be a "threshold" dose level at and above which the syndrome comes into existence Clinical signs include agitation, apathy, disorientation, loss of equilibrium, loss of coordination of muscular movements diarrhea, vomiting, tetanic spasms, convulsive seizures, coma, and death The principal changes noted are infiltration into the meninges, vasculitis of the brain, and edema Neuronal cells of the cerebellum undergo pyknosis and nuclear shrinking indicating a disturbance in fluid balance in these cells Death is attributed to neuronal damage due to vaculits, edema, and increased intracranial pressure

Late Effects

Effects in this category fall into a category which are the genetic effects and the late somatic effects of radiation Genetic damage is not always expressed until mutant genes find themselves in a genetic environment that permits expression This section will only consider the late somatic effects of radiation

The late effects following total body exposure in low dose ranges are impaired fertility, shortening of life span, cancer induction, and the induction of cataracts

Impairment of fertility occurs because of radiosensitivity of precursor cells to the gametes However, exposure to radiation in males does not appear to affect sexual capacity (libido or potency) Of course, exposure to radiation often produces a kind of "sickness" (previously described) which is debilitating, and as in most illnesses, there is a loss of sexual desire and responsiveness

Shortening of life span is a true radiation effect but its genesis is not known The amount of life shortening of small animals after total body irradiation appears to be dose dependent In addition, life shortening appears to be dose rate dependent

Ionizing radiations are carcinogens (cancer formers), exposure to ionizing radiation carries the risk of cancer induction in the irradiated organism Ionizing radiation is a general carcinogen, that is radiation induces cancers of any tissue in nearly any animal tested, irrespective of species Radiation is not the only carcinogen There are a multitude of other carcinogens, e.g., chemicals, physical chronic irritants and living agents (viruses) However, among these only radiation is at present known to be so general a carcinogen

Cataracts form as a result of an exposure to ionizing radiation in which the eye is involved A rather large dose is required to induce the formation of cataracts, and therefore cataracts formation is a relatively uncommon late effect of total body radiation These cataracts are not the same as those which occur as a result of senility In appearance and development, radiation induced cataracts are quite distinct Some data indicate that neutron irradiation can produce cataracts in good quantity after rate low doses

BIBLIOGRAPHY

1 D E Lea, *Actions of Rad iations on Living Cells Second Edition* Cambridge University

Press, 1955.

2. E. P. Cronkite and V. P. Bond, *Radiation Injury in Man*, Charles C. Thomas, Publishers, Springfield, Illinois, 1960.

3. Z. M. Bacq and P. Alexander, *Fundamentals of Radiobiology, Second Editiion*, Pergamon Press, New York, 1961.

4. D. J. Pizzarello and R. L. Witcofski, *Basic Radiation Biology*, Lea and Febiger, Philadelphia, 1967.